

DEPOSITIONAL ENVIRONMENT AND PROVENANCE OF THE LATE APTIAN
TO EARLY ALBIAN CUMMINGS FORMATION, EAST CENTRAL ALBERTA,
AND A DISCUSSION CONCERNING SECONDARY SOURCE ROCK POTENTIAL

Robert Pelkey

Submitted in Partial Fulfilment of the Requirements
for the Degree of Bachelor Sciences, Honours
Department of Earth Sciences
Dalhousie University, Halifax, Nova Scotia
March 2006



Dalhousie University

Department of Earth Sciences

Halifax, Nova Scotia

Canada B3H 3J5

(902) 494-2358

FAX (902) 494-6889

DATE: March 13, 2006

AUTHOR: Robert Pelkey

TITLE: Depositional Environment and provenance of late
APTIAN to EARLY ALBIAN Cummings formation,
east central Alberta, and a discussion
concerning secondary source rock potential

Degree: B.Sc Convocation: May Year: 2006

Permission is herewith granted to Dalhousie University to circulate and to have copied for non-commercial purposes, at its discretion, the above title upon the request of individuals or institutions.

Signature of Author

THE AUTHOR RESERVES OTHER PUBLICATION RIGHTS, AND NEITHER THE THESIS NOR EXTENSIVE EXTRACTS FROM IT MAY BE PRINTED OR OTHERWISE REPRODUCED WITHOUT THE AUTHOR'S WRITTEN PERMISSION.

THE AUTHOR ATTESTS THAT PERMISSION HAS BEEN OBTAINED FOR THE USE OF ANY COPYRIGHTED MATERIAL APPEARING IN THIS THESIS (OTHER THAN BRIEF EXCERPTS REQUIRING ONLY PROPER ACKNOWLEDGEMENT IN SCHOLARLY WRITING) AND THAT ALL SUCH USE IS CLEARLY ACKNOWLEDGED.

DEPOSITIONAL ENVIRONMENT AND PROVENANCE OF THE LATE
APTIAN TO EARLY ALBIAN CUMMINGS FORMATION, EAST
CENTRAL ALBERTA, AND A DISCUSSION CONCERNING
SECONDARY SOURCE ROCK POTENTIAL

Robert Pelkey

Through the interpretation of one cored section located within the Provost Oil Field of east central Alberta, the late Aptian to early Albian Cummings Formation, found within the Lower Mannville Group, has been interpreted as a transgressive estuary deposit. Basal channel incision followed by valley-fill deposits exhibit progressive marine influence through the presence of characteristic tidal bundles and asymmetrical current ripples demonstrating subordinate current flow. A low diversity suite of biogenic sedimentary structures, mixed *Skolithos* and *Cruziana* ichnofacies, also adhere to a transgressive estuarine depositional model. Abundant detrital chert, volcanic and lithic fragments observed through mineralogical analyses indicate a Cordilleran provenance. Organic petrographic analyses of organic matter within the Cummings Formation suggest a terrestrial source of potential gas producing type III kerogen. Vitrinite reflectance and rock evaluation results suggest the Cummings Formation is thermally immature. Poor total organic carbon percentages designate the Cummings Formation as being inadequate as a secondary source rock for the Provost Oil Field. Further understanding of depositional environments and sequence stratigraphic relationships within the Western Canadian Sedimentary Basin (WCSB) provides insight into hydrocarbon emplacement. This study also provides further stratigraphic resolution of the complex interval between the Lower and Upper Mannville Groups.

Key Words: Western Canadian Sedimentary Basin, depositional environment, Cummings Formation, Mannville Group, physical and biogenic sedimentary structures, provenance, organic petrography, source rock, hydrocarbons.

TABLE OF CONTENTS

ABSTRACT	i
TABLE OF CONTENTS	ii
TABLE OF FIGURES	iii
LIST OF PLATES	iv
TABLE OF TABLES	iv
ACKNOWLEDGEMENTS	1
CHAPTER 1 – INTRODUCTION	1
1.1 Objectives	1
1.2 Geological Setting	1
1.2.1 A Rising Cordillera and the Formation of the Western Canadian Sedimentary Basin	1
1.2.2 The Western Canadian Sedimentary Basin	4
1.2.3 Stratigraphic Framework of the Western Canadian Sedimentary Basin	5
1.2.4 Stratigraphy of the Study Area	5
1.3 Previous Work	9
CHAPTER 2 – DEPOSITIONAL ENVIRONMENT OF THE FORELAND BASIN SUCCESSION	11
2.1 Cretaceous Deposition	11
2.1.1 First Clastic Wedge	11
2.1.2 Second Clastic Wedge	15
2.1.3 Third Clastic Wedge	19
2.2 Mannville Deposition	19
CHAPTER 3 – METHODS	24
3.1 Methods	24
3.1.2 Core Descriptions	24
3.1.3 Transmitted and reflected-light microscopy	25
3.1.4 X-ray Diffraction	25
3.1.5 Vitrinite Reflectance	26
CHAPTER 4 – RESULTS	28
4.1 Core Descriptions	28
4.1.1 Lithofacies F	31
4.1.2 Lithofacies E	33
4.1.3 Lithofacies D	33
4.1.4 Lithofacies C	34
4.1.5 Lithofacies B	34
4.1.6 Lithofacies A	35
4.2 Thin Section Mineralogy	36
4.2.1 Transmitted and reflected-light microscope observations	38
4.3 X-ray Diffraction results	45
4.4 Organic Petrography and Hydrocarbon Maturity using Vitrinite Reflectance	49
CHAPTER 5 – DISCUSSION	66
5.1 Depositional Environment and Sequence Stratigraphy of the Cummings Formation	66

5.1.1 Lithofacies F	66
5.1.2 Lithofacies E	70
5.1.3 Lithofacies D	71
5.1.4 Lithofacies C	72
5.1.5 Lithofacies A and B	73
5.2 Provenance of the Cummings Formation	76
5.3 Source Rock Potential and Thermal Maturity of Organic Matter and Reservoir Compartmentalization	79
CHAPTER 6 – CONCLUSIONS	83
6.1 Conclusions	83
6.2 Recommendations for Further Work	84
Reference	86

APPENDICES

- A-Plates of Core
- B-Core Description Sheets
- C-XRD analyses Raw Data
- D-Rock Evaluation Data

TABLE OF FIGURES

Figure 1.1 – Map of the Study Area	2
Figure 1.2 – Cross Sectional View of the Evolution of the Rocky Mountain Thrust and Fold Belt	3
Figure 1.3 – Stratigraphic Column of the Study Area	7
Figure 2.1 – Structural Elements of the Western Canadian Sedimentary Basin	12
Figure 2.2 – a) Map view of the Sedimentary Basin showing major geographical areas and cross section line b) Cross Sectional map of foreland basin succession	14
Figure 2.3 – Paleogeographical map of Alberta during Early Aptian	17
Figure 2.4 - Paleogeographical map of Alberta from Late Aptian to Early Albian	18
Figure 2.5 – Cross sectional view of sequence stratigraphic relationships within the study area	21
Figure 2.6 – Isopach map of the transgressive systems tract of the basal unconformity of the foreland basin succession	22
Figure 2.7 – Interpretive map of the drainage networks on the basal unconformity of the foreland basin succession	23
Figure 4.1 – Core Summary of the upper cored interval of Well 3B	29
Figure 4.2 – Bulk mineralogy of thin section 3B-1 of Lithofacies F	39
Figure 4.3 – Bulk mineralogy of thin section 3B-2 of Lithofacies F	41
Figure 4.4 – Bulk mineralogy of thin section 3B-3 of Lithofacies B	43
Figure 4.5 – Spectral plots acquired from XRD analyses	45
Figure 4.6 – Maceral types located in Sample 1	50
Figure 4.7 – Maceral types located in Sample 2	53

Figure 5.1 – Example of a tide-dominated estuary	66
Figure 5.2 – Basal Cummings Formation contact	67
Figure 5.3 – Summary of interpretations	75
Figure 5.4 – Hydrocarbon generation model	81

LIST OF PLATES

Plate 1 – Matrix supported silt rip-up clasts	57
Plate 2 – Imbricated silt rip-up clasts along a bedding plane	58
Plate 3 – Vertical <i>Skolithos</i> burrows	59
Plate 4 – <i>Skolithos</i> and <i>Planolites</i> burrows	60
Plate 5 – Reaction halos surrounding sulfide mineralization	61
Plate 6 – Tidal couplets	62
Plate 7 – Current ripples	63
Plate 8 - Lenticular bedding	64
Plate 9 – Reactivation surface	65

TABLE OF TABLES

Table 1 – Identified lithofacies, with corresponding thicknesses	30
Table 2 – Summary of mineralogy of the upper cored interval of well 3B	37
Table 3 – Vitrinite reflectance results	55

ACKNOWLEDGEMENTS

First and foremost I would like to thank my supervisor, Dr. Grant Wach, for providing me the opportunity to learn from his vast experience in sedimentology and sequence stratigraphy. I would also like to thank him for encouraging me in the field of earth sciences. I would like to thank visiting scholar Dr. Yawooz Kettaneh for his support and guidance in my mineralogical analysis. I am also grateful for the opportunity to work with Mike Avery of the Geological Society of Canada (Atlantic). His dedication to my work and success are very much appreciated. One must mention Gordon Brown and his expertise in thin section preparation. I would like to thank my fellow classmates for making this experience real and enjoyable. Finally, I would like to thank my family and friends for their everlasting support.

CHAPTER 1 - INTRODUCTION

1.1 Objectives

The purpose of this thesis is to determine the depositional environment, sequence stratigraphic relationships and provenance of the Lower Cretaceous Cummings Formation in east central Alberta (Fig. 1.1). This is done through the interpretation of the upper cored interval and lower cored interval of the Suncor well 3B-23-36-06WO4M (3B) from the Provost oil field. The provenance is determined through an investigation of the mineralogy using transmitted and reflected- light microscopy supported by X-ray diffraction (XRD). Source rock potential and thermal maturity of organic matter found within the Cummings Formation were assessed using vitrinite reflectance values and rock evaluation data. Maceral characterization is completed through the use of an incident and fluorescent light microscope. This study provides greater understanding to the complexity and ambiguity of the boundary between the Lower and Upper Mannville Group.

1.2 Geological Setting

1.2.1 A Rising Cordillera and Western Canadian Sedimentary Basin

The westward drift of the North American plate, initiated by the rifting of the Atlantic Ocean beginning in the Mid-Jurassic, created a rising Cordillera leading to the development of the Western Canadian Sedimentary Basin (WCSB) (Mossop and Shetsen 1994). This westward movement resulted in the collision of converging oceanic terranes and amalgamated super terranes from the converging plate to the west (Fig. 1.2).

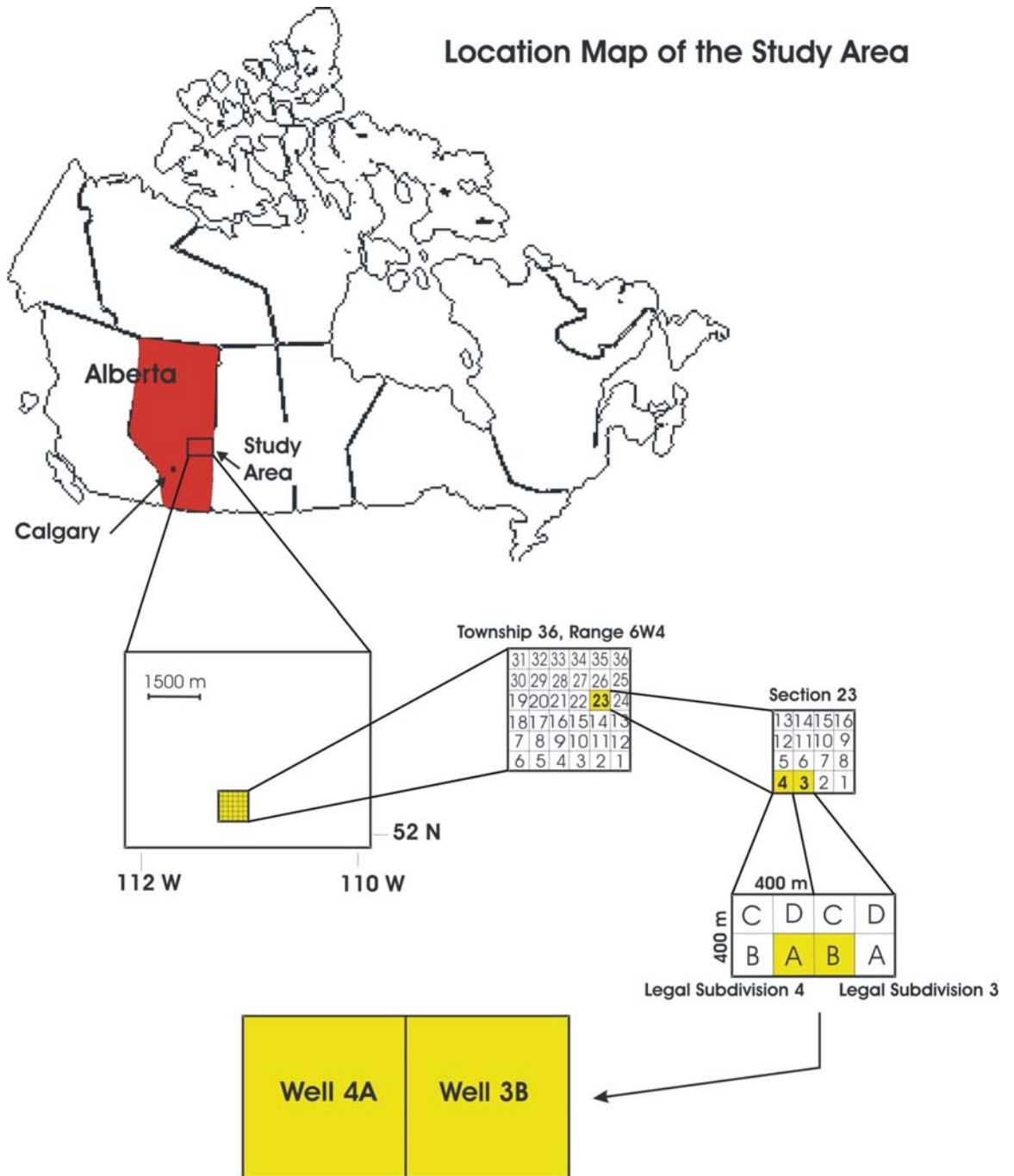


Figure 1.1- Map of the study area including location plots of the wells using the Dominion Land Survey System

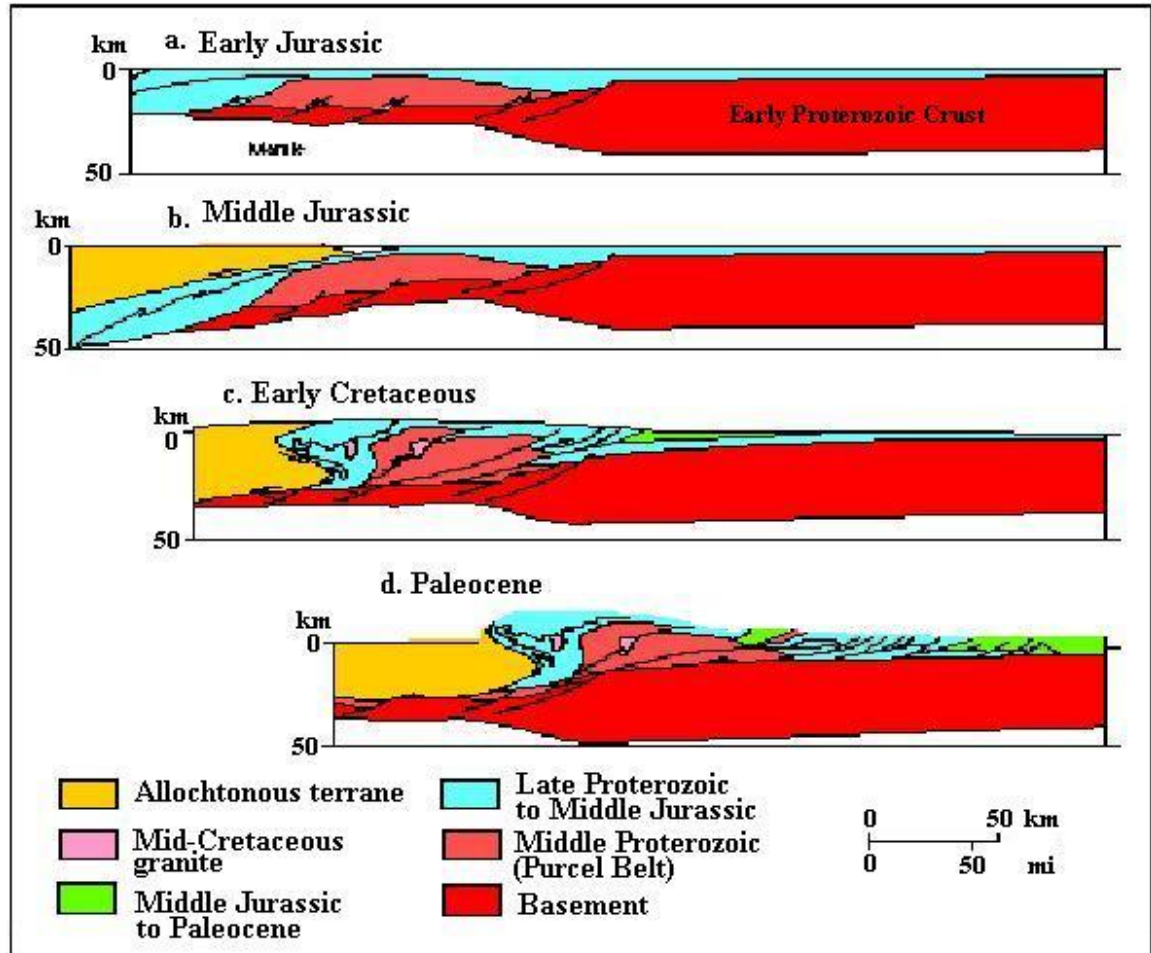


Figure 1.2- Cross sectional view of the evolution of the Rocky Mountain Foreland Thrust and Fold Belt along 49° 45' N latitude (from Mossop and Shetsen, 1994). Terrane accretion induced by a westward drift of the North American plate resulting in compressional tectonism.

Convergence resulted in compressional accretion and crustal thickening of the west coast margin (Monger and Price, 1979), inducing the early phases of the Cordilleran orogeny (Poulton 1984). Mossop and Shetsen (1994) describe the Cordillera as a collage of accreted allochthonous terranes that have been thrust and stacked in overlapping sheets over supracrustal rocks through collisional tectonism. These features are illustrated in Figure 1.2. The stacked sheets stimulated crustal thickening of the Cordillera thrust and

fold belt, generating an overpowering imbalance in isostatic equilibrium resulting in isostatic flexure of the supracrustal rocks and continental lithosphere. This flexure caused significant subsidence initiating the formation of the foreland basin to the west (Mossop and Shetsen 1994). The rise of the Cordillera coupled with increasing sedimentation rates triggered migration of the depo-axis of the foreland basin (Mossop and Shetsen 1994). The shift of the foreland basin to the northeast was comparable to a moving wave controlled by variations in subsidence driven by increased crustal thickening and increased sediment influx from erosion of the rising Cordillera (Mossop and Shetsen 1994). Topographic lows provided accommodation space for sediment transported from the rising Cordillera and the Precambrian Canadian Shield.

1.2.2 The Western Canadian Sedimentary Basin

The WCSB consists of a wedge of Mid-Proterozoic to Cenozoic strata thickening from east to west, bounded by the Cordillera to the west and the edge of the Canadian Shield to the east. The WCSB extends into the United States to the south and the Tathlina Highlands of the North West Territories to the north (Mossop and Shetsen 1994). The strata ranges in thickness from zero on the edge of the Canadian Shield to three to five km along the eastern margin of the foreland thrust and fold belt (Mossop and Shetsen 1994). As mentioned, the origin and development of the Cordillera controlled the geometry and structure of the WCSB (Price 1994). High relief and topographical positive areas within the WCSB controlled alluvial sediments flanking the eastern margin of the Cordillera as well as the sediment transport through a series of complex drainage networks during low relative sea level (Cant & Abrahamson 1996). The stratigraphy of

the WCSB is controlled by accommodation space with variations in sedimentation, subsidence, and eustasy creating multiple cycles of transgression and regression (Stott 1984). These cycles of deposition will be discussed in Sections 1.2.3 and 1.2.4.

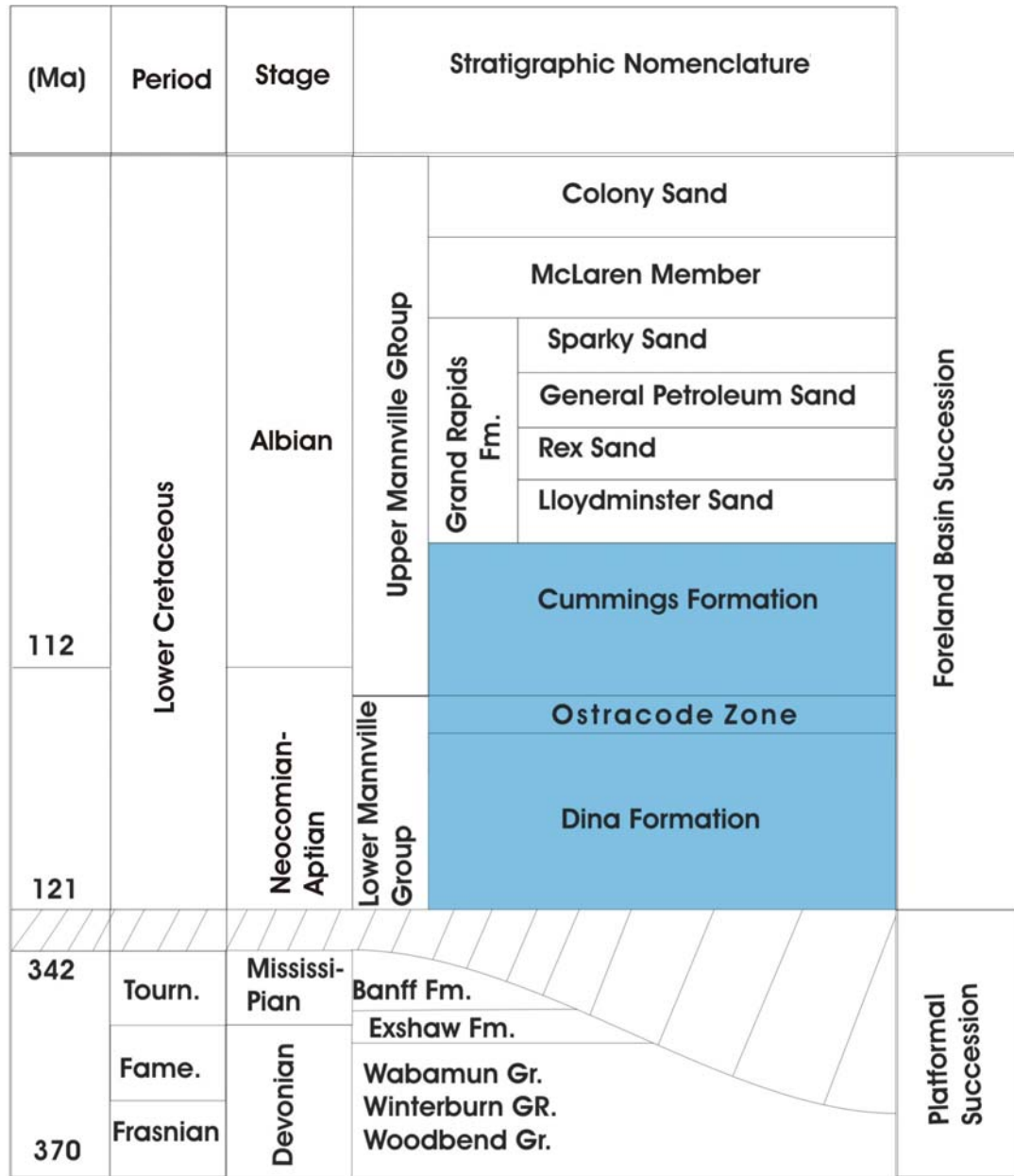
1.2.3 Stratigraphic Framework of the Western Canadian Sedimentary Basin


The WCSB can be separated into two major stratigraphic components, the platformal and the foreland basin successions, separated by an unconformity of approximately 20Ma signifying an extended period of uplift and erosion (Mossop and Shetsen 1994). The platformal succession comprises Paleozoic to Jurassic sediments deposited on the passive margin of the stable North American Craton, preceding the evolution of the foreland basin. The platformal sediments portray transgressive/regressive cycles of shale, carbonates, and shoreface sandstones (Mossop and Shetsen 1994). The overlying foreland basin successions are dominated by clastic sediments deposited during active orogenic advancement of the Cordillera from Mid-Jurassic to Oligocene. These clastic successions exhibit transgressive/regressive cycles of the western interior seaway (Stott 1984). The Cummings Formation is a part of the foreland basin succession located within the Mannville Group, discussed in Section 1.2.4.

1.2.4 Stratigraphy of the Study Area

The Stratigraphic succession of the study area described from oldest to youngest begins with Devonian to Mississippian carbonates deposited within the platformal succession on the western passive margin overlying the basement rocks of the stable North American craton (Fig. 1.3) (Christopher 1984). The upper contact of the platformal

succession is defined by a large-scale unconformity representing a second order sequence boundary as defined by Vail (1977) (cited in, Mossop and Shetsen 1994). The Cretaceous Mannville Group defines the base of the foreland succession. The Mannville Group is divided into the Lower Mannville and the Upper Mannville. As shown in the stratigraphic column of Figure 1.3, the basal unit of the Lower Mannville is the Dina Formation in the study area.



 - Infilled fields represent cored intervals and the focus Interval of this study


 - illustrates 2nd order sequence boundary marked by a large scale unconformity. Also depicts transition from Platformal to Foreland Basin Succession.

Figure 1.3 – Stratigraphic column of the study area (modified from Riediger et al 1999 and Christopher, 1999)

The Mannville Group and Dina Formation are not continuous throughout the WCSB and do not consistently represent the basal unit of the foreland basin succession. Other units such as the Bullhead Group in North-eastern B.C and in the Peace River area and the Fort St. John Group in the Liard River area represent the basal unit of the foreland basin succession (Hayes et al 1994).

According to Mossop and Shetsen (1994), the Dina Formation is accepted as Aptian in age and is the main oil producing unit in the Provost Oil Field. Fluvial incision into pre-existing Mississippian and Devonian strata during a lowstands systems tract provided space for subsequent deposition of the Dina Formation into paleo-valleys during an Aptian transgression (Cant 1996). The Ostracode Zone of the Lower Mannville was deposited during the high stands systems tract marking the maximum flooding surface during the Aptian transgression. According to Riediger et al. (1999) and Christopher (1984), the Cummings Formation lies stratigraphically above the Ostracode Zone within the Upper Mannville Group, deposited between late Aptian to early Albian. The depositional environment of this formation has been interpreted as coastal sandstones deposited during the transition from a highstand to a falling stand systems tract (Riediger et al., 1999). Riediger et al. (1999) characterizes the Cummings Formation as a shallowing-upward succession of mudstone, interlaminated mudstone with siltstone and fine-grained sandstone capped by coals and carbonaceous mudstones followed by fluvial incision during a regional regressive event.

The sediments of the foreland basin succession have been difficult to date due to the lack of biostratigraphic control particularly in the southern region of the WCSB where

fully marine conditions rarely infiltrated (Mossop and Shetsen 1994). This created ambiguous nomenclature when defining stratigraphic units, for example, according to Williams (1963) the Cummings Formation is straddling the division of the Lower and Upper Mannville groups, whereas, according to Christopher (1984) and Riediger et al. (1999) the Cummings Formation is located in the Upper Mannville. According to Cant and Abrahamson (1996) the Cummings Formation is located in the Lower Mannville. The Geological Atlas of the Western Canadian Sedimentary Basin (Mossop and Shetsen, 1994) does not subdivide the Mannville Group where the Cummings Formation is present. This study will use the stratigraphic nomenclature of Riediger et al. (1999) and Christopher (1984) presented in Figure 1.3 based on the proximity of their study areas as well as similar sequences of stratigraphic units observed within the cores described in this study.

1.3 Previous Work

The WCSB is an area with considerable oil and gas exploration. Numerous boreholes riddle the WCSB providing superior quality of geologic control. Rudkin provided a regional analysis of the WCSB in 1964 while Glaister, Williams, Mellon, Stott, and Jackson provided more geographically limited studies in 1959, 1963, 1967, 1982 and 1984 respectively (cited in Mossop and Shetsen 1994). Restricted stratigraphic intervals such as: the Moose Bar Sea deposits, Central Foothills, Deep Basin, and Lower Mannville of the Southern Plains have been studied and published by McLean and Wall (1981), Macdonald et al. (1988), Smith et al. (1984), and Hayes (1986) respectively (cited in Mossop and Shetsen 1994). More recent publications by Cant (1996) discuss the

stratigraphic framework of the Lower Mannville, whereas, Riediger et al. (1999) provides an in-depth study of the distribution and oil types found within the Mannville Group within the Provost oil field. However, the Mannville Group has been difficult to correlate on a regional scale due to the widespread lithologic heterogeneity and the lack of biostratigraphic control (Mossop and Shetsen 1994). The Cummings Formation has been mapped into Saskatchewan by Christopher (1984) and possible correlative outcrops in Manitoba, however these correlations are uncertain.

CHAPTER 2 - DEPOSITIONAL ENVIRONMENTS OF THE FORELAND BASIN SUCCESSION

2.1 Cretaceous deposition

Deposition throughout the Cretaceous can be characterized by three unconformity-bounded clastic sequences deposited in the migrating foredeep of the West Coast Sedimentary Basin (Stott, 1984). From the Late Jurassic to the Late Cretaceous, cyclic patterns of marine shale, alluvial to fluvial sandstone, prodeltaic sandstone and nearshore siltstone and sandstone are a result of transgressive/regressive successions of the Western Interior Seaway and orogenic evolution of the Cordillera (Stott, 1984). The distribution and thickness of the sediments within the WCSB can be attributed to structural controls illustrated in Figure 2.1. These controls include the rate of uplift and erosion of the Cordillera, the rate of subsidence and paleogeography of the Alberta and Williston basins, topographical highs such as the Sweetgrass and Peace River arches, dissolution of underlying limestone resulting in karst topography, and topographical lows created by dissolution of underlying Devonian salts (Mossop and Shetsen 1994).

2.1.1 First Clastic Wedge

The oldest clastic wedge of the Foreland Basin succession consists of Jurassic to Early Cretaceous sediments of the Fernie and Nikanassin formations and the Minnes and Kootenay groups (Fig. 2.2 B). Maximum development of this succession occurs in the Fernie Basin, located in the western foothills between the Smoky and Peace rivers and in southeastern British Columbia (Fig. 2.2 A) (Stott, 1984).

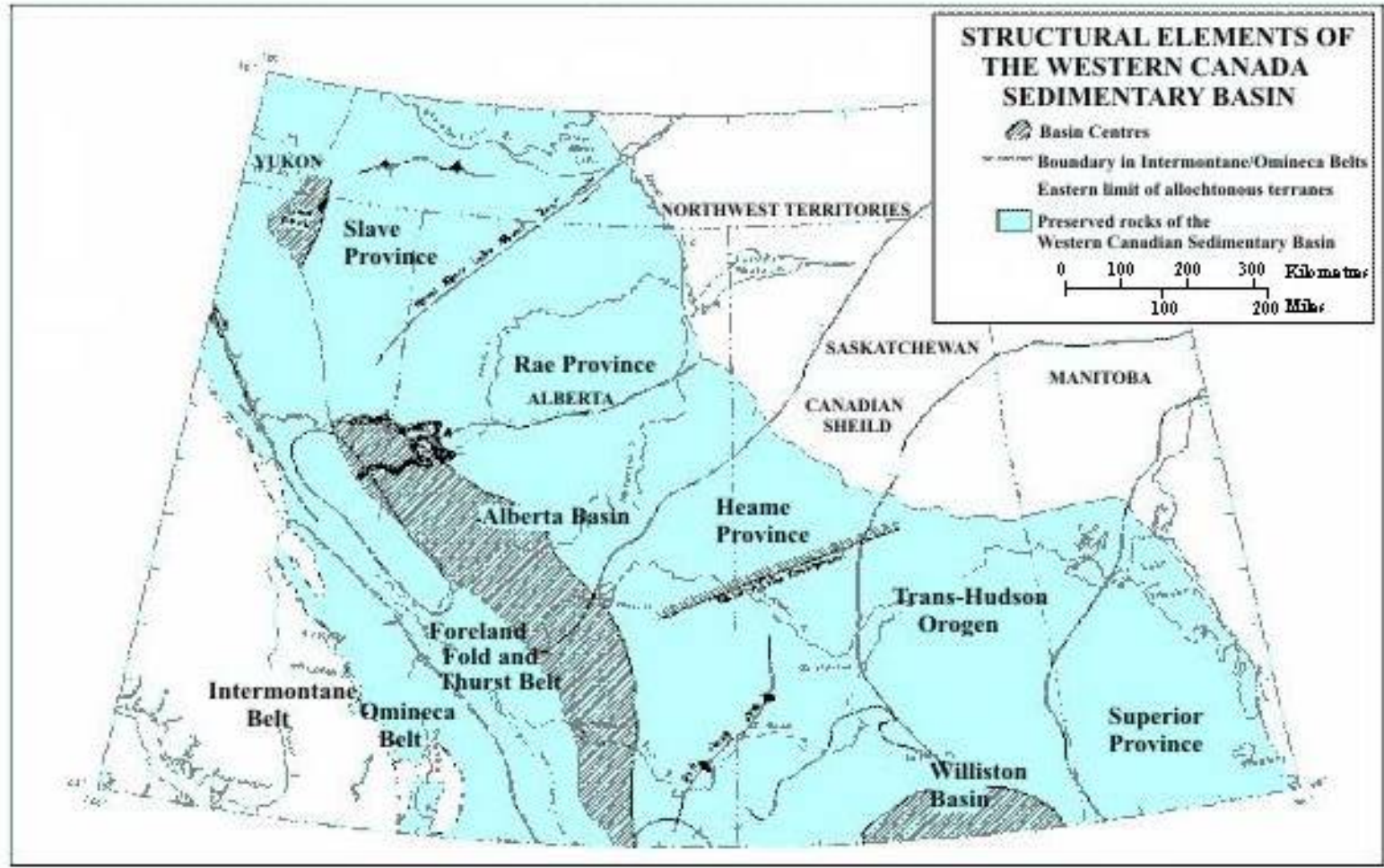
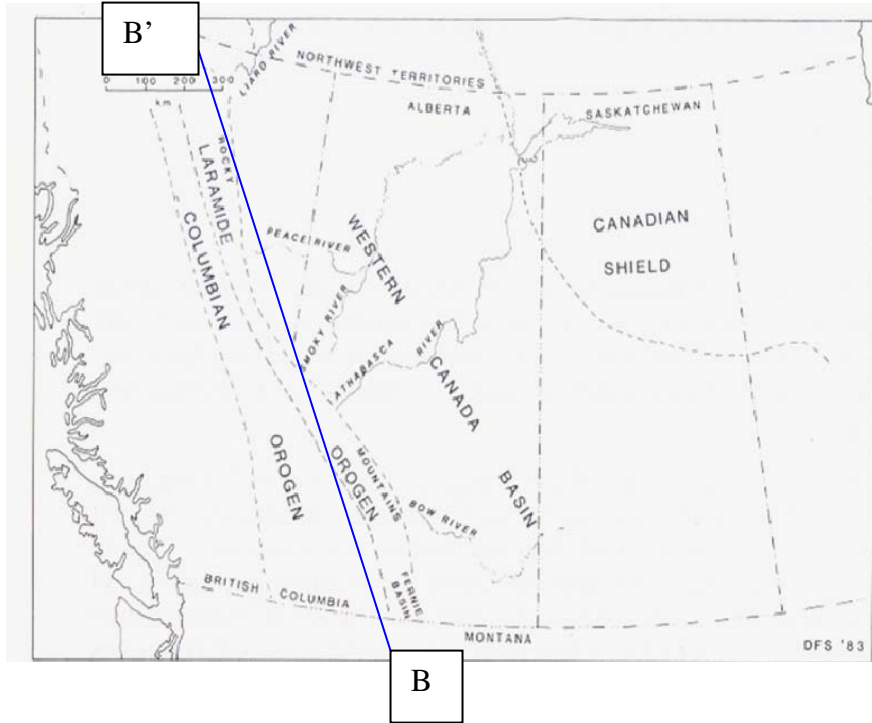


Figure 2.1 - Map of WCSB depicting structural controls creating depositional divisions during Late Jurassic to Late Cretaceous, (after Mossop and Shetsen 1994).

The thickness of this succession is approximately 2.7km in the north decreasing to zero within the eastern plains of Alberta. The total succession generally lies unconformably over Triassic rocks and is overlain unconformably by the diachronous Cadomin conglomerate within the Blairmore, Mannville and Bullhead groups (Fig. 2.2) (Stott 1984). The Fernie Formation was deposited during a regional transgression during Oxfordian time and comprises a condensed marine sequence of black shale, thin sandstone and limestone, evidently derived from the craton to the east (Stott 1984). Following deposition of the Fernie Formation, increased rates of sedimentation mark a change in source from the stable eastern craton to the western margin of the rising Cordillera (Stott 1984). Continuous sedimentation from the Cordillera resulted in deposition of the Kootenay and Minnes groups of the lowermost Cretaceous. These groups comprise of coarsening upward massive sandstone, interbedded sandstone, mudstone, and coal that are commercial seams. According to Stott (1984) these lithofacies illustrate an alluvial to fluvial plain, grading into a deltaic shoreface environment.

The sediment accumulated and filled the foredeep and the marine embayment retreated northward, exposing the southern limits of the deep basin east of the Cordillera. This exposure led to an extended hiatus in deposition from the mid to Late Valanginian through to the Late Barremian/Early Aptian, representing approximately 20 Ma of non-deposition and erosion interrupted by episodic intervals of regional deposition (Fig. 1.4) (Stott 1984).

a)



b)

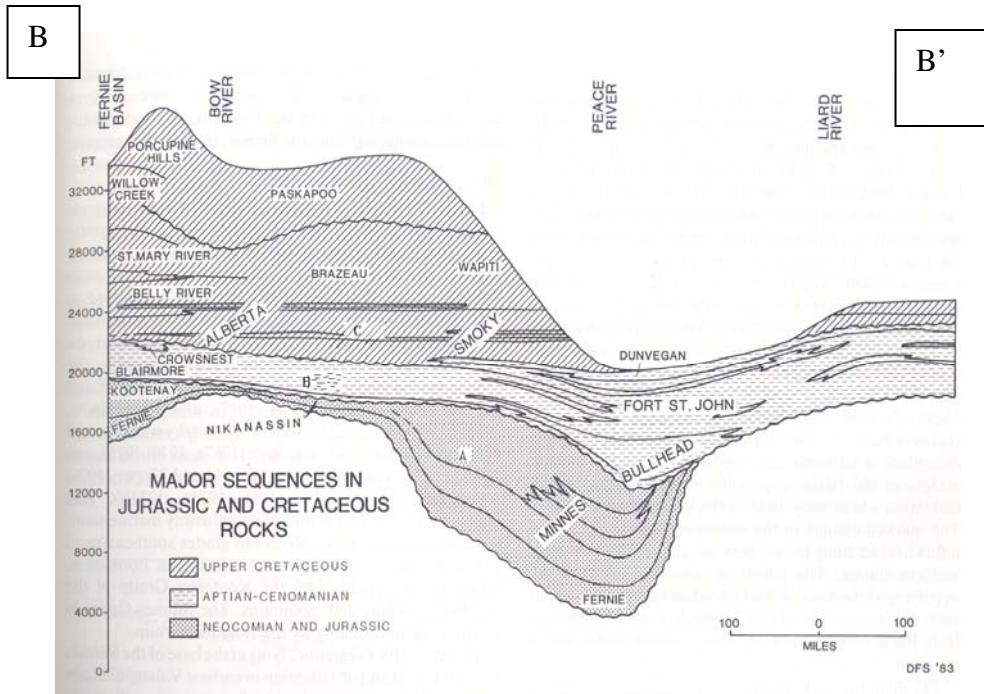


Figure 2.2 - a) Map of the WCSB showing geographic features and geological divisions. Blue line represents the cross section from B to B' depicted in figure b; a) A= first clastic wedge, B= second clastic wedge and C= third clastic wedge (after Stott 1984).

2.1.2 Second Clastic Wedge

Uplift continued along the Columbian Orogeny with renewed subsidence of the foredeep allowing for infiltration of a marine embayment and deposition of marine sediments (Stott 1984). This transgressive systems tract marked the end of a large-scale unconformity with the deposition of the second clastic wedge within the WCSB (Fig. 2.3) (Cant and Abrahamson 1996). This depositional succession comprises of the Blairmore Group of the southern and central foothills of Alberta, the Bullhead and Fort St. John Group of the Peace River area and the Mannville Group spanning from southern Alberta to east central Alberta (Fig. 2.2 b). The Bullhead and Lower Blairmore groups consist of chert-conglomerates and coal-bearing beds approximately 1km thick in the western foothills of the Cordillera decreasing to a few metres thick southward (Stott 1984). The chert-conglomerate beds grade laterally into fine-grained sandstones, then into mudstones marking an early Aptian transgression (Stott 1984). This transgression did not extend much further south than the Peace River area and is marked by a large-scale delta at the mouth of an ancestral Peace River with more deltas believed to be present along the paleoshoreline of the marine embayment (Stott 1984). The seaway was bordered in the south by poorly drained alluvial plains and extensive shallow lacustrine and estuarine environments (Stott 1984).

Following the early Aptian transgression, the Albian Fort St. John Group and the Cenomanian Dunvegan Formation (Fig. 2.2 b) represent four transgressive/regressive cycles within the second clastic wedge (Stott 1984). The first cycle deposited about 400

m of marine shale and extended westward beyond the present day foothills of north eastern B.C. and southwest into the WCSB. Studies by Hopkins et al. (1982) suggest that the embayment may have extended into the northwestern U.S. (Stott 1984). Delta front sandstones, overlying marine shale, on the western margin of the WCSB mark the transition from transgression to regression terminating the first cycle within the Fort St. John and Upper Blairmore groups (Stott 1984).

The second cycle is marked by a 400m thick marine shale overlain by delta front and prodeltaic sandstones deposited at Liard River (Fig. 2.2) (Stott 1984). The extent of the marine shale suggest that the southward advancing marine embayment only extended as far south as Smoky River in the foothills of the Cordillera (Stott 1984).

The third transgression within the Albian Fort St. John Group and the Cenomanian Dunvegan Formation proved to be the most extensive and is believed to have connected the Boreal Sea to the north with the Gulf of Mexico to the south (Stott 1984). This transgression deposited a 1.1km thick succession of marine shale overlying pre-existing shore face and terrestrial sediment, while two autonomous regressive lithofacies suggest two distinct phases of regression within this cycle (Stott 1984).

The fourth transgression/regression cycle exhibits shifts in the paleoshoreline position (Stott 1984). The changes in shoreline position, basin configuration and complex depositional history can be attributed to tectonic movement resulting in fluctuations in sediment supply and subsidence of the migrating foredeep (Mossop and Shetsen 1994).

Early Aptian: (Cadomin, Ellerslie, Dina, Gething Paleogeography

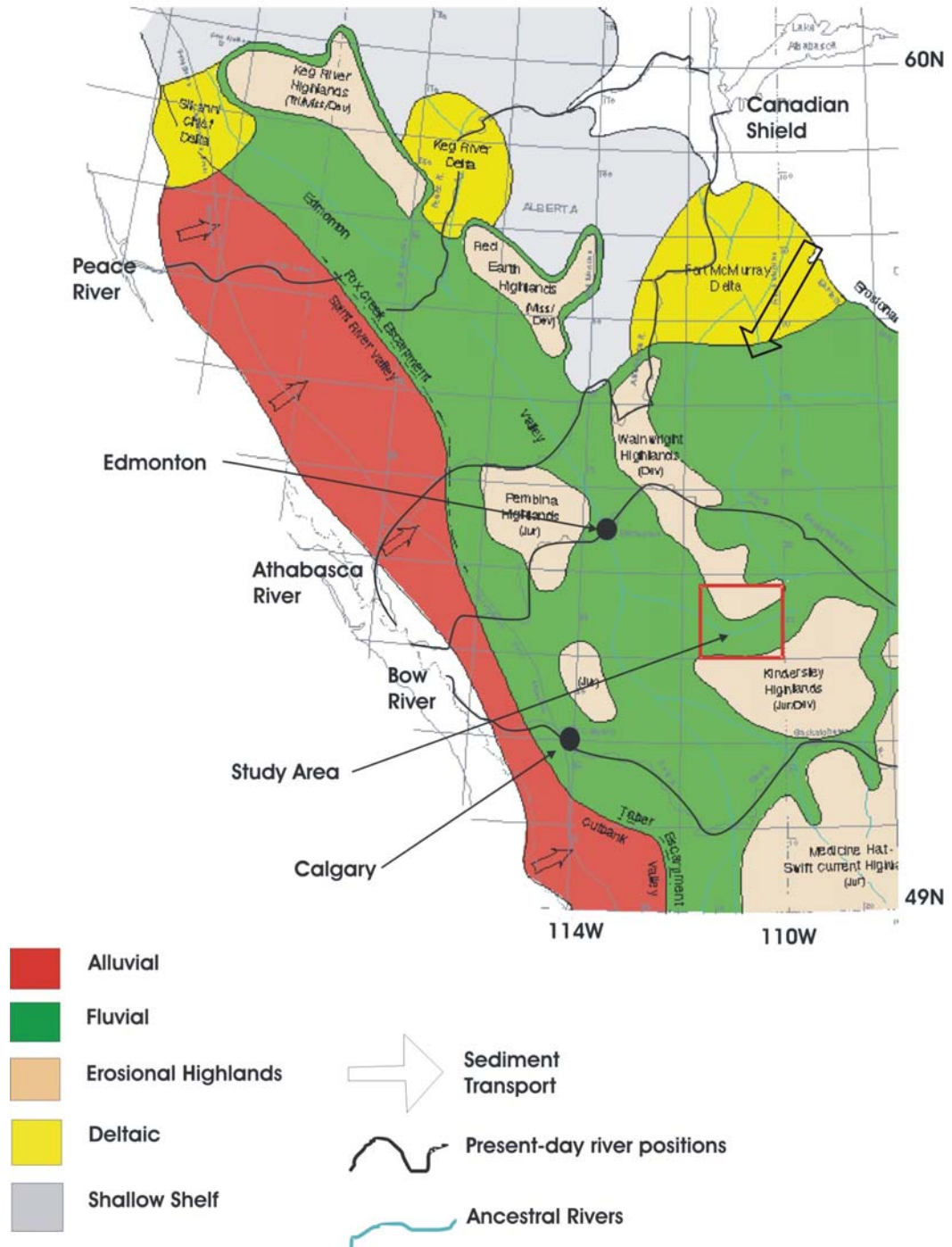


Figure 2.3 - Paleogeography of Alberta and the study area during early Aptian (after Mossop and Shetsen, 1994)

Late Aptian to early Albian paleogeography: (Calcareous, Ostracod, Cummings)

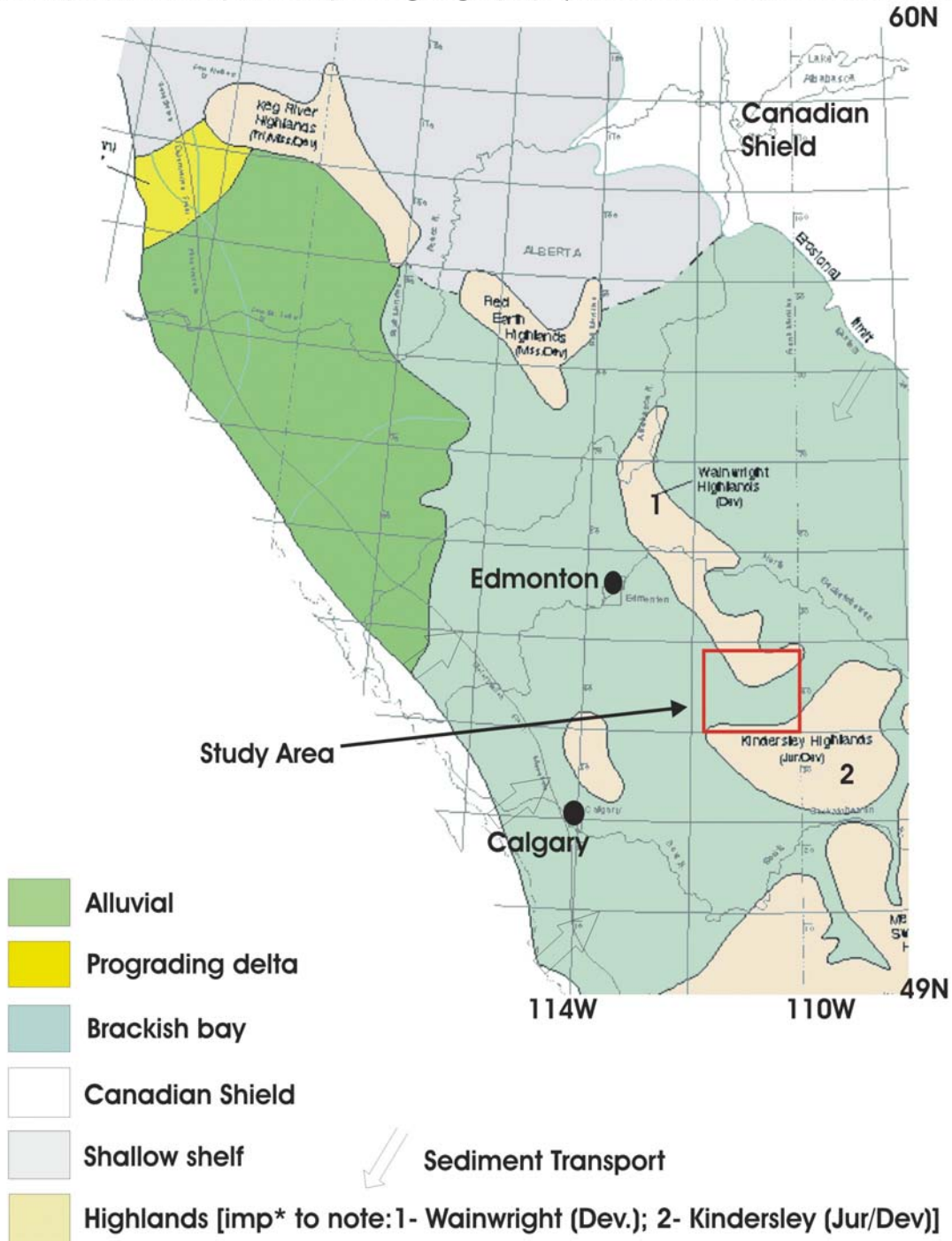


Figure 2.4 - Paleogeography of Alberta and the study area during late Aptian to early Albian (after Mossop and Shetsen, 1994) with modifications from the result of this study.

2.1.3 Third Clastic Wedge

The third clastic wedge consists of Upper Cretaceous strata with thicknesses up to 4km in the western foothills of the Cordillera thinning to 1.2km in the Alberta Plains (Fig. 2.2 B). The Alberta and Smoky groups lay unconformably on the Blairmore Group in the south and the Dunvegan Formation in the north (Stott 1984). These strata consist of thick basal marine shales overlain by terrestrial sediments deposited following the mid-Campanian. Upper Cretaceous sediments overlain by Paleocene sediments are assigned to the Upper Willow Creek, Porcupine Hills and Paskapoo formations (Stott 1984). The third clastic wedge is located stratigraphically above the focus interval of this study, and will not be discussed in detail.

2.2 Mannville Deposition

Interpretation of the stratigraphic columns from Christopher (1984), Cant and Abrahamson (1996) and Riediger et al (1999), suggest the transgressive/regressive cycle of the Mannville Group, (Figs. 2.3 and 2.4) can be correlated to Stott's early Aptian transgressive/regressive cycle within the second clastic wedge. The Lower Mannville consists of non-marine fluvial sediments, incised valley fill and coal seams accompanied by coastal to shoreface sandstones (Cant and Abrahamson 1996). Deposition is a function of relative sea level and structural controls, which define paleodrainage networks responsible for eroding transporting and depositing sediment. Figures 2.6 and 2.7

illustrate interpretive maps created by Williams (1963) and Cant and Abrahamson (1996) exhibiting paleotopography of the basal unconformity surface. These maps display paleotopography resulting in drainage divides, which control provenance, transportation and deposition throughout the basin.

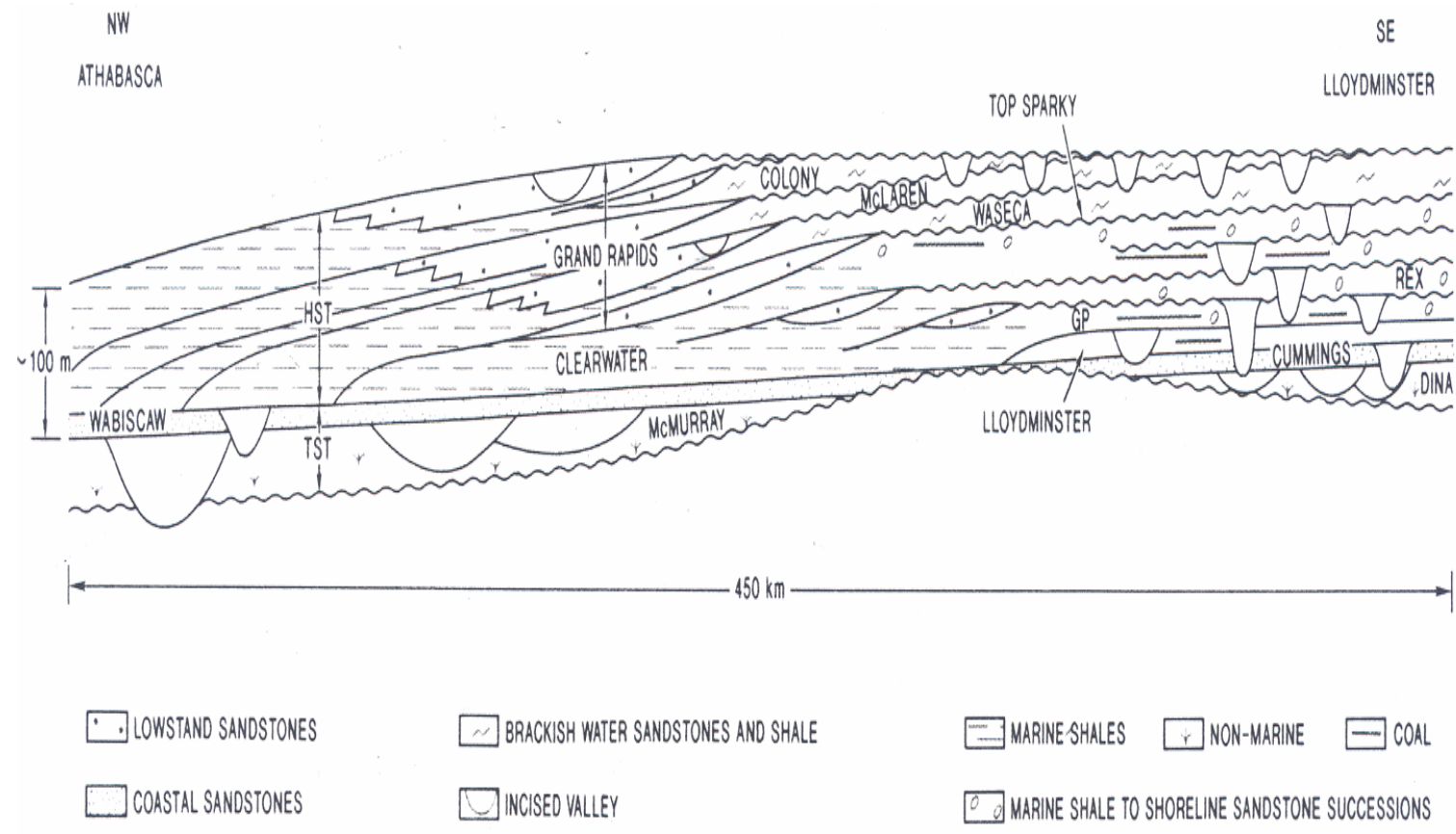


Figure 2.5 - Cross sectional view of sequence stratigraphy relationships including transgression and highstand systems tract (TST and HST) of the Cretaceous Mannville Group (from Cant and Abrahamson, 1996).

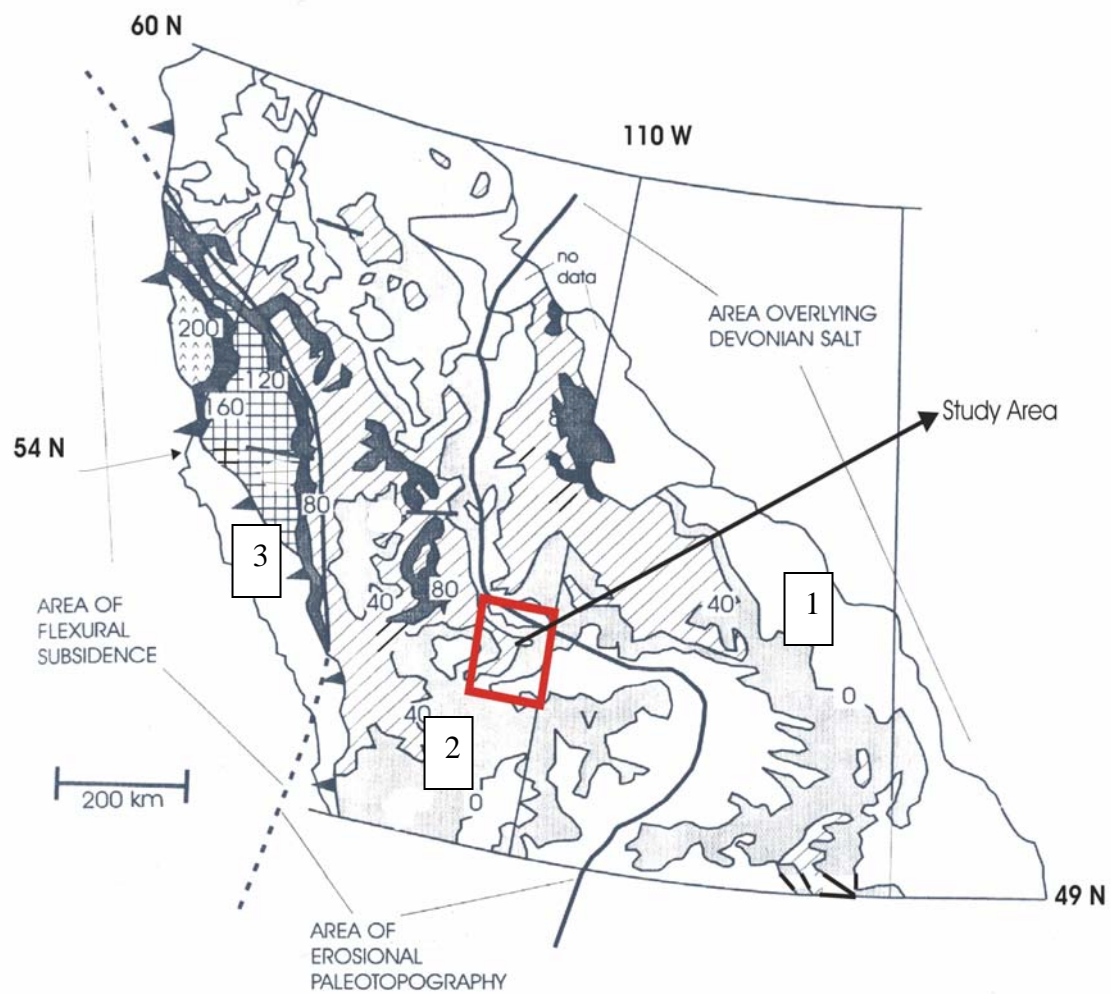


Figure 2.6 – Isopach map of the transgressive systems tract of the basal unconformity showing structural controls. Contour intervals are in meters. 1) Eastern basin extending from Saskatchewan into Alberta overlying Devonian salts; 2) area of erosional paleotopography, central zone with incised valley fill and non-depositional uplands; 3) area of flexural subsidence due to compressional tectonism and the rising Rocky Mountains (after Cant and Abrahamson, 1996).

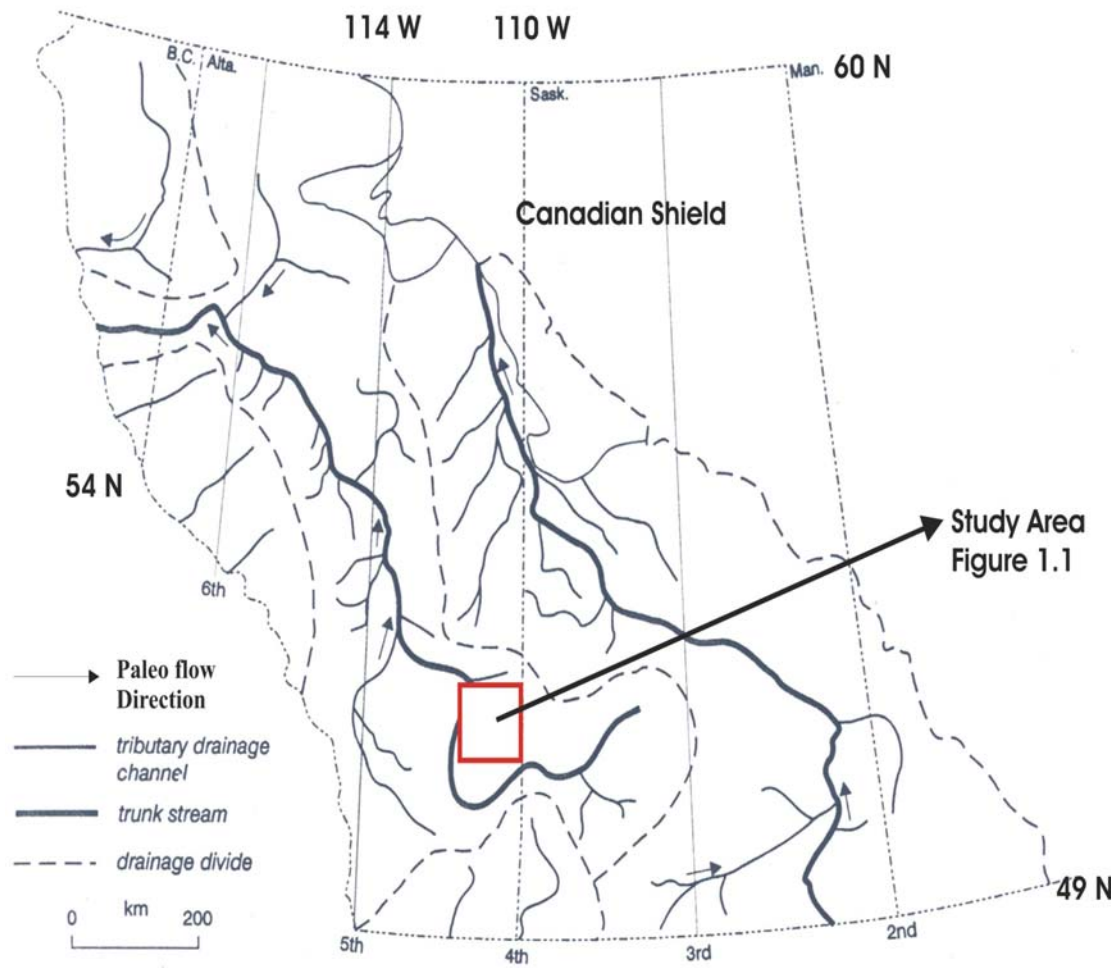


Figure 2.7 – Interpretive map of drainage networks on the basal unconformity of the foreland basin succession, derived from isopach map in figure 2.6 (after Cant and Abrahamson, 1996).

CHAPTER 3 - METHODS

3.1 Methods

3.1.2 Core descriptions

The Canadian Society of Petroleum Geologists in Alberta and Petrol Roberts in donated three cored intervals from two separate wells. Well 3B-23-36-06WO4M (3B) is comprised of two cored intervals termed “upper” (905.00-918.15m) and “lower” (918.25-933.25m) revealing a separation of 10cm. These cored intervals consist of the Cummings Formation, the Ostracode zone and underlying Dina Formation. Only the upper cored interval (Cummings Formation) of well 3B and the top 1m of the lower cored interval representing the Cummings Formation is described in detail within this thesis. The lower core of 3B and 4A was previously discussed in a detailed analysis of the Dina Formation by Joe Kidston in 2003. The lower contact of the Cummings Formation is important and will be discussed later in Chapter 5. Similarly, well 4A-23-36-6W4 (4A) consists of one cored interval only including approximately 1m of the Cummings Formation.

Description of the upper core from Well 3B is presented in Chapter 4. The upper core of well 3B is 13.15m long contained in 6 boxes, whereas, the lower-cored interval is approximately 15m long contained in 7 boxes. The core within well 3B totals 28.15m. Both cores are split into 8cm surfaces and mostly remain in good condition. Some intervals are broken and missing while others appear to have been previously sampled. This study adds to Kidston’s (2003) study of the underlying Dina Formation while presenting an exceptional opportunity to study 30m of continuous core.

Core description sheets with legend are attached in Appendix B. Each core description sheet provides 2cm resolution resulting in 2m of core per sheet. Description sheets document grain size, lithology, surface descriptions, laminae geometry, sedimentary structures, bioturbation and interpretation of lithofacies, and depositional environments. Detailed photographs of defining sedimentary structures are provided in Chapter 4. Plates of the cored intervals are in Appendix A.

3.1.3 Transmitted and reflected-light microscopy

Three polished thin sections were prepared for analyses from the upper core from well 3B. Thin sections are labelled 3B-1, 3B-2, and 3B-3 and were sampled at depths of 917.23 m, 911.08 m and 906.15m respectively. Thin sections provided from previous studies are labelled 7, 8, and 9 and sampled at depths 911.40, 910.60 and 905.00 m respectively. Thin sections were cut and prepared at Dalhousie University by Gordon Brown. Observations and results of mineralogy through a transmitted and reflected-light microscope are presented in Chapter 4.

3.1.4 X-ray diffraction

Three samples from the upper core of well 3B were analyzed using X-ray diffraction. The purpose of this method is to determine the composition of clay particles, composition of cement, and to confirm mineralogical observations obtained under the transmitted and reflected microscope. The samples were prepared from remaining core following the cutting of thin sections. The first XRD sample corresponds to thin section 3B-1 at a depth of 917.23m. The second XRD sample corresponds to thin section 3B-2 at

a depth of 911.08m. The third XRD sample corresponds to thin section 3B-3 at a depth of 906.15m. The samples were ground up with a mortar and pestle into the appropriate grain size, then formed into dry mounts, and placed into the XRD machine for analysis. The results from these measurements are in Table 2 and Appendix C accompanied by spectral plots presented in Chapter 4.

3.1.5 Vitrinite Reflectance

Two whole rock samples from the upper core of well 3B were prepared at the Bedford Institute of Oceanography (BIO) to analyze the organic material through maceral characterization and thermal maturity based on vitrinite reflectance values. One oil stained sample from the underlying Dina Formation (Well 4A) was also sampled. However, due to heavy oil staining no representative reflectance values could be obtained therefore will not be discussed in this thesis. Samples were prepared under the supervision of Mike Avery of the Geologic Survey of Canada (Atlantic Division). Sample 1 consisted of organic-rich rubbly shale ranging in depth from 907.48 to 907.89 m. Sample 2 consisted of sandstone with laminations of detrital organic material from depths ranging from 910.13 to 910.23 m.

Preparation commenced by crushing the organic matter samples to approximately 500 micrometers (10-20 mesh) grain size, split to form a representative sample, then prepared as 2.5 cm (1") diameter plastic stubs to fit the polisher. Two stages of fix material (epoxy resin) were then added in preparation for polishing. The samples were then polished with diamond-based suspension to obtain a low relief, scratch-free surface for examining under an oil lens with incident and fluorescent light at

approximately 1000x magnification in order to interpret the maceral composition source rock potential. Sixteen Vitrinite Reflectance measurements were taken from both samples and presented in Table 3 of Chapter 4. Representative digital photos are also presented in Chapter 4.

Both organic samples 1 and 2 were also used for Rock Evaluation (Rock Eval). The rock evaluation was conducted by Dr. Hans Wielens of the Geological Society of Canada (Atlantic). This data provides total organic carbon (TOC), max temperature (Tmax) values concerning the thermal maturity of the Cummings Formation discussed in Chapter 5. Rock evaluation data is presented in Appendix D.

CHAPTER 4 - RESULTS

4.1 Core Descriptions

The upper core of well 3B consists entirely of the Cummings Formation. The lower contact is located at 918.33 m, within the lower core of well 3B, and was previously described by Kidston (2003). Kidston (2003) described the basal contact of the Cummings Formation in well 3B as a fining-upward, poorly sorted pebble conglomerate defining the basal lag of a fluvial channel. However, well 4A also described by Kidston, only separated by 500m to the west, reveals the basal contact of the Cummings Formation as a sandy siltstone with wavy contorted bedding characteristic of a shallow marine embayment. This will be discussed further in chapter 5.

The upper core of well 3B is described in this chapter in terms of lithofacies. Table 1 identifies each lithofacies and their cumulative thicknesses throughout the cored interval. Figure 4.1 depicts the summary of the upper core of well 3B. Detailed core description sheets are presented in Appendix B. Detailed photos of defining sedimentary and biogenic structures are presented at the end of this chapter through plates 1 to 9 and also in Appendix A.

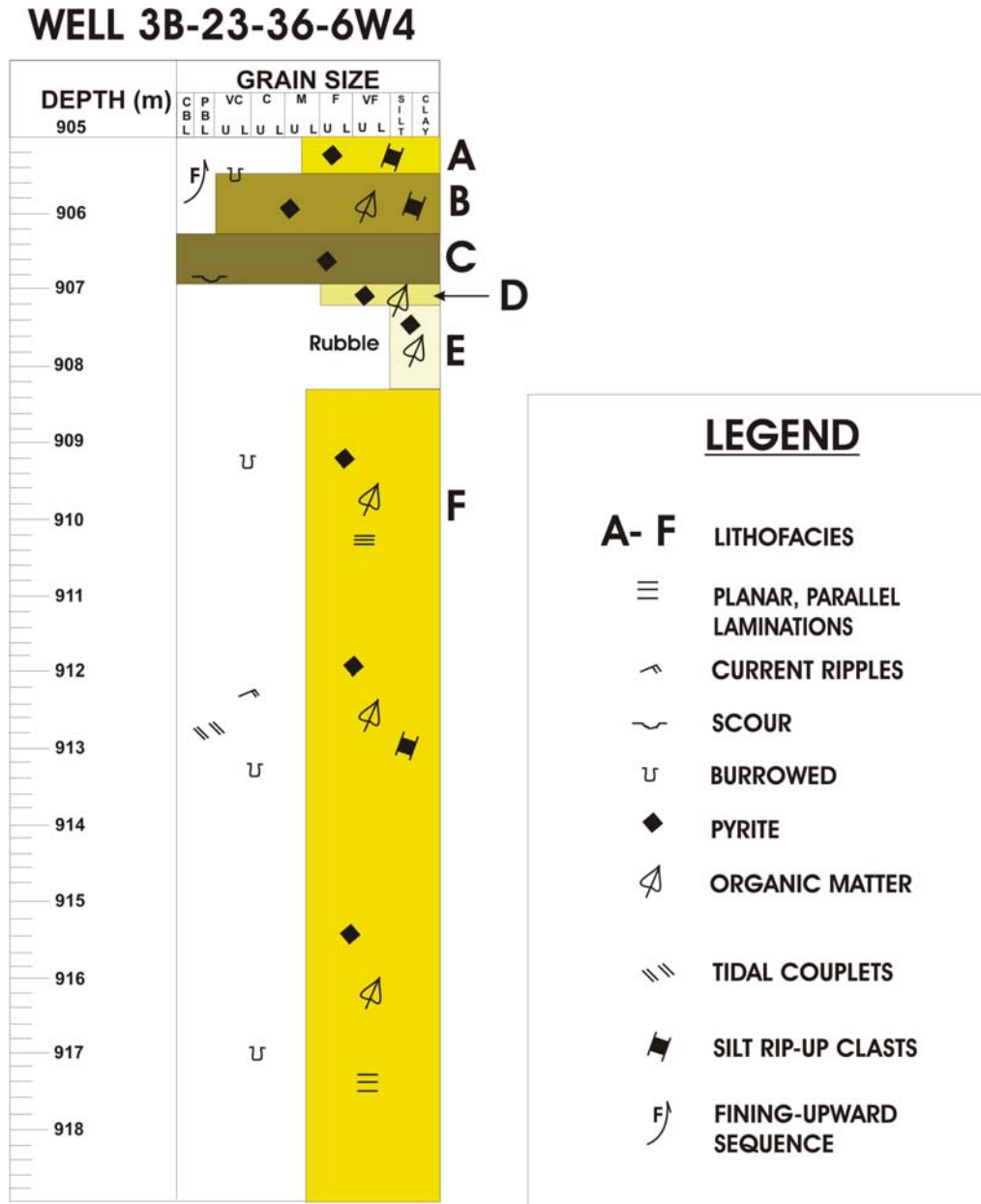


Figure 4.1 – Core summary of the upper cored interval of well 3B. Detailed core descriptions available in Appendix B. Colours give a rough sense of grain size (pale = fine-grained, dark = coarse-grained material).

Box number	Depth (m)	Lithofacies (A – F)	Thickness (m)	Cumulative Thickness (m)
1	905.00 – 905.65	A. Fine (upper) to medium (lower) grained sandstone with rare matrix supported clasts	0.65	0.65
1	905.65 – 906.30 (core break)	B. Fining upward, poorly sorted imbricated granule sized clasts supported by medium (upper) grained sandstone	0.65	1.30
1	906.30 – 906.90 (core break)	C. Poorly sorted conglomerate with granule to cobble size clasts.	0.60	1.90
1	906.90 – 907.30	D. Micro-faulted, coarsening upward very fine (upper) to fine (lower) grained sandstone with parallel laminations of fine (upper) siltstone.	0.40	2.30
2	907.30 – 908.58	E. Rubbly organic-rich siltstone with rare very fine (lower) grained wavy sand drapes and siderite concretions.	1.28	3.58
2 - 6	908.58 – 918.15 (core break)	F. Cleaning upward cycles of parallel laminated, bioturbated, fine (lower) to medium (upper) grained sandstone with abundant sulphides and wavy contorted laminations of organic matter.	9.57	13.15

Table 1 – Identified lithofacies, with corresponding box location and thicknesses within core 3B. Cumulative thickness depicts total length of core (13.15 m). Letters A – F pertain to lithofacies descriptions in the following sections. Note missing core locations assumed from core breaks and lithofacies' boundaries.

4.1.1 Lithofacies F: 908.58 – 918.15 m

This lithofacies is characterized by cleaning upward cycles of light grey sandstone with abundant laminations of organic matter. Grain size ranges from fine (lower) to medium (upper) typically remaining consistent throughout the lithofacies.

Organic matter is rare to common at the base becoming more abundant towards the top. The organic matter demonstrates fine-scale cyclic patterns. Each cycle is defined by an abundance of organic laminae at the base grading upwards into cleaner sandstone. Interlaminated organic material and sandstone observed over approximately 60% of the lithofacies exhibit parallel planar to wavy laminae geometry with dips ranging from 0° to 35°. Laminations range in thickness from mm scale to approximately 2 cm. Minor sections comprising of mud drapes with lenticular bedding and a finer grained (very fine upper) bed of silicified sandstone are also observed within this lithofacies (see core description sheets in Appendix B).

The extent of cementation fluctuates through the lithofacies due to cement composition and diagenetic processes. No reaction with HCl was observed suggesting the presence of siliceous or non-reactive carbonate cement, possibly ankerite. Cement composition and porosity will be discussed later within the mineralogy and XRD sections of this chapter.

As cycles grade to cleaner sandstone, more sedimentary structures become visible. These relatively clean sandstones reveal sharp scoured surfaces demonstrating reactivation, minor elongated silt rip-up clasts with sand drapes, similar to lithofacies E, and current ripples lined with organic matter and dark silty material (Plate7). Tidal

influence is evident through the presence of tidal bundles with a possible location at 911.69 m and very well conserved set of couplets at 916.82 m with approximately 28 observable couplets (Plate 6).

Concretions of marcasite with sizes ranging from mm scale to 10cm in diameter are observed, as well as coarse (granule sized) concretions of pyrite with circular reaction rims or halos (Plate 5). Sulphides occur more readily in association with the laminations of organic matter and are abundant throughout the lithofacies suggesting reducing conditions.

Biogenic structures are common within this lithofacies. These structures include trace fossils from the *Skolithos* and *Cruziana* (*Planolites*) ichnofacies (Plate 4). *Skolithos* burrows are common toward the top of the lithofacies in sections of high sand content and range in scale from 1cm to 5cm in length. The *Skolithos* burrows are infilled with finer grained sandy material. *Planolites* are common throughout and appear to have a strong association with the laminations of organic material. Bioturbation index (see core sheet legend) varies from 0 to 3, which in certain areas deforms the organic laminations.

The upper contact of this lithofacies is sharp and planar with abundant preserved biogenic sedimentary structures lined and infilled with silty material (Plate 3). The lower contact is located within the lower core of well 3B. Discussion of this contact will be discussed later in chapter 5.

4.1.2 Lithofacies E: 907.30 – 908.58 m

Due to the rubbly nature of this section of the core it is difficult to observe continuous structures throughout the lithofacies, thereby presenting difficulties in making a complete description.

Lithofacies E is characterized by rubbly, organic-rich dark grey to black siltstone with rare very fine (lower) grained grey wavy sand drapes ranging in thickness from mm scale to 2cm. Some drapes include minor granule size clasts of light grey sandstone. The cement does not react with HCl suggesting siliceous or non-reactive carbonate cement (ankerite). This lithofacies exhibits no evidence of preserved biogenic sedimentary structures. A continuous siderite concretion (5cm thick) marks the lower contact of this lithofacies and minor concretions are found throughout. The upper contact is not present due to missing core at the core break.

4.1.3 Lithofacies D: 906.90 – 907.30 m

Lithofacies D is characterized by micro-faulted, coarsening upward very fine (upper) to fine (lower) grained grey sandstone with parallel laminations of fine (upper) dark grey siltstone.

Laminations of sandstone and siltstone typically 0.5cm thick, display a horizontal planar parallel laminae geometry, which is highly disturbed by listric-style microfaulting throughout the lithofacies.

No observable reaction occurred with HCl suggesting the presence of siliceous or non-reactive carbonate cement (ankerite).

Minor amounts of organic particles are found within the upper (coarser) margin of this lithofacies. No evidence of preserved biogenic sedimentary structures are observed. The core representing this lithofacies is also in poor condition. A large portion is believed to be lost due to fracturing perhaps due to drilling and handling or intermediate faulting resulting in the missing core.

4.1.4 Lithofacies C: 906.30 – 906.90 m

Lithofacies C is characterized by a reddish brown poorly sorted conglomerate with subrounded to subangular granule size clasts supported by a poorly sorted coarse (upper) to medium (lower) grained grey-brown sandstone.

This lithofacies is in poor condition and a majority is assumed to be lost due to reasons stated above. The small amount of remaining core is structureless and shows no imbrication of clasts and no evidence of preserved biogenic sedimentary structures.

The upper contact is lost at the core break and there is probably missing core. The basal contact is scoured and represents an erosional surface with flame structures and load casts immediately above the contact.

4.1.5 Lithofacies B: 905.65 – 906.30 m

Lithofacies B is characterized by fining upward sequences of poorly sorted imbricated angular granule sized silt rip-up clasts supported by a medium (upper) grained

light grey sandstone matrix interbedded with clean medium (upper) grained grey sandstone.

The base of granule beds display erosional scoured surfaces marking reactivation. Bed thicknesses vary from 10 cm to mm scale lamination sets interbedded with clean grey sandstone. Laminae geometry is planar parallel with some evidence of rippled or wavy surfaces dipping from 0° to 10° (Plate 2).

No observable reaction to HCl suggesting siliceous or non-reactive carbonate cement. No evidence of preserved biogenic sedimentary structures are present, however, rare particles of organic matter lining lamination surfaces are observed.

The lower contact is lost at the core break. The upper contact of this lithofacies is gradational over approximately 10 cm into lithofacies A as granule sized silt rip-up clasts become less abundant with increasing amounts of medium (upper) to (lower) grained sandstone.

4.1.6 Lithofacies A: 905.00 – 906.65 m

Lithofacies A is characterized by coarsening upward light grey sandstone with grain size varying from fine (upper) to medium (lower).

The laminae geometry is defined by planar parallel laminations at the base changing to wavy and back to planar parallel at the top, typically dipping at <5°. Laminations are typically less than 1 cm in thickness and defined by rare traces of elongated particles of organic matter with rare angular to subangular granules (0.5 – 3.0 cm in diameter) with matrix-supported silt rip-up clasts (Plate 1).

No reaction was observed when HCl was applied to the face of the core suggesting siliceous or non-reactive carbonate.

No sulphide mineralization is visible; however, the presence of a reddish- brown siderite concretion lining the lamination plane 2.5cm thick located at approximately 905.20 m is observed.

Biogenic sedimentary structures are rare to non-existent within this lithofacies and can be attributed to the trace fossil ichnofacies *Skolithos*. Possible vertical *Skolithos* burrows are located within the planar parallel laminations of this lithofacies.

4.2 Thin Section Mineralogy

This section describes the observations made with transmitted- and reflected- light microscopes. Three thin sections were prepared and described from well 3B at locations; 3B-1 at a depth of 917.23m (lithofacies F), 3B-2 at a depth of 911.08m (lithofacies F including organic laminae), and 3B-3 at a depth of 906.15m (lithofacies B including granule sized silt rip-up clasts). Each thin section was prepared using blue epoxy to visually enhance the pore spaces for analyses. Table 2 summarizes the data obtained from these samples and also includes XRD data from the three locations mentioned above. These observations provide the basis for a discussion concerning the provenance of the Cummings Formation in Chapter 5. The descriptions of the thin sections will begin at the lowest sample interval then move upward.

Location on core 3B	Transmitted-light microscope	Reflected-light microscope	XRD	Bulk mineralogy
3B-1 917.23m	Quartz and orthoclase cemented by ankerite and silica. Chert fragments.	Pyrite, marcasite accessory illmenite	Quartz, kaolinite, orthoclase microcline, illite	Quartz and orthoclase cemented by ankerite and silica. Chert fragments. Pyrite, marcasite accessory illmenite
3B-2 911.08m	Quartz and orthoclase cemented by ankerite and silica. Chert fragments	Pyrite, marcasite accessory illmenite	Quartz, ankerite, kaolinite, orthoclase, clinochlore, illite, albite	Quartz and orthoclase cemented by ankerite and silica. Chert fragments Pyrite, marcasite accessory illmenite kaolinite, illite, albite
3B-3 906.15m	Quartz, orthoclase cemented by ankerite and silica. Fragments of radiolarian chert plagioclase	Pyrite, marcasite accessory illmenite	Quartz, ankerite, kaolinite, aragonite, orthoclase, illite, albite, microcline	Quartz, Plagioclase orthoclase cemented by ankerite and silica. Fragments of radiolarian chert Pyrite, marcasite accessory illmenite kaolinite, aragonite, illite, albite, microcline

Table 2 – Summary of mineralogy observed within the upper cored interval of well 3B using various analytical techniques

4.2.1 Transmitted and reflected-light microscope observations

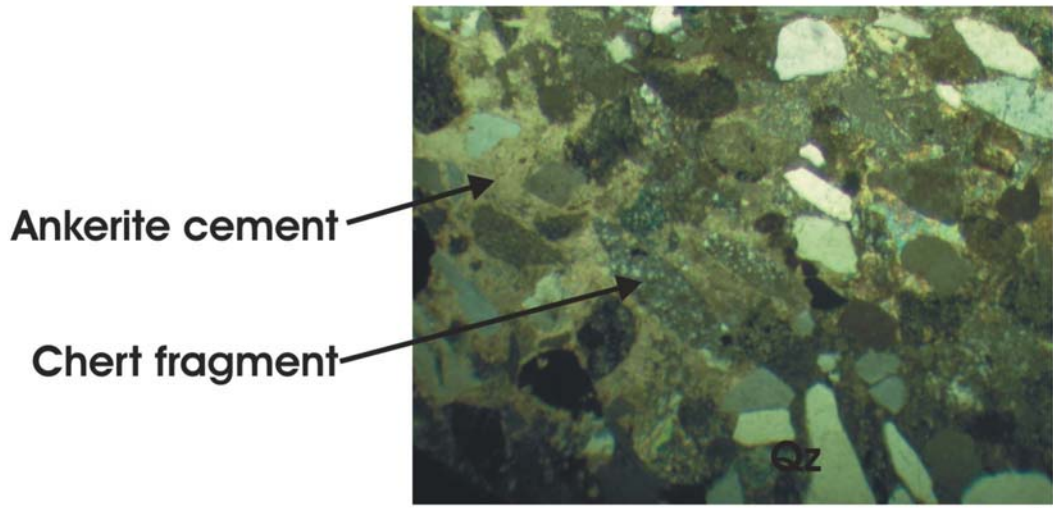
Thin section 3B-1 (917.23 m) – Lithofacies F - This sample comprises approximately 30 to 40% grains, supported by ~60 to 50% cement with porosity accounting for 10% of the entire thin section. Subrounded to subangular grains of quartz and feldspar (mostly orthoclase) are dominantly supported by silica cement with minor amounts of ankerite. This thin section exhibits coarser grains than samples 3B-2 and 3B-3 (Fig. 4.2). Approximately 65% of the cement is comprised of silica while sporadic rhombic ankerite composes the remaining 35%. Typical detrital fragments of chert are observed as well as quartzite rock fragments. Visible overgrowth textures appear on several quartz grains demonstrating optical continuity during mineral growth. Accessory tourmaline grains were also observed. The remaining minerals consist of ~5% clays and <5% opaques with minor plagioclase of the 30 to 40% grains.

The opaque minerals within this thin section are characterized by marcasite and pyrite grains. Marcasite was defined by its elongate to rhombic shape whereas pyrite is identified by its cubic outlines. Both opaque minerals have varying grain size (<0.5 to <1mm). Accessory ilmenite was identifiable from lamellar twinning, a relict texture still apparent within the ilmenite grains.

Figure 4.2 – Detailed photos of bulk mineralogy of thin section 3B-1 (907.23m) of lithofacies F.

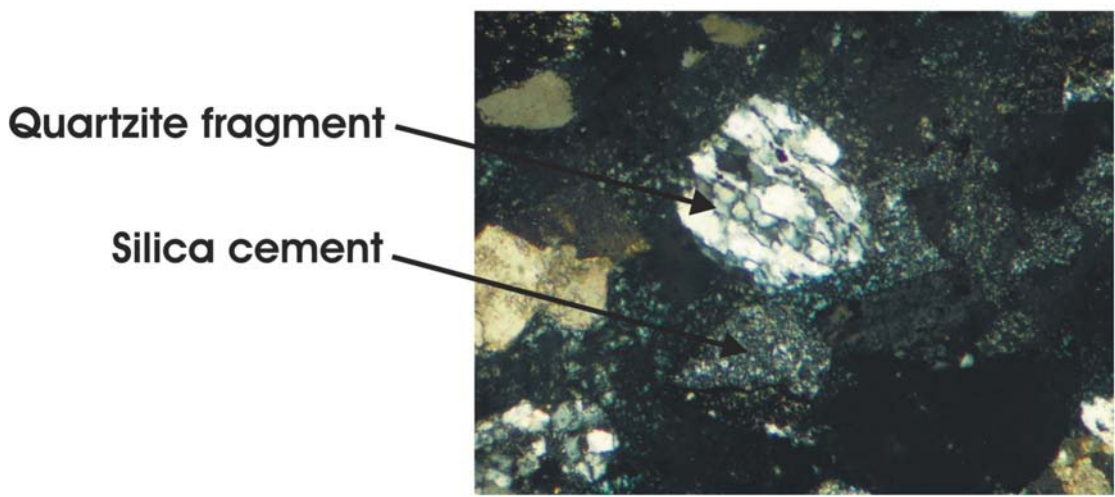
- A) Chert fragment with associated ankerite cement. Note the grain size with respect to samples shown below.
- B) Quartzite fragment supported by silica cement. Note the fused boundaries between quartz grains within the rock fragment.

Sample 3B-1 (917.23 m)



A)

0.35mm



B)

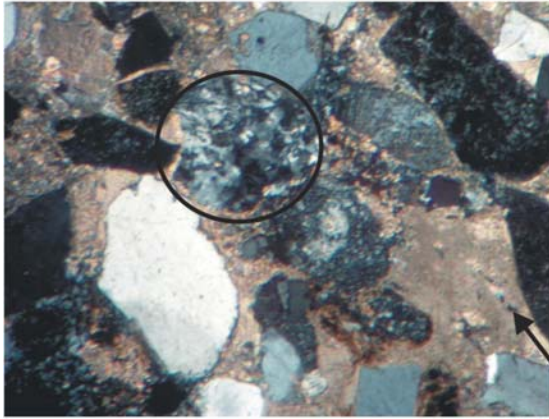
Thin section 3B-2 (911.08 m) – Lithofacies F – This sample is comprised of approximately 30 to 40 % grains is supported by ~60 to 50% cement with porosity accounting for <5% of the entire thin section. Moderate to poorly sorted subangular to angular fragments of detrital chert, angular to subrounded quartz and subangular to subrounded perthitic orthoclase and plagioclase cemented by carbonate (ankerite) cement (Fig. 4.4) are present of the ~60 to 70% cement, approximately 70% is ankerite and 30% silica. Therefore, detrital fragments of granite characterized by intergrown plagioclase and quartz crystals as well as detrital quartzite fragments characterized by fused quartz crystals with fused boundaries (Fig. 4.4). The remaining portion consists of ~5% clays and <5% opaques of the 30 to 40% grains. The opaque minerals within this thin section are characterized by marcasite and pyrite grains. This sample is consistent with the findings in thin section 3B-1.

Figure 4.3 - Detailed photos of bulk mineralogy for thin section 3B-2 (911.08m) of lithofacies F. Pictures exhibiting grain size, composition and porosity observable from the use of blue epoxy.

- A) Granitic rock fragment surrounded by quartz and feldspar grains. Also note the abundance of ankerite cement vs. silica cement.
- B) Quartzite rock fragment with visible chert fragments, quartz and feldspars.
- C) Bulk mineralogy of thin section 3B-2 (plane polarized light).
- D) Same image as C but in cross nicols. Note the perthitic nature of the feldspar.

Sample 3B-2 (911.08 m)

Granitic rock fragment



A)

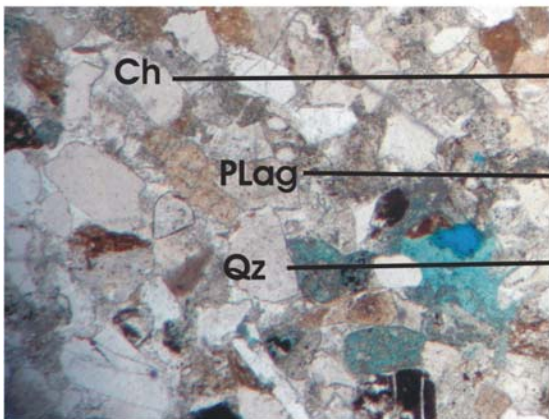
Quartzite rock fragment



B)

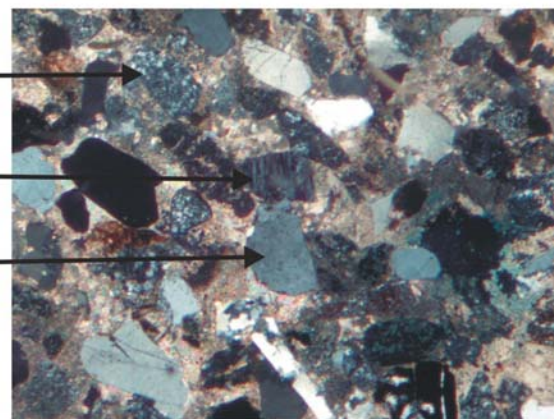
Abundant carbonate cement

Plane polarized



C)

XN



D)

0.4mm



Thin section 3B-3 (906.15 m) – Lithofacies B. This sample comprises approximately 35% grains supported by ~65% cement with porosity accounting for ~5% of the entire thin section. Poorly sorted angular to subrounded detrital fragments of radiolarian chert, supported by angular to subrounded grains of quartz, orthoclase and plagioclase are dominantly (~50%) cemented by chert and ankerite (Fig. 4.5). Approximately 10% of the cement was determined to be ankerite, identified by its rhombic shape and supported by XRD results (Figs. 4.5, raw data available in Appendix C). Minor amounts of aragonite make up ~5% of the total 15% carbonate cement within this thin section. Opaques and clays form <10%.

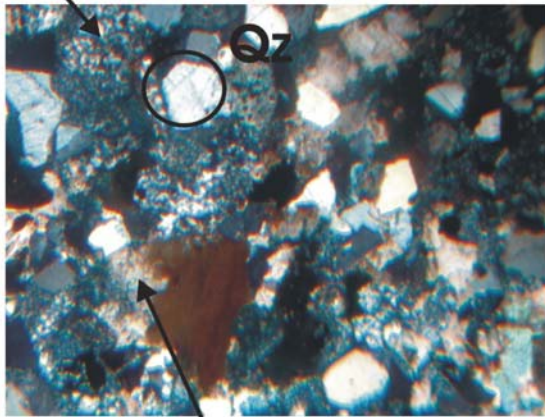
The opaque minerals within this thin section are pyrite, marcasite and titanium-bearing minerals. Leucoxene was also observed within this sample. Nesse (2000) defines leucoxene as an alteration product that is associated with Ti and Fe bearing oxides, hydroxides, and other minerals. It was identified by its characteristic fine-grained brownish color. The grain size is consistent with samples 3B-1 and 3B-2.

Figure 4.4 – Detailed photos of bulk mineralogy for thin section 3B-3 (906.15m) of lithofacies B. Pictures exhibiting grain size, composition and porosity observable from the use of blue dye. (Ch = chert)

- A) Angular quartz grains with associated silica and ankerite cement.
- B) Detrital radiolarian chert fragment with microfossils. Typical detrital chert grain in polarized light with blue pore spaces
- C) Typical detrital chert grain in polarized light with blue pore spaces
- D) Same image as C, but in cross nicols.

Sample 3B-3 (906.15m)

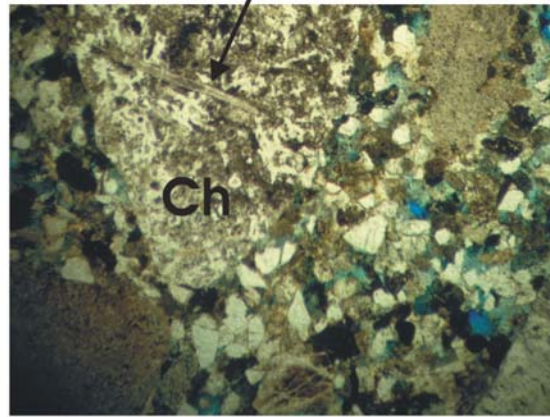
Silica Cement



A)

3.0mm

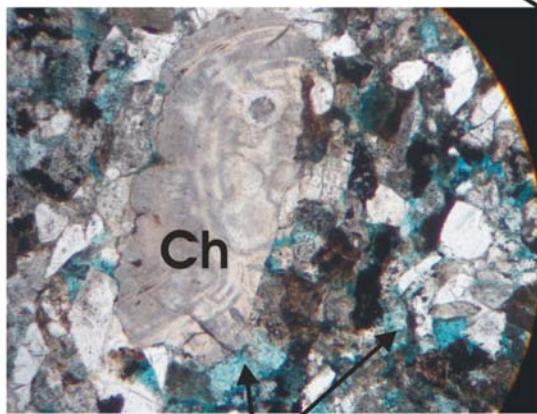
Microfossils



B)

Carbonate Cement
(Ankerite)

Plane polarized

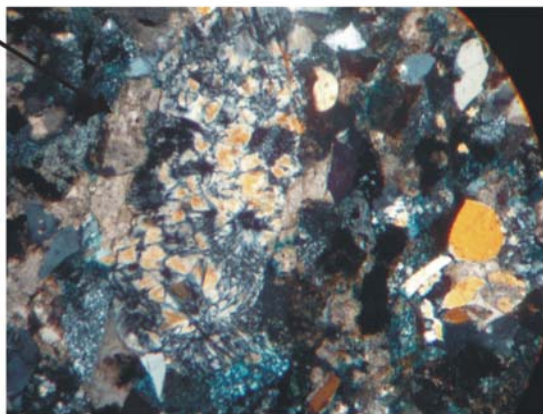


Blue pore spaces

C)

2.0mm

Cross-Nicols (XN)



D)

4.3 X-ray diffraction results

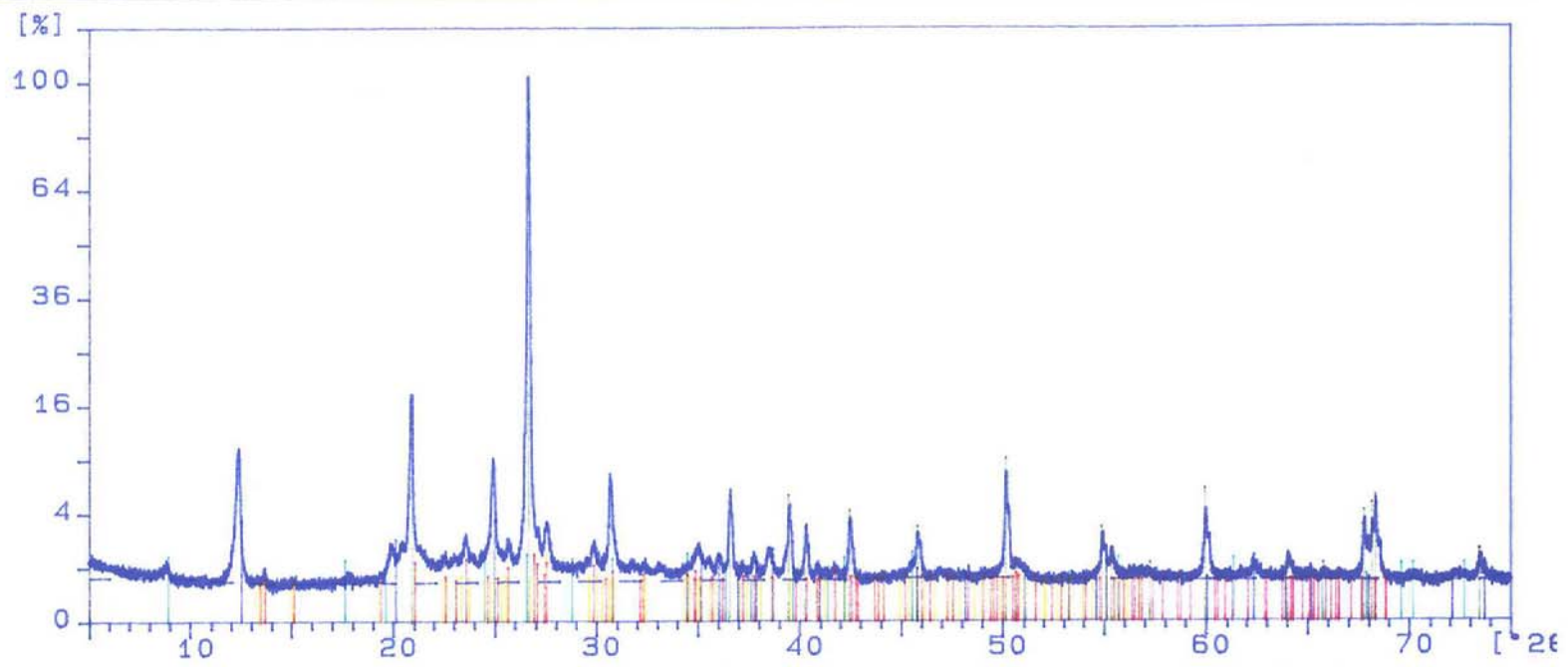
Three XRD samples were analysed and the results are presented within this section. Results support descriptions of the thin sections. The results of the analyses are presented in Table 2 and Appendix C along with the mineralogy observed under the reflected and transmitted microscope. Figure 4.5 depicts three spectral plots attained from the XRD machine. Each mineral on the plots shows its respective peak locations. A strong correlation is found between quartz, orthoclase, microcline and ankerite as illustrated on the spectral plots. Raw data from the XRD analyses is presented in Appendix C. Clays are amongst the minerals identifiable by XRD.

The XRD results presented in Table 2 and the spectral plots (Fig. 4.5) comply with the microscope observations. The clay minerals (illite, kaolinite) found by the XRD were the only minerals which were unable to be viewed under the microscope due to grain size.

Figure 4.5 – Spectral plots acquired from XRD analyses. Samples obtained from upper cored interval of well 3B. Plots display mineral correlations through peaks located from 0 to 75° (diffraction angle).

Sample ident.: 3B-1

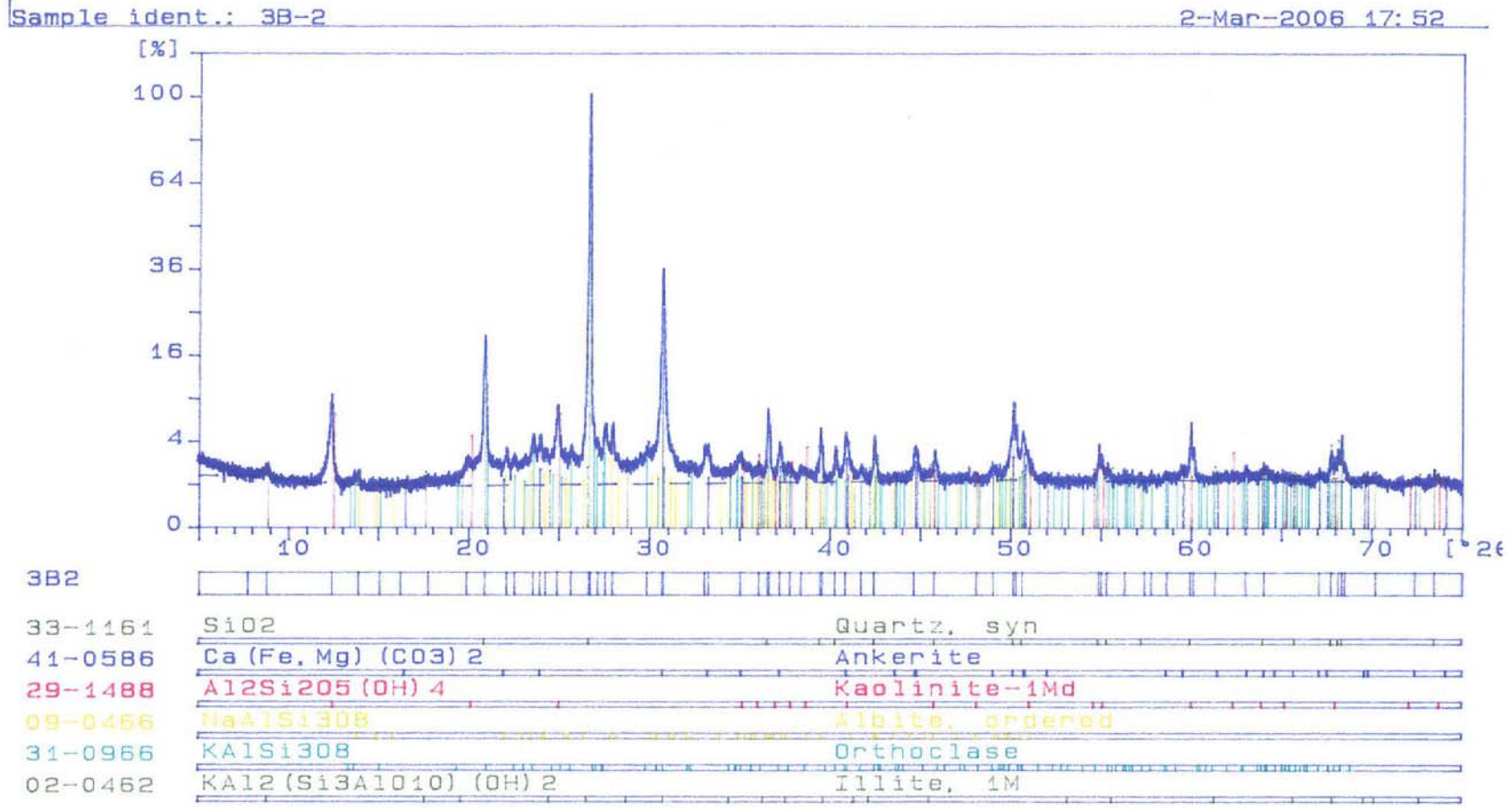
2-Mar-2006 18:12



3B1

33-1161	SiO2	Quartz, syn
29-1488	Al2Si2O5(OH)4	Kaolinite-1Md
31-0966	KAlSi3O8	Orthoclase
19-0932	KAlSi3O8	Microcline, intermediat
02-0462	KAl2(Si3AlO10)(OH)2	Illite, 1M

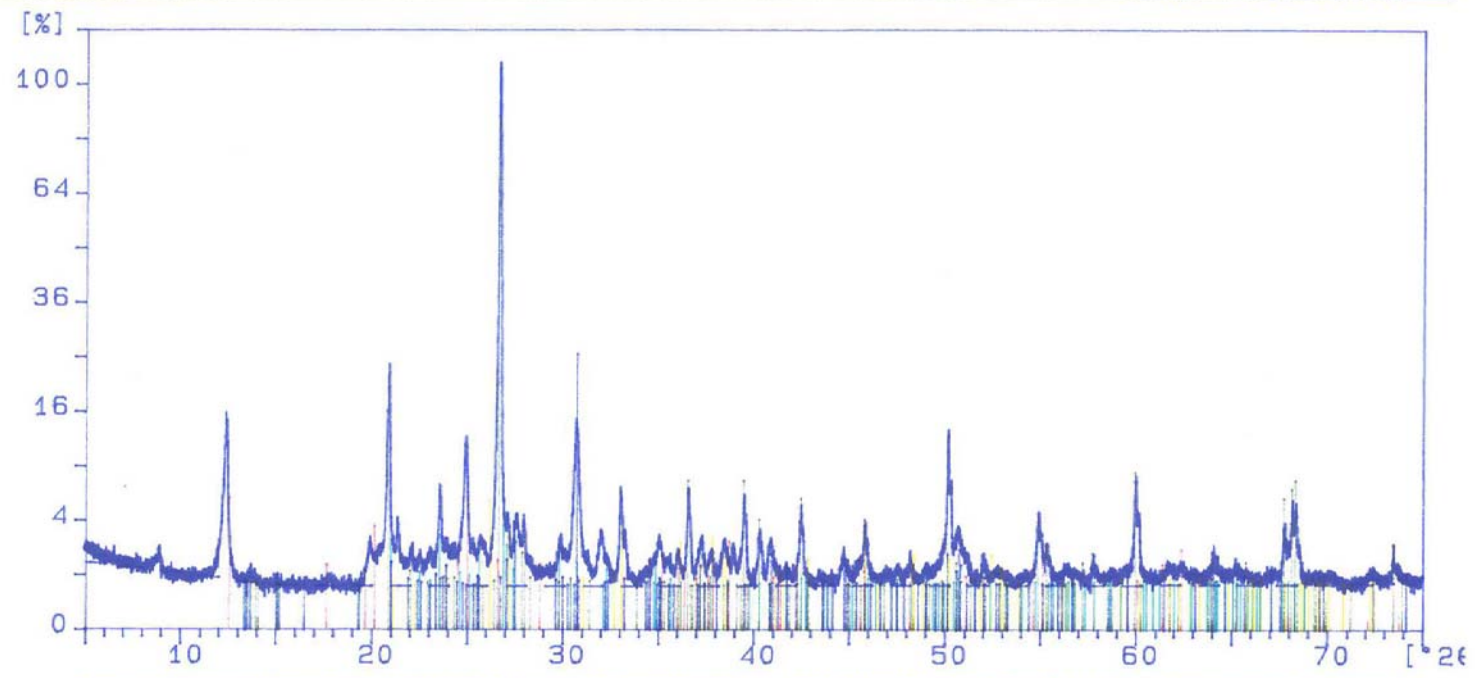
3B-1: green = quartz; blue = kaolinite; red = orthoclase; yellow = microcline; aqua = illite



3B-2: green = quartz and illite; blue = ankerite; red = kaolinite; yellow = albite; aqua = orthoclase.

Sample ident.: 3B-3

2-Mar-2006 17:21



3B3

33-1161	SiO ₂	Quartz, syn
41-0586	Ca (Fe, Mg) (CO ₃) ₂	Ankerite
29-1488	Al ₂ Si ₂ O ₅ (OH) ₄	kaolinite, 1M
41-1475	CaCO ₃	Aragonite
31-0966	KAlSi ₃ O ₈	Orthoclase
41-1480	(Na, Ca) Al (Si, Al) ₃ O ₈	Albite, calcian, ordere
19-0932	KAlSi ₃ O ₈	Microcline, intermediat
02-0462	Al ₂ (Si ₃ AlO ₁₀) ₂ (OH) ₂	Illite, 1M

3B-3: green = quartz and albite; blue = ankerite and microcline; red = kaolinite and illite; yellow = aragonite; aqua = orthoclase.

4.4 Organic Petrography and Hydrocarbon maturity using Vitrinite Reflectance

This section will discuss aspects of the hydrocarbon system, namely the source rock potential and thermal maturity related to the Cummings Formation and provides a brief organic petrographic description obtained from incident and fluorescent light microscopy at approximately 640x magnification. Hydrocarbon maturity was assessed by vitrinite reflectance measurements using modified methods from Davis, (1998).

Observations of maceral composition and hydrocarbon producing potential from two whole rock stubs, samples 1 and 2, from the upper core of well 3B are described. Detailed photos of organic particles taken in incident and fluorescent light are presented in Figures 4.6 and 4.7. In total, 16 vitrinite reflectance values were obtained from each sample and are presented in Table 3. Further, maceral classification schemes and the hydrocarbon generation model are presented in Appendix D.

Vertical spacing between samples 1 and 2 is approximately 3m and no significant variations in maturity were detected.

Sample 1 – (907.48 – 907.89m)

Sample 1 was obtained from organic-rich rubbly shale within lithofacies E. Organic particles found within this sample are coarse grained with an abundance of vitrinite (possibly telovitrinite) and semifusinite. Reflectance results are presented in Table 3. Minor particles of liptinite macerals were also observed consisting of resinite infilling pore spaces of vitrinite particles and bituminite.

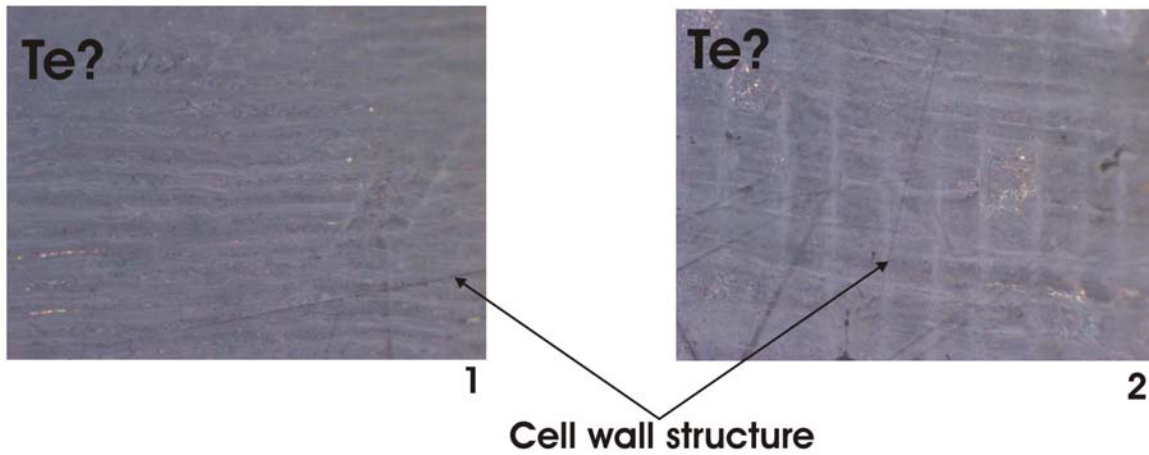
Figure 4.6 – Detailed photos of maceral type found in sample 1 (907.48 – 907.84m). Figure continued on following page. Fluorescent images were also used for classification of liptinite macerals found within sample 1.

- 1 and 2) Possibly telovitrinite (Te) displaying remnants of cellular structure.
- 3 and 4) Semi fusinite (SF) displaying collapsed cellular structure.
- 5 and 6a) Resinite (R) infilling pore spaces of vitrinite.
- 6 b) Fluorescence image of same area as 6A.
- 7) a) Bituminite.
b) Same area under fluorescence.

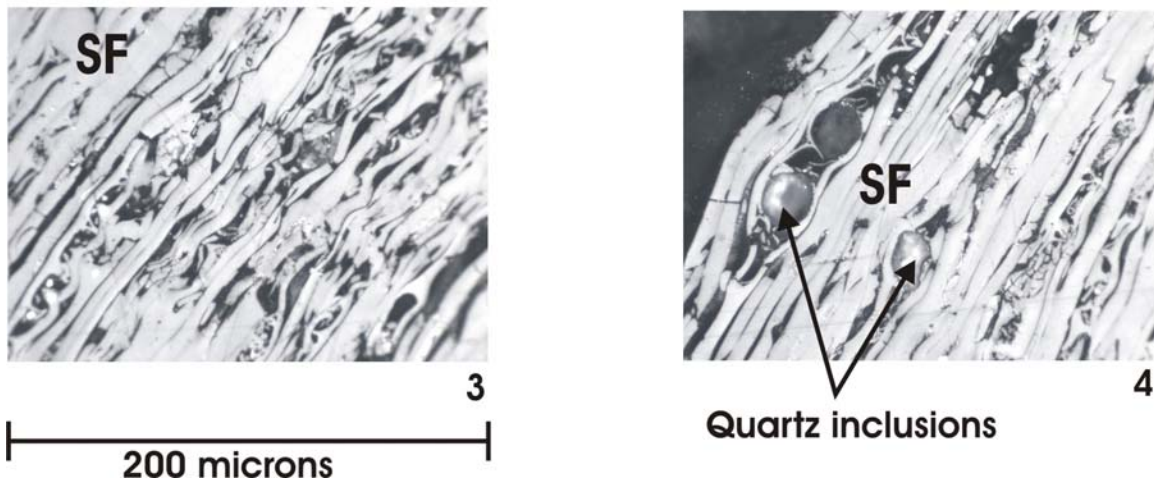
Sample 1: 907.48 - 907.89m

Eye piece magnification 640x

Macerals of the huminite/vitrinite group



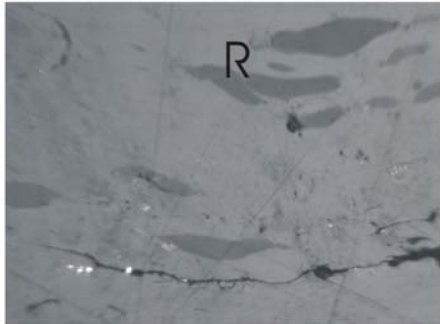
Macerals of the inertinite group



Sample 1: (cont.)

Macerals of the liptinite group

Eye piece magnification 640x



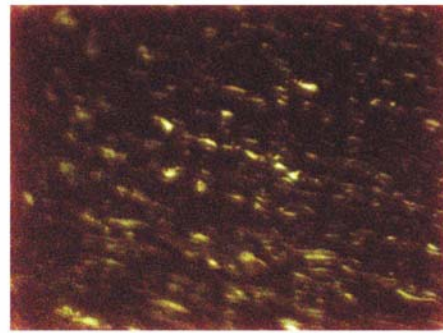
5

Fluorescent light



6a

Resinite

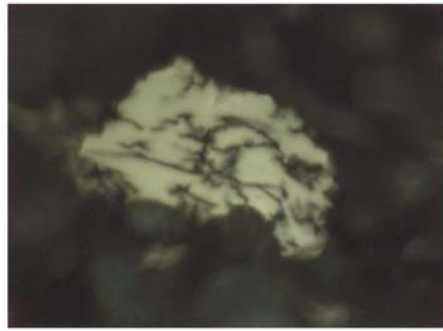


6b



7a

Bituminite



7b

200 microns

Sample 2 – (910.13 – 910.23m)

Sample 2 was obtained from consolidated light grey sandstone laminated with organic detrital material located within lithofacies F. Organic particles observed were rare and very fine-grained. The maceral types observed consisted of vitrinite, liptinite (rare) and inertinite (Fig. 4.7). Common particles observed consisted of semi fusinite and vitrinite. Organic particles were minor compared to the amount of mineral matter found within the samples. Reflectance values are presented in Table 3 and detailed photos are presented in Figure 4.7.

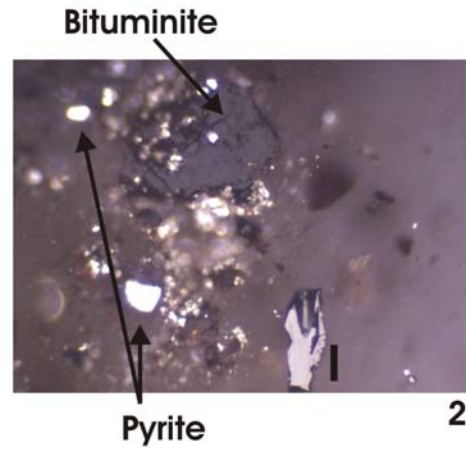
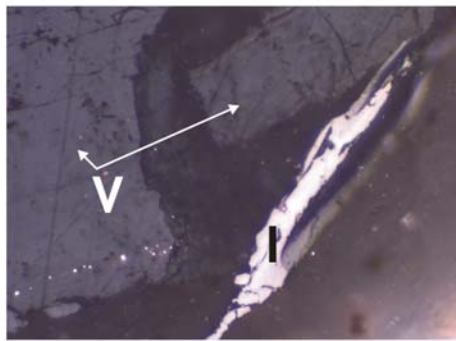
Figure 4.7 – Detailed photos of maceral types observed in sample 2 of well 3B.

- 1) Vitrinite associated with semi fusinite of the inertinite group (I).
- 2) Vitrinite with associated semi fusinite surrounded by mineral matter. Note the abundance of pyrite.
- 3) Vitrinite with associated semifusinite.
- 4) Semifusinite (SF).

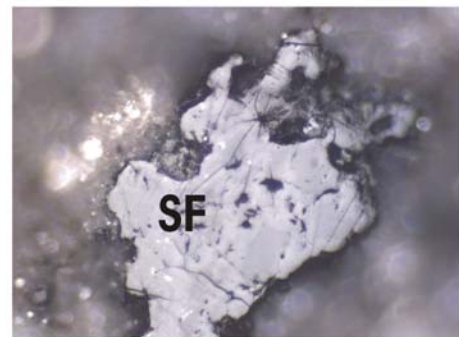
Sample 2: 910.13 - 910.23m

Eye piece magnification 640x

Mixed maceral types: Vitrinite, Liptinite, Inertinite



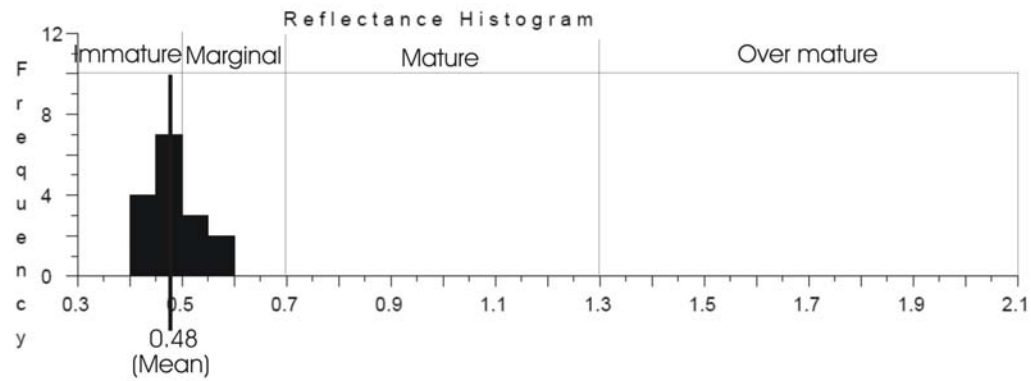
200 microns



Data listings and basic statistics for:

Sample 1

Col >	1	2	3	4	5	6	7	8	9	0
Row	(0.53)	(0.47)	(0.48)	(0.49)	(0.54)	(0.49)	(0.57)	(0.50)	(0.57)	(0.45)
1	(0.47)	(0.45)	(0.41)	(0.40)	(0.42)	(0.43)				
Total	Mean	Stand Dev	Pts	Min	Max	Sum				
(Edit)	0.48	0.05	16	0.40	0.57	7.67				
	0.48	0.05	16	0.40	0.57	7.67				



Sample 2

Col >	1	2	3	4	5	6	7	8	9	0
Row	(0.43)	(0.58)	(0.49)	(0.38)	(0.49)	(0.41)	(0.52)	(0.46)	(0.45)	(0.40)
1	(0.44)	(0.54)	(0.46)	(0.48)	(0.46)	(0.47)				
Total	Mean	Stand Dev	Pts	Min	Max	Sum				
(Edit)	0.47	0.05	16	0.38	0.58	7.46				
	0.47	0.05	16	0.38	0.58	7.46				

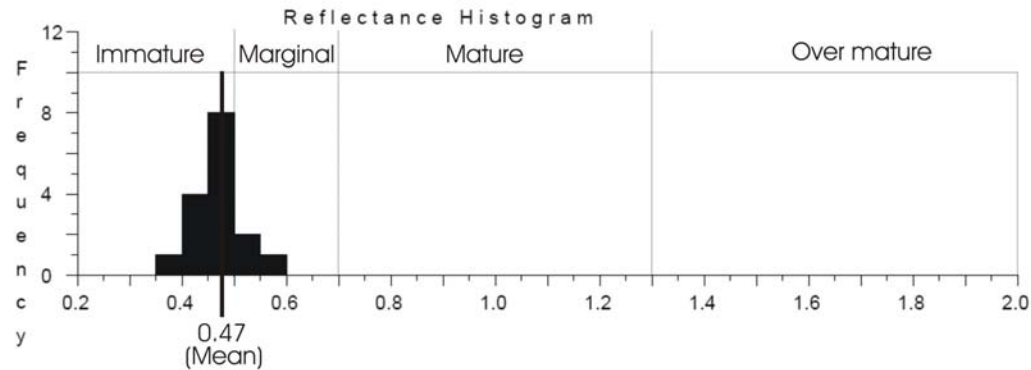


Table 3 – Data listings and basic statistics associated with vitrinite reflectance results obtained from the upper core of well 3B.

Plate 1 – 9: Detailed photos of defining sedimentary structures observed within well 3B. Photos are assorted from the top of the core downward and presented from plates 1 through 9.

Plate 1 – Matrix supported silt rip-up clasts, box 1, lithofacies A

Plate 2 – Imbricated silt rip-up clasts along bedding plane, box1, lithofacies B

Plate 3 – Vertical *Skolithos* burrows, box 2, lithofacies F

Plate 4 – *Skolithos* and *Planolites* burrows, box 2, lithofacies F

Plate 5 – Reaction halos surrounding sulfide mineralization, box 2, lithofacies F

Plate 6 – Tidal couplets, box 4, lithofacies F

Plate 7 – Current ripples, box 4, lithofacies F

Plate 8 – Lenticular bedding, box 5, lithofacies F

Plate 9 – Reactivation surface, box 6, lithofacies F

905.55m

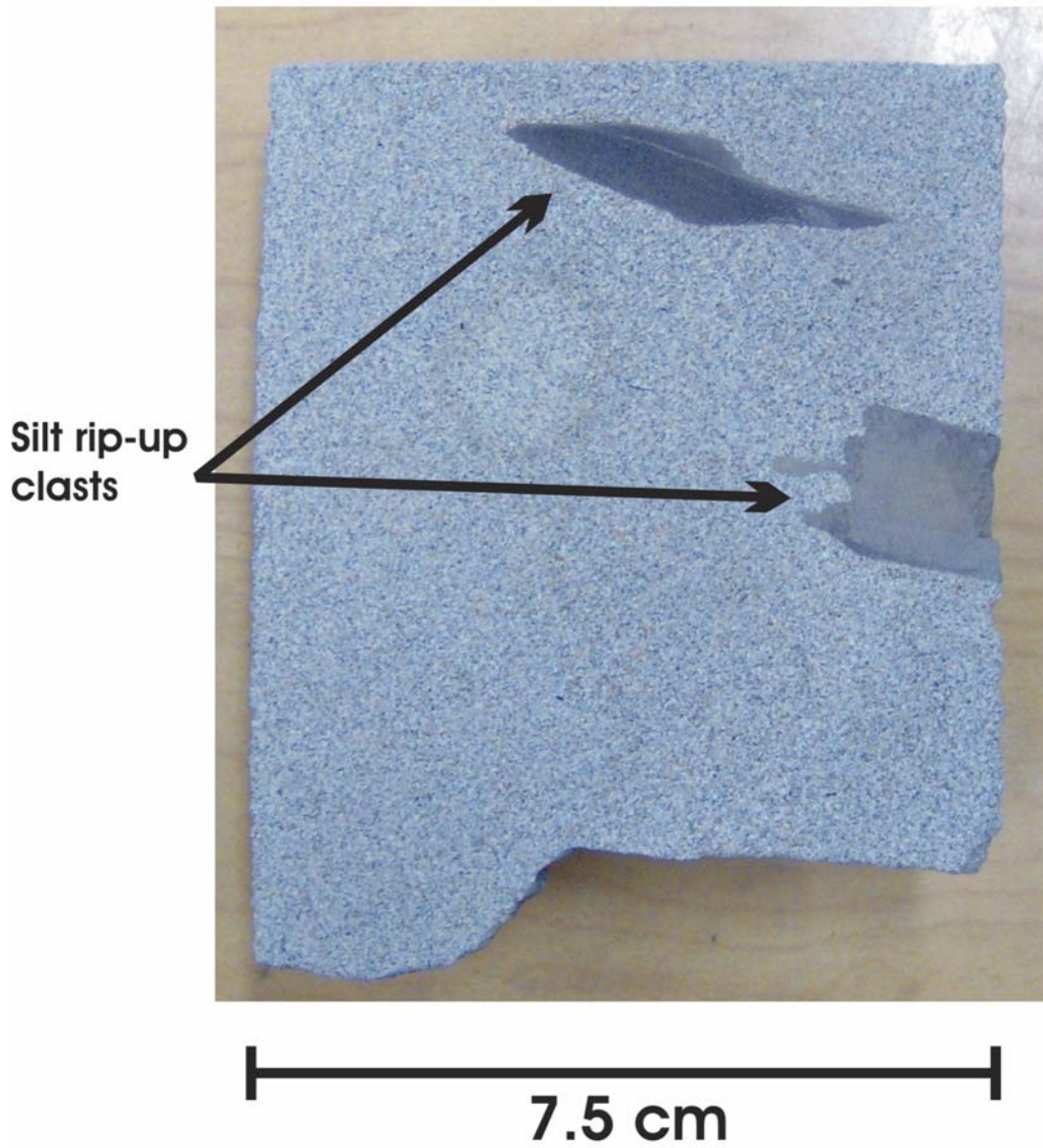


Plate 1- Matrix supported silt rip-up clasts suspended in light grey sandstone of Lithofacies A

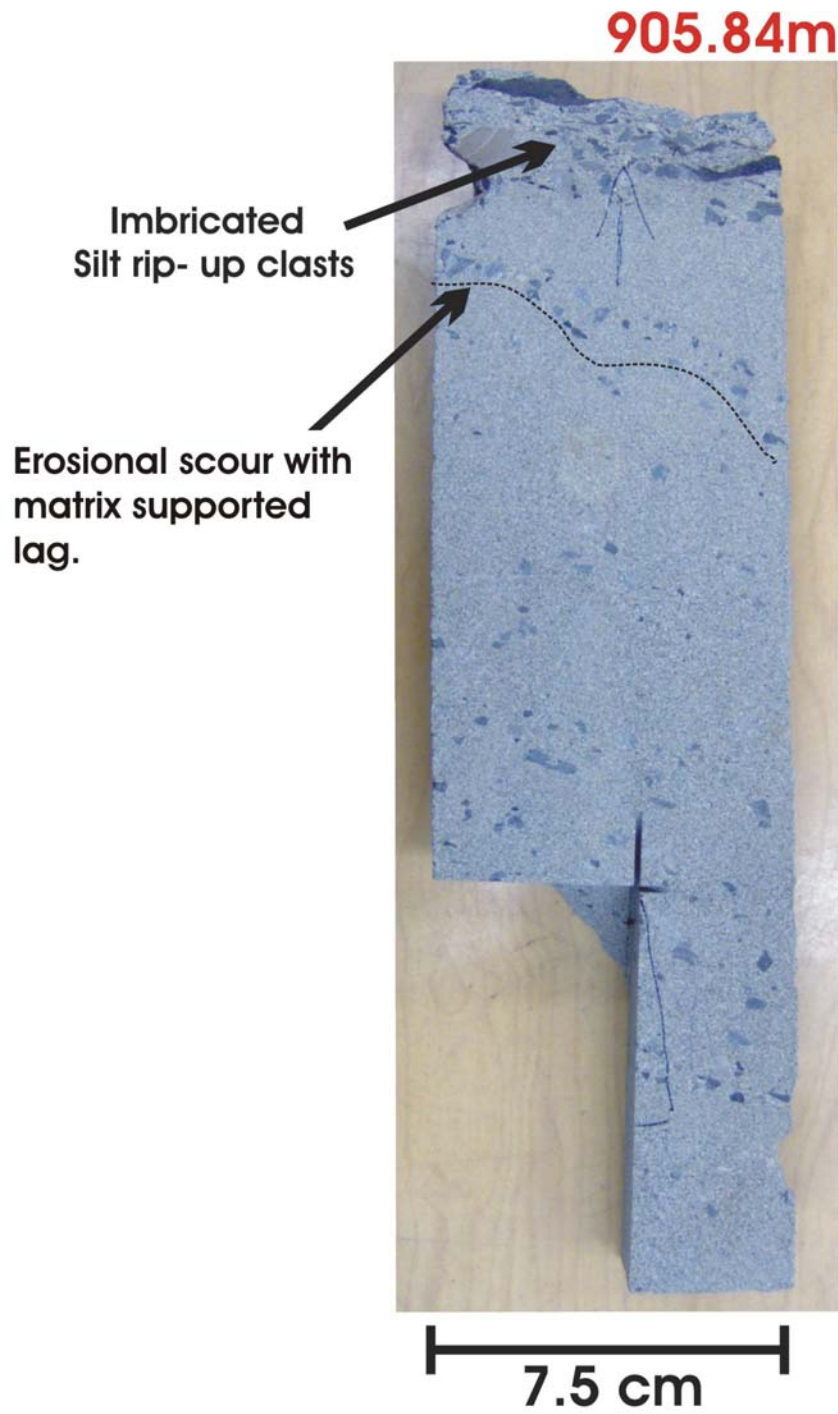


Plate 2- Imbricated silt rip-up clasts lining (possible) rippled bedding surfaces of Lithofacies B.

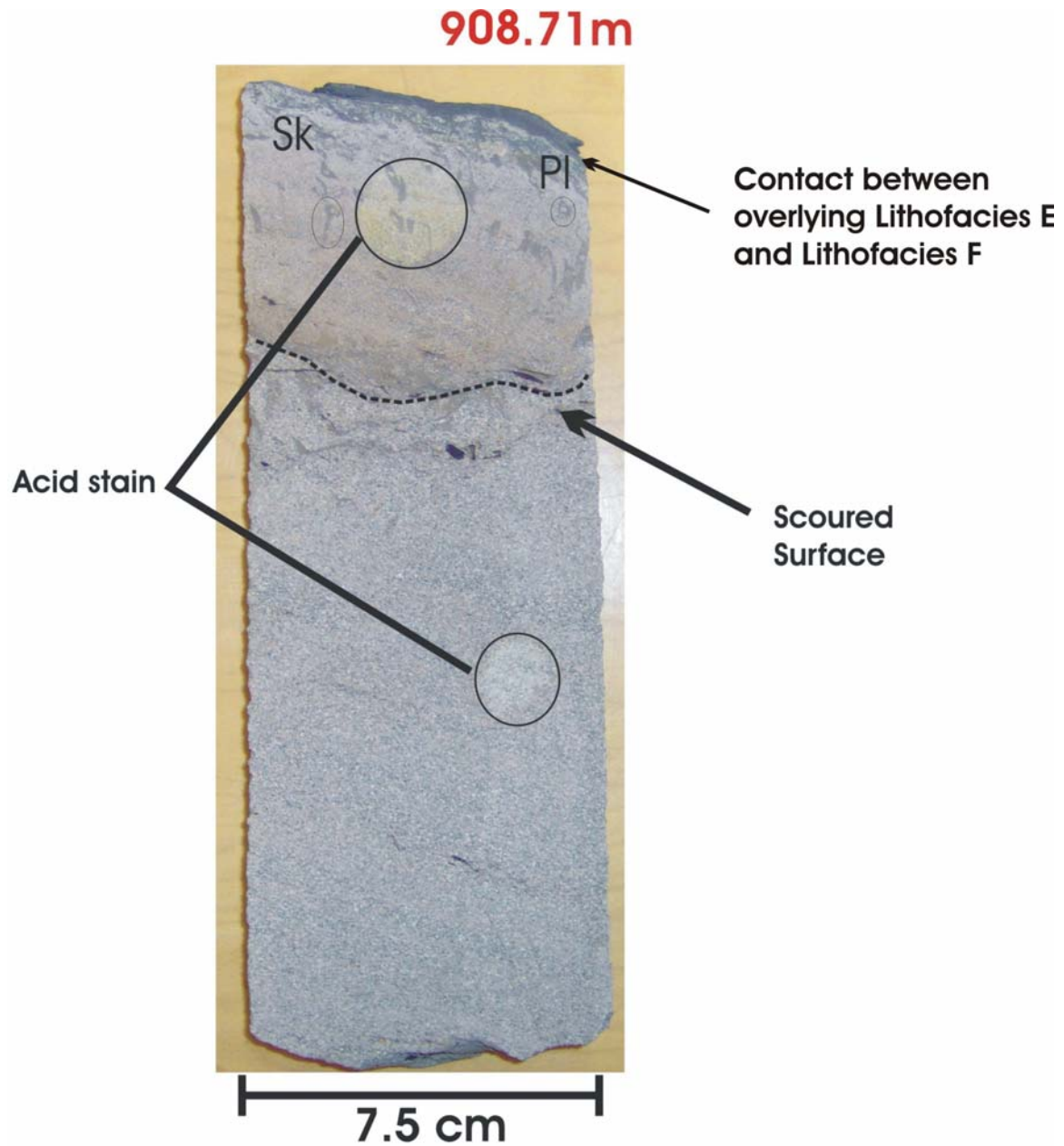


Plate 3 - Vertical *Skolithos* and horizontal *Planolites* burrows lined and infilled with silty material within light grey sandstone. Burrows cross scoured contact between Lithofacies E and F.

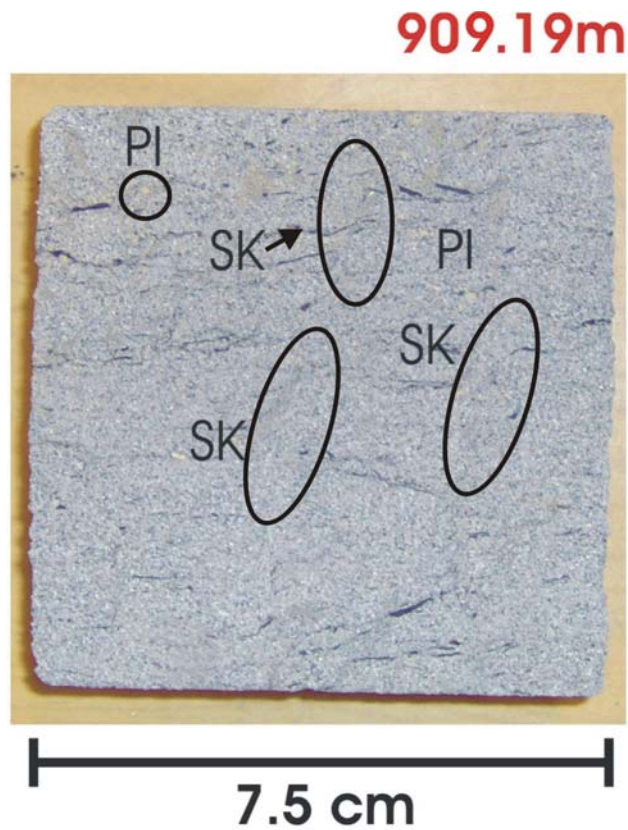


Plate 4 - Vertical *Skolithos* and horizontal *Planolites* burrows infilled with finer grained sand. Trace fossils found in organic laminated light grey sandstone of Lithofacies F

909.50m



7.5 cm

Plate 5 - Reaction halos surrounding sulfide mineralization in organic-rich light grey sandstone of Lithofacies F. Notice how sulfides appear to grow within organic laminations.

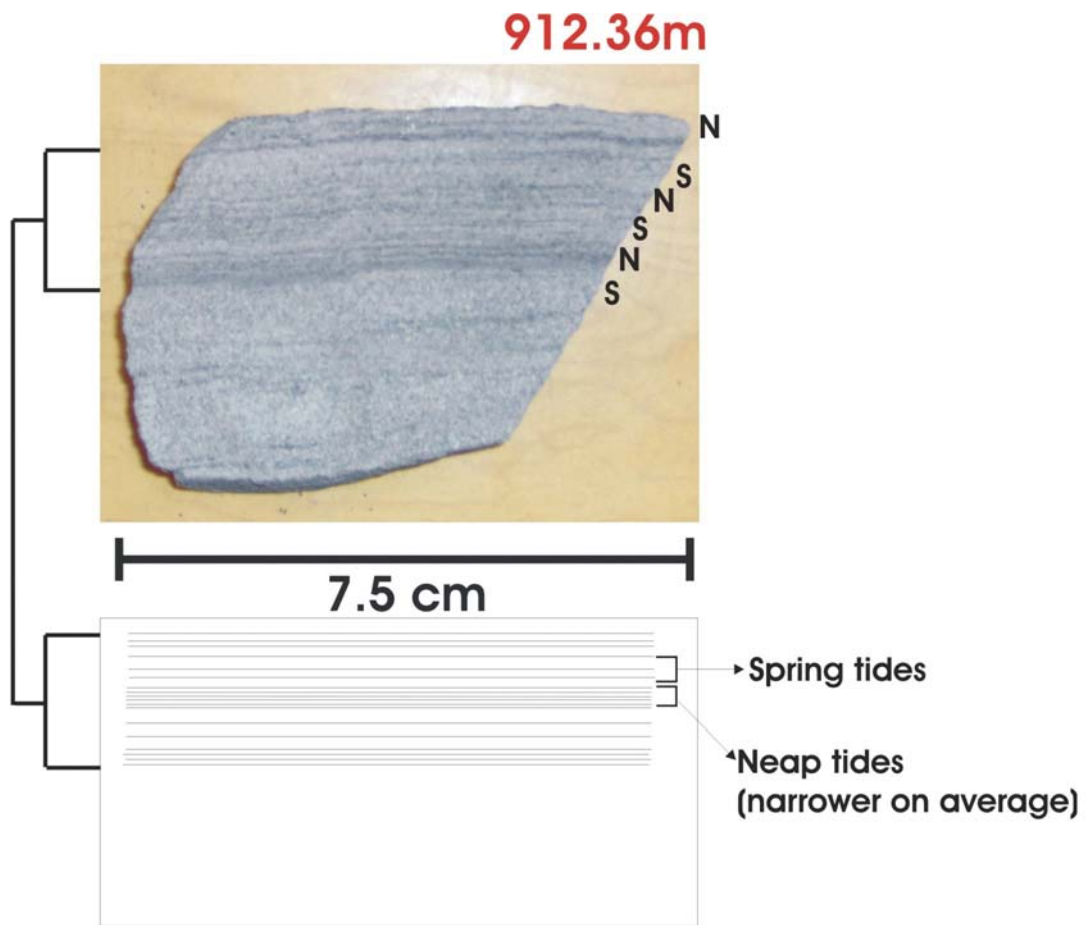


Plate 6 - Tidal Couplets representing neap-spring tidal bundles. These couplets exhibit both high slackwater and low slackwater organic rich laminae reflecting deposition under subtidal conditions, compared to the intertidal conditions where the low slackwater drape is not deposited. It is rare to preserve the 28 couplets representing a lunar month due to erosion but three thin and three thicker laminae sets are present, interpreted to be neap-spring tidal bundles. These tidal couplets are found within Lithofacies F.

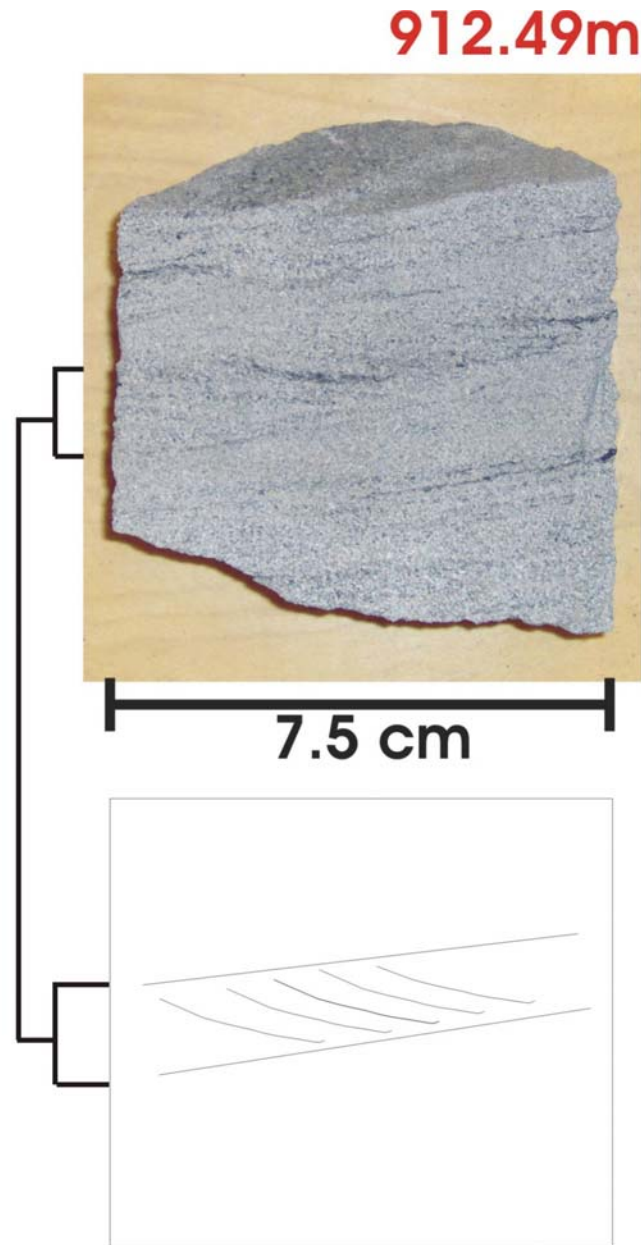


Plate 7 - Current Ripples; laminations lined with dark organic finer grained sediment. Current ripples found within clean light grey sandstone of Lithofacies F.

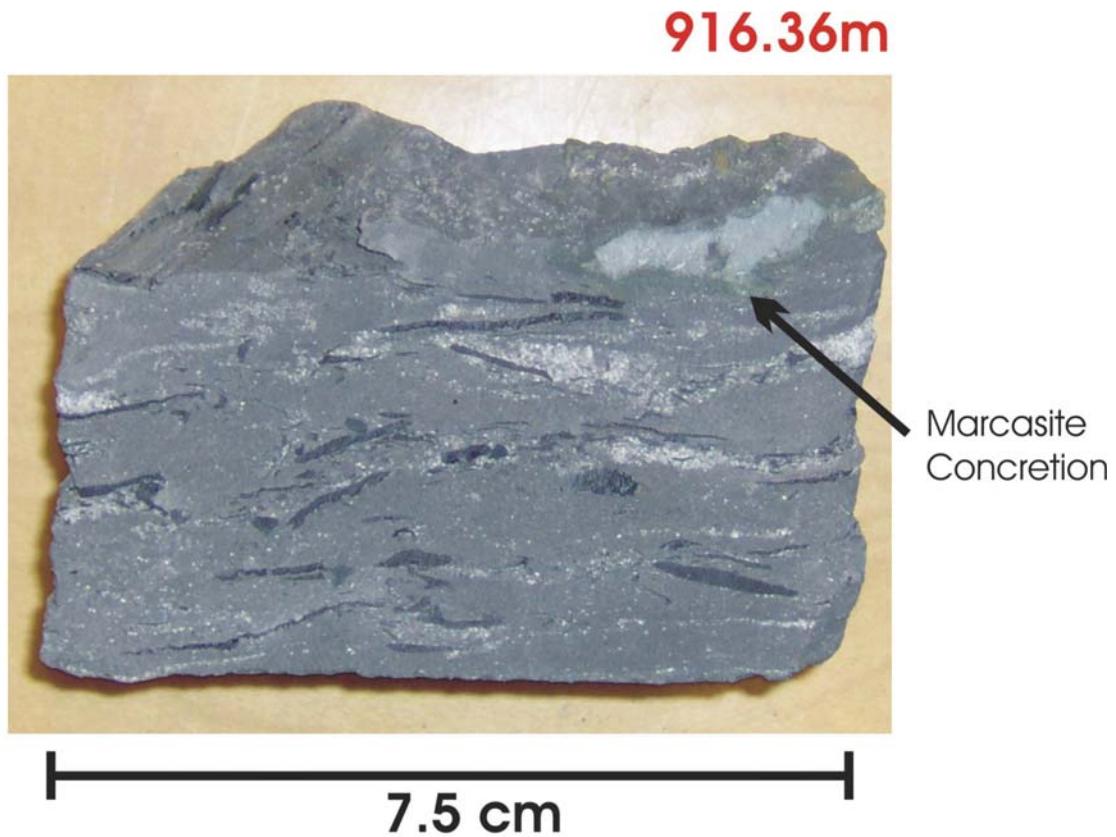


Plate 8 - Lenticular bedding with abundant elongated particles of organic or dark grey mudstone matter. Marcasite concretion (2.5cm). Lenticular bedding only found in example shown within Lithofacies F. This mixture of coarser grained sand and rip-up clasts, with several being matrix supported, of organic rich dark grey silty claystone may represent waning from after storm deposition.

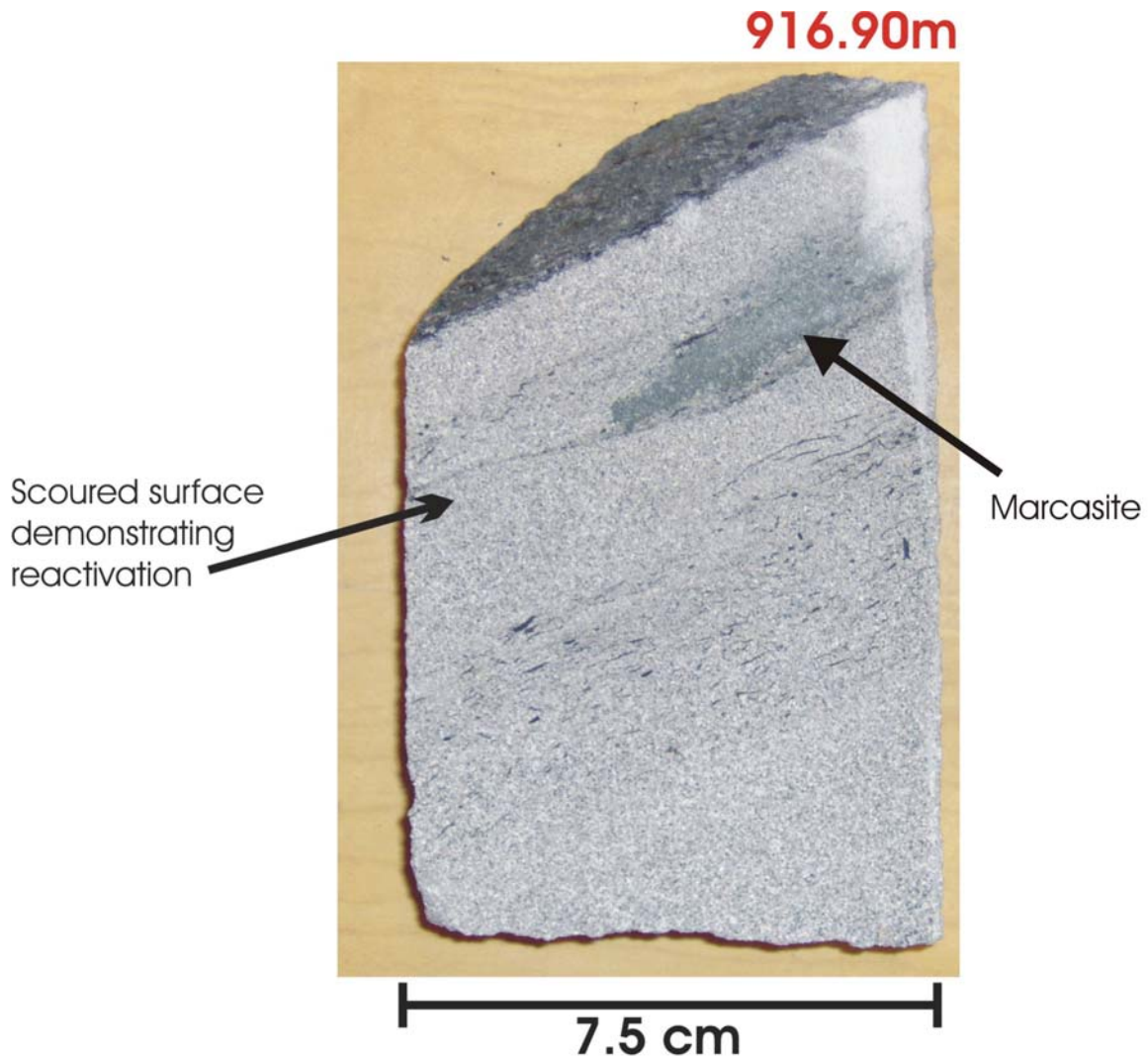


Plate 9 - Scoured irregular surface lined with fine grained organic rich sediment demonstrating reactivation following a parallel laminated section. Common fine grained particles of organic matter. These sedimentary structures are found within Lithofacies F.

CHAPTER 5 - DISCUSSION

5.1 Depositional Environment and Sequence Stratigraphy of the Cummings Formation



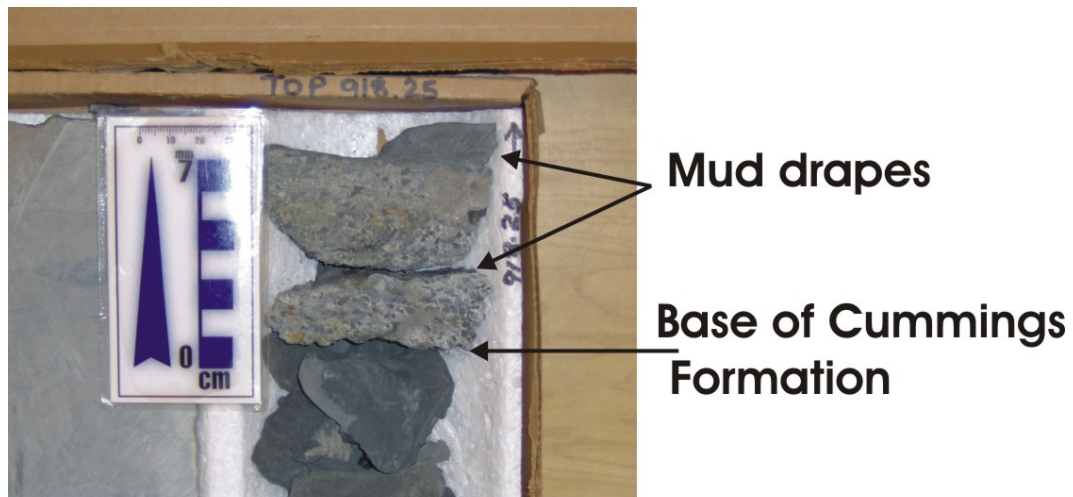
Figure 5.1 – Example of a tide-dominated estuary (East Alligator River, Northern Territory, Australia).

5.1.1 Lithofacies F

Biogenic and sedimentary structures observed within this lithofacies are indicative of relatively high current or wave energies typically associated with marine-influenced channel bar complexes within estuarine environments. These features observed in lithofacies F have been previously attributed to marine-influenced channel bar complexes (Pemberton et al, 1992). An estuarine environment constitutes a partially enclosed body of water with direct contact to the open ocean (Fig. 5.1). This lithofacies

has been interpreted as an estuarine shallow channel bar complex grading into an estuarine bay-fill. Similar lithofacies have been described by Leckie and Singh, (1991) within the WCSB, such as the Albian Paddy Member of the Peace River Formation.

The basal contact of the Cummings Formation is located within the lower cored interval of well 3B (Fig. 5.2). Less than 7cm of the Cummings Formation is exposed within this cored interval. The basal contact is lost at the core break. The remaining core consists of granule sized silt rip-up clasts supported within medium grained grey sandstone. Visible mud drapes (mm-2cm) are also observed. The basal contact of the Cummings Formation is interpreted as a basal lag of an incising channel deposit, congruent with the interpretation of Kidston (2003). This unit would have initially been deposited in a lowstand systems tract marking a sequence boundary, transition to a transgressive system tract and deposition of a transgressive estuarine (valley fill) deposit.



**Top of Box 1 of Core 2
in Well 3B**

Figure 5.2 – Picture of basal Cummings Formation contact in lower cored interval of well 3B.

Freshwater input from river runoff coupled with saline water from tidal activity and turbidity creates a transitional phase from fresh to brackish to saline water resulting in low diversity ecosystems due to biological stress (Wightman, Pemberton and Singh 1987). This is observed in lithofacies F through the presence of a low diversity suite of the *Skolithos* and rare *Planolites* trace fossils, both characteristic of channel bar estuarine deposits (Pemberton et al, 1991). Leckie and Singh, (1991) also observed low diversity suites of *Skolithos* burrows within the Paddy Member. *Skolithos* burrows observed at the base of lithofacies F are infilled and lined with fine-grained sandstone. The *Skolithos* burrows located near the upper contact of lithofacies F are lined and infilled by silt, there presence suggests increasing marine influence as you move up section (Wightman, Pemberton and Singh, 1987). *Skolithos* are generally found within clean sandstone, whereas, the *Planolites* feeding and grazing traces (Pemberton et al., 1992) are commonly associated with detrital organic laminations suggesting lower energy conditions.

Marine influence is not only evident from the lined *Skolithos* trace fossils, but also the presence of physical sedimentary structures such as; tidal bundles and cross-bedded current ripples. Current ripples observed in lithofacies F portray foresets lined by dark silty mud drapes indicating slack water deposition and rounded lee surfaces indicating a subordinate current stage (tidal influence) resulting in reactivation (Plate 7 and 9). These structures are diagnostic of tidal flow responses found in ancient estuary deposits (Dalrymple, 1992). Silt rip-up clasts and wavy bedding surfaces at the base of the lithofacies also provide evidence of channel deposits, which, grade upwards into more horizontal planar or parallel bedding structures suggesting a decrease in current velocities

(Reineck and Singh, 1980). This is typically observed in the transition from incision to transgressive estuarine deposition (Reinson, 1992).

A 9cm section (possibly thicker, but difficult to discern due to a core break) of lenticular bedding is also observed within this lithofacies. According to Dalrymple (1992) and Reineck and Singh (1980), lenticular bedding is commonly associated with mud flats of tidally influenced systems. This may also be demonstrating a local meander of the tidally-influenced channel resulting in channel abandonment and formation of mud plugs (Leckie and Singh 1991). Minor sand drapes found within the lenticular bedding are most likely emplaced by washover induced by high energy storm surges.

Reineck and Singh, 1980, suggest that abundant organic matter is typically found within the basinal or lagoonal area of an estuary, however they also suggest the associated lithotype would be shale, which, does not comply with the fine-grained sandstone observed in this lithofacies. Abundant parallel laminations of organic detrital material are observed throughout this lithofacies suggesting rapid sedimentation rates, compatible with channel deposition within an estuarine environment. The organic matter is mostly concentrated within the middle of this lithofacies and demonstrates cyclic patterns of abundant organic laminae grading into clean sandstone.

Sulphide precipitation with surrounding reaction halos closely associated with the organic material is also observed. The abundance of sulphides furthermore indicates deposition within a chemically reducing environment also known to be a subaqueous environment associated with estuarine deposits (Berner et al, 1985).

5.1.2 Lithofacies E

The rubbly nature of the core limits interpretation of lithofacies E. The basal contact of lithofacies E is sharp and characterized by a diagenetic siderite concretion approximately 7cm thick; observed in similar studies of the foreland basin succession lithofacies by Leckie and Singh (1993). The paleotopography of the underlying Devonian carbonates demonstrates a highly irregular surface formed over millions of years of exposure and erosion. Exposure of the Kindersley and Wainwright topographical highs (see Figs. 2.3 and 2.4) during the Early Cretaceous may have provided a source of carbonate for percolating meteoric water. This carbonate-rich meteoric water could contribute to the formation of diagenetic carbonate-rich concretions such as the siderite concretions described above. The underlying sandstone shows a fining upward sequence approximately 10cm thick to basal contact of lithofacies E. An approximately 1.2m section (possibly thicker, but difficult to tell due to core break) of organic-rich shale is observed within this lithofacies.

This lithofacies is interpreted as a tidal flat or possibly a mud plug deposit associated with a tidally-influenced channel bar complex within an estuarine environment similar to those described by Leckie and Singh (1991). This interpretation is based on stratigraphical association with the underlying lithofacies and the presence of sand drapes throughout the lithofacies suggesting a section of lenticular bedding, similar to the thin unit of lenticular bedding described above. As stated, lenticular bedding is can be associated with mud flats found in the upper regions (landward) of the intertidal zone of tidally influenced systems. This may also related to a local meander of the tidally-

influenced channel resulting in channel abandonment and formation of mud plugs (Leckie and Singh, 1991). Other studies with similar observations of lithofacies association such as Buatois et al, (1999) and Pattison (1992) suggest that parallel laminated organic-rich shale has been deposited within the central basin of an estuarine system. Absence of rootlets suggests a subaqueous environment (also evident in mud plugs) and rare sand lenses can be attributed to periodic floods from storm surges increasing the basinward spread of fluvial sedimentation.

This lithofacies was sampled for organic petrological analyses and results show that the organic particles are very abundant and coarse grained, suggesting proximity between death and burial. This suggests the interpretation of a tidal flat or mud plug within a channel bar complex disagreeing with Buatois' (1999) and Pattison's (1992) depositional interpretations in regards to lithofacies E.

5.1.3 Lithofacies D

Lithofacies D consists of a coarsening upward parallel laminated fine (upper) to (lower) grained sandstone grading into fine (upper) siltstone. This lithofacies has been highly disturbed by syndepositional, soft-sediment listric-style microfaulting possibly due to bank instability induced by intertidal high water bankfull accumulation and dry low water slumping cycles. The high water stage supports bank stability and during low water this stability is reduced. This lithofacies exhibits no preserved biogenic sedimentary structures. The basal contact of this lithofacies has been lost due to missing core. Therefore, no surface or gradational contact can be attested between the tidal flat/mud plug depositional environments of lithofacies E to lithofacies D.

According to Reineck and Singh (1980), evenly laminated sand and horizontal bedding is abundantly distributed on beaches and coastal environments exposed to wave action. This suggests that this lithofacies was deposited in a low energy shoreface environment near the mouth of the estuary, susceptible to wave action (Leckie and Singh, 1991). Swash and backwash wave movements can rework the sediments obliterating any evidence of biogenic structures (Reinick and Singh, 1980). This is an energy stress suppressing organic activity (Wach, pers. Comm.). This interpretation corresponds to the transgressive depositional model of sandy estuarine bay-fill constructed from a cored interval of the Lower Albian Viking Formation in south-central Alberta produced by Pemberton et al. (1992). It also agrees with the depositional model proposed by Leckie and Singh (1991) concerning the transgressive estuarine environment of the Lower Albian Paddy Member of the Peace River Formation.

The coarsening upward sequence observed within this lithofacies suggests a transition from basinward stepping aggradation to landward stepping aggradation marking a maximum flooding surface deposited within a highstands systems tract followed by regional regression (Vail et al, 1977)

5.1.4 Lithofacies C

Lithofacies C consists of unconsolidated poorly sorted granule to cobble conglomerate resulting in substantial core loss. The basal contact exhibits flame structures, diagnostic features of an erosional surface. The sequence stratigraphic relationship between lithofacies D and lithofacies C is indicative of regional regression followed by channel incision demonstrating a lowstands incised valley surface, also termed a transgressive sequence boundary (Leckie and Singh, 1991). This surface

represents a recommencing period of estuarine bay-fill deposits within the paleovalley. According to Reinson, (1992), estuary valley fill deposits usually consist of several successions due to the fact that they occupy the same valley through multiple sea level fluctuations.

This surface could also be interpreted as a transgressive lag resulting in a ravinement surface. Reinson (1992) defines a ravinement surface is defined as a bounding unconformity that must be identified in order to apply concepts of sequence stratigraphy to estuarine environments. Ravinement surfaces are indicative of continuous transgression resulting in overlying offshore open marine deposits. However, this is not the case in the overlying lithofacies within this succession.

5.1.5 Lithofacies A and B

Due to the similar nature and stratigraphic relationships shared between lithofacies A and B, they have been combined in the following section. Lithofacies A and B consist of a fining upward sequence with multiple beds including imbricated granule-sized silt rip-up clasts. This unit is interpreted as inner estuary channel fill deposited in a high energy flow regime. The base of this unit has been lost to missing core, therefore, the nature of the contacts from the conglomerate of lithofacies C described above can only be assumed.

Abundant imbricated rip-up clasts interpreted as lag deposits of active channels (Leckie and Singh, 1991) and scoured irregular surfaces towards the base of the unit indicate very high energy flow velocities eliminating the preservation of biogenic structures. The high current energy remains consistent moving up through the unit with

parallel bedding structures with elongated silt rip-up clasts (3cm in diameter). Reinick and Singh (1980) describe channel deposits as having basal conglomerates and Prothero and Shwabb (1996) indicate that following the lag deposits (basal conglomerates), continuous high energy flow regimes may demonstrate parallel laminations, which are both observed within this unit. Discontinuous siderite concretions (2-3 cm diameter) are also observed along bedding planes, which are consistent with estuarine channel fill deposits (Reinson et al., 1988).

This unit resembles the basal contact of the Cummings Formation observed in the lower cored interval of well 3B and appears to be the foundation of a typical transgressive estuarine depositional model (Leckie and Singh, 1991) and (Reinson et al., 1988).

Figure 5.3 is a summary of the lithologic, depositional environment and sequence stratigraphic relationships of the Cummings Formation within well 3B. The base of the Cummings Formation is defined by a fining upward pebble conglomerate (918.5m) marking channel incision during a lowstand systems tract. The erosional basal contact of the Cumming Formation can also be interpreted as a sequence boundary. Channel incision is followed by deposition of approximately ten metres of medium-grained sandstone (lithofacies F). This lithofacies is interpreted as a channel bar complex infilling the inner estuarine valley, deposited during a transgressive systems tract. Lithofacies E, is interpreted to have been deposited during channel abandonment such as tidal flat or mud plug environments. Dark, organic-rich siltstone with interlaminated sand drapes found within this lithofacies is indicative of the tidal flat or mud plug depositional models (see section 5.1.2). The parallel laminated very fine-grained sandstone of

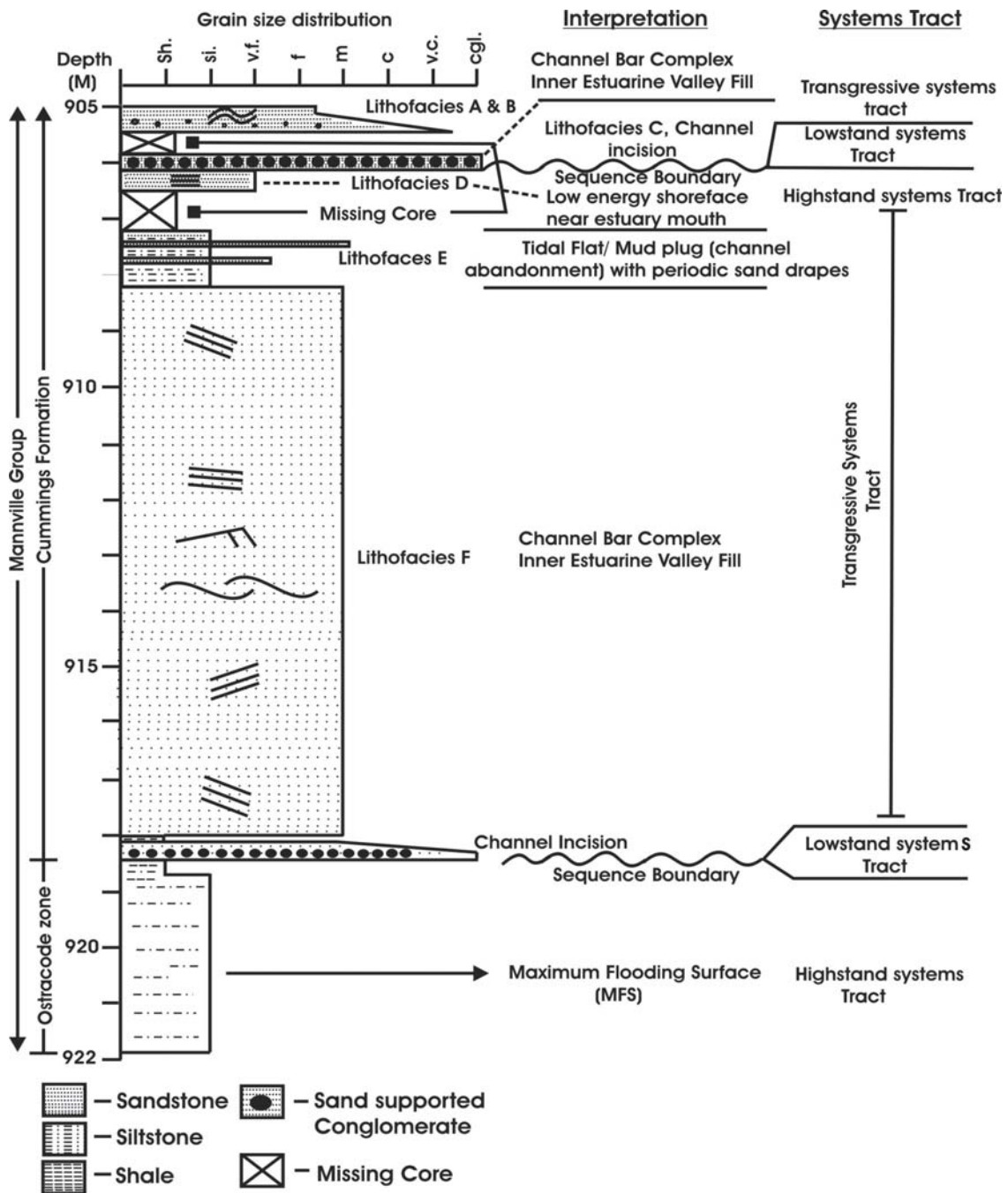


Figure 5.3 – Summary of interpretations as related to depositional environment and sequence stratigraphic relationships of the Cummings Formation (after Leckie and Singh, 1991).

lithofacies D suggests deposition during a highstand systems tract (see section 5.1.3) and is interpreted as a near estuary mouth sand deposit. This lithofacies also marks the transition from a transgressive systems tract to highstand systems tract (maximum flooding surface) and the end of the transgressive estuarine cycle. A poorly sorted pebble to cobble conglomerate, deposited in a lowstand systems tract within lithofacies C, represents an erosional sequence boundary similar to the base of the Cummings Formation previously described. This channel incision demonstrates renewal of the transgressive estuarine cycle. The overlying lithofacies A and B are interpreted to have been deposited under similar conditions as lithofacies F, a transgressive inner estuarine valley fill.

5.2 Provenance of the Cummings Formation

In order to determine the provenance of the Cummings Formation, textural and compositional mineralogical interpretations of the thin section mineralogy and XRD (sections 4.2 and 4.3) have been made. The source rock(s) of the Cummings Formation can not be broken down to specific formations with certainty due to the complexity produced by diverse ancient outcrop exposure, paleodrainage divides, the possibility of recycled grains, and diagenetic processes resulting in mineral alteration. Therefore, the analytical methods used for mineralogy will be used to provide evidence of either a western provenance, namely the Cordillera and the Rocky Mountain Fold Belt, or an eastern provenance derived from the Canadian Shield.

Previous work done by Williams (1963) concludes that sandstones located at the base of the Mannville Group, the Eilerslie Member (central Alberta), which is analogous

to the Dina Formation, exhibit clastic sediments and metasediments derived from the Precambrian Shield. This holds true with the conclusive statements provided by Kidston (2003) come to the same conclusion regarding the provenance of the Dina Formation. Williams (1963) also demonstrated that during the deposition of the Clearwater Fm. (Athabasca area), which is stratigraphically equivalent to the Cummings Formation, an abundance of detrital rock fragments and feldspars began to appear, suggesting an increase in westerly Cordilleran derived sediments. These conclusions were drawn from textural and compositional data compiled from core sample analyses. Williams (1963) found that quartz grains derived from the Cordillera are not as texturally mature as the sediments derived from the Shield. This means that mature quartz grains from the Shield have been recycled through multiple generations of lithologies and lithofacies and display rounded grain boundaries. Compositionally mature simply implies a high proportion (>90%) of quartz due to its resistant nature. The conclusions presented by Williams (1963) have also been supported by Hopkins (1981) in this study of the Lower Mannville of Central Alberta.

More recent work concerning provenance within the WCSB has been presented by Hyde and Leckie (1994). Their study corresponds to the Upper Albian Paddy Member of the Peace River Formation. This study is located proximal to the western border of Alberta (Peace River Area) and therefore a Cordilleran provenance can be interpreted rather easily from texturally immature sandstones. The purpose was to deduce specific formations as a source for the Paddy Member. It is important to note that Hyde and Leckie (1994) observed detrital chert fragments containing circular dark spots interpreted as microfossils. Some grains include radiating spine-like appendages suggesting the

preservation of radiolarians. Important conclusions from Hyde and Leckie (1994) relevant to the provenance of the Cummings Formation include: 1. the presence of metamorphic and plutonic rock fragments; 2. drainage networks providing sediment influx to the foreland basin were able to weather metamorphic rocks from the Omineca Belt west of the Front and Main ranges in northern British Columbia. Their Findings support suggestions by Stott (1968) that Cretaceous rocks of the foreland basin succession were derived from a westerly source (Rocky Mountains) and crystalline rocks from central British Columbia (Hyde and Leckie, 1994).

Abundant detrital chert fragments (many including radiolarian structures described above), volcanic and metamorphic lithic fragments and angular to subangular quartz grains make up the majority of sandstones within the Cummings Formation (Figs. 4.3, 4.4, and 4.5). Each of which are diagnostic of a westerly Cordilleran source (Williams, 1963; Hopkins, 1981; Hyde and Leckie, 1994). Observed sandstones are compositionally mature (see spectral plots, Fig. 4.6), however the angularity of the quartz grains suggest that the sandstones within the Cummings Formation are texturally immature, also supporting a Cordilleran provenance. According to Williams (1963) and Cant and Abrahamson (1996) the paleotopography of the basal unconformity produced drainage networks that were the primary control on valley fill sediments throughout the early Cretaceous (Figs. 2.6 and 2.7). Based on the mineralogy studied within the Cummings Formation, it can be concluded that the main source of sediment supply to the study area from these drainage networks would have been derived from the Cordillera and rising Rocky Mountain Thrust and Fold belt. It is unclear, however, if the surrounding topographical highs such as Wainwright and Kindersley, surrounding the

study area (Figs. 2.4 and 2.3) would have generated significant sediment input. These topographical highs comprise Devonian to Jurassic quartz-rich clastics and carbonates (Smith, 1984), therefore it is likely that some sediment was derived from these areas.

Based on the results obtained by Kidston (2003) concerning the source of the Dina Formation, coupled with the results presented in this study concerning the overlying Cummings Formation, it is apparent that provenance follows findings made by Williams (1963) and Hopkins (1981). The provenance of the Lower Mannville Group is initially easterly derived, progressively shifting to the west from the Aptian to Early Albian in part influenced by the marine transgression from the northwest and by the rising Cordillera.

5.3 Source rock potential and thermal maturity of organic matter and reservoir compartmentalization

The Cummings Formation., Ostracode zone and underlying Dina Formation within the study area of this thesis are located within the Provost Oil Field, of which the Dina Formation is the main hydrocarbon producing unit (Hayes et al, 1994). According to Riediger et al (1999), the source rocks generating hydrocarbons trapped within the Dina's channel sands (Kidston, 2003) consist of the Devonian/Mississippian Exshaw Formation and the Early Cretaceous Ostracode zone to the southwest. The Cummings Formation exhibits no oil staining within core 3B; therefore, reservoir compartmentalization between the Dina and Cummings Formations can be inferred. This most likely occurs due to the lithologically-dependant distribution of hydrocarbons within the Dina Formation

(Kidston, 2003) and possibly due to the pervasive silicification resulting in low porosity within the Cummings Formation.

This section provides a brief discussion concerning the secondary source rock potential of the Cummings Formation within the Mannville Group and the Provost Oil Field. Source rock potential and thermal maturity of the Cummings Formation was determined by analyses of the organic matter through vitrinite reflectance (V %Ro) and rock evaluation. The rock evaluation results are presented in Appendix D and a hydrocarbon generation model (from Snowdon and Powell, 1984) based upon proportions of maceral compositions, source (marine vs. terrestrial) and V %Ro is presented in Figure 5.4.

The source of organic matter of the Cummings Formation has been determined to be terrestrial with an abundance of vitrinite and inertinite (semifusinite) with lesser (~2 to 10%) amounts of liptinites (resinite). According to Snowdon and Powell's (1984) hydrocarbon generation model, the organic matter found within the Cummings Formation would constitute a potential gas producing type III kerogen. Mean V %Ro values (see Table 3) obtained from two samples within the upper core of well 3B exhibit immature results. The total organic carbon (TOC) obtained from rock evaluation analyses shows poor to fair results with pyrolysis chemical parameters T(max) and P.I. (production index) values also found in the immature range (only slightly – hydrocarbon generation begins at T(max) 435°C and obtained T(max) range is 415 - 428°C).

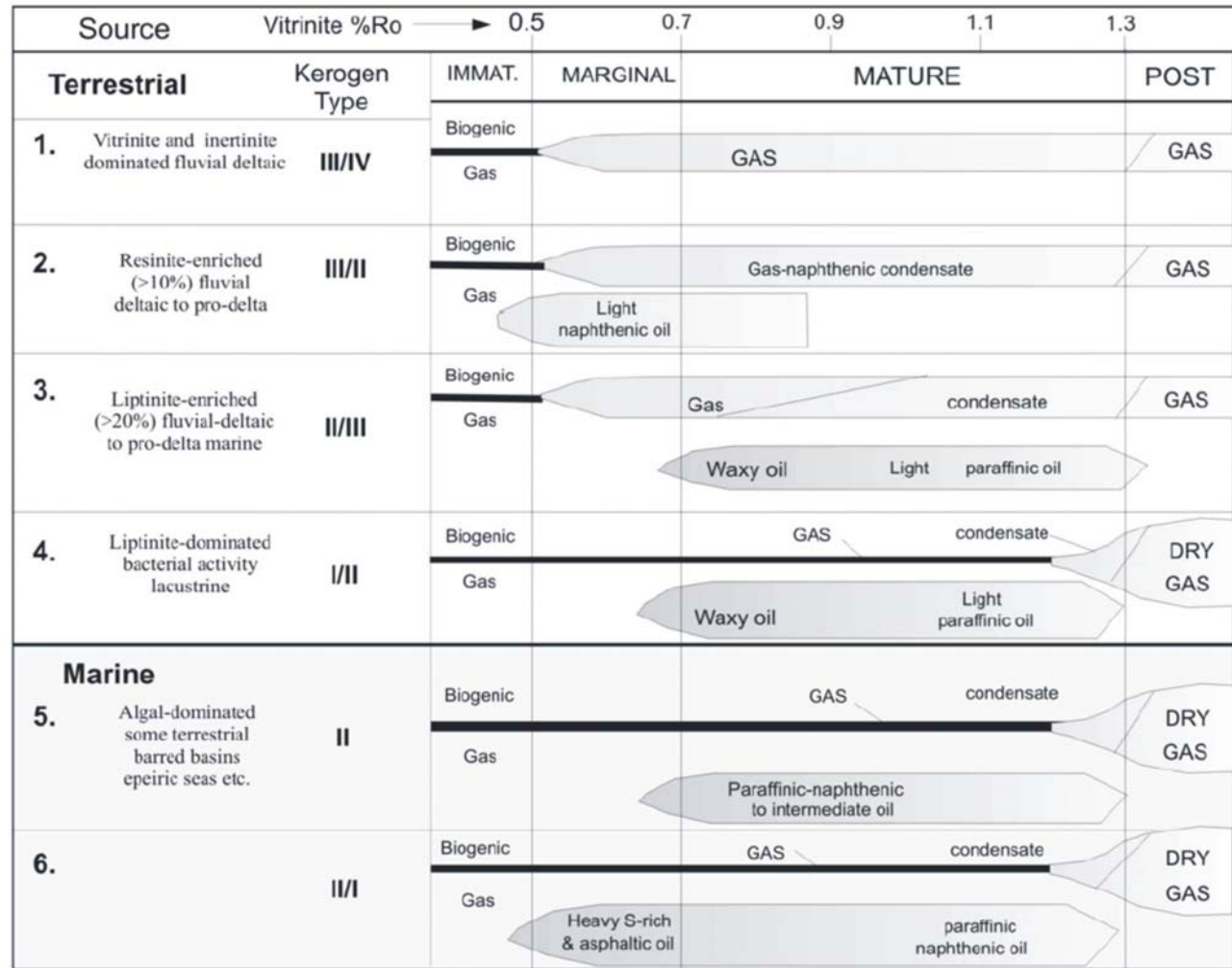


Figure 5.4 – Hydrocarbon generation model (from Snowdon and Powell)

Results presented above demonstrate that the Cummings Formation does not possess the thermal conditions required for hydrocarbon production and is therefore, immature. The TOC within this formation is only marginal and should not be considered as a secondary source rock for overlying formations. Lateral variations and channel margins, stratigraphically equivalent to the Cummings Formation estuary deposits observed in the upper core of well 3B, may generate a higher rank in source rock potential due to the increased concentrations of biological productivity and burial in flood plain or tidal flat (swamp) environments. The presence of ankerite cement, only chemically stable up to approximately 1 km in depth (Dr. Yawooz Kettaneh pers. comm), and consistent V% Ro populations suggest that the Cummings Formation has not been considerably uplifted and therefore would not have previously cooked in situ organic matter and generated hydrocarbons.

CHAPTER 6 – CONCLUSIONS

6.1 Conclusions

- 1) The Cummings Formation was deposited within at least two cycles of a transgressive estuarine environment. Lithofacies exhibit a transition from channel incision and channel bar complexes to channel abandonment and shoreface deposits followed by regression marked by a second incised channel deposit. The second incised channel deposit indicates a recommencing of the transgressive estuarine deposit.
- 2) Through mineralogical analyses, it has been determined that the Cummings Formation has a westerly provenance. This can be attributed to a rising Cordillera and Rocky Mountain Thrust and Fold Belt, paleodrainage networks resulting from paleotopography of the Western Canadian Sedimentary Basin and marine incursions from the north.
- 3) The organic matter within the Cummings Formation was derived from a terrestrial source. Vitrinite reflectance and rock evaluation data indicate that the Cummings Formation is thermally immature and does not possess sufficient total organic matter to be considered a secondary source rock for overlying formations.

Previous work by Cant (1996) suggests that the Cummings Formation was deposited as coastal sandstones during the transition from a highstand to a falling stand systems tract. However, evidence from core 3B suggests an estuarine depositional model deposited during a transgressive systems tract. Increased marine influence is observed indicating a landward stepping depositional sequence, demonstrating the opposite affect seen in either highstand or falling stand systems tracts. Lateral variation beyond channel

margins of the Cummings Formation in this study area may account for the differences observed by Cant (1996).

Abundant detrital chert fragments, volcanic and metamorphic lithic fragments and angular to subangular quartz grains within the Cummings are diagnostic of a westerly Cordilleran source (Williams, 1963; Hopkins, 1981; Hyde, 1994). According to Williams (1963) and Cant (1996) the paleotopography of the basal unconformity produced drainage networks controlling valley fill sediments throughout the Early Cretaceous. From the analyses completed in this thesis, it can be concluded that the main source of sediment supply to the study area from these drainage networks would have been derived from the Cordillera and rising Rocky Mountain Thrust and Fold belt. It is unclear, however, if topographical highs such as Wainwright and Kindersley, surrounding the study area would have generated significant sediment input. Results obtained by Kidston (2003) concerning the source of the Dina Formation coupled with the results presented in this study concerning the overlying Cummings Formation, provide provenance relationships that follows findings by Williams (1963) and Hopkins (1981). The provenance of the Lower Mannville Group is initially easterly derived progressively shifting to the west from the Aptian to Early Albian in part influenced by the marine transgression from the northwest and furthermore by the rising Cordillera.

6.2 Recommendations for further work.

Further work should be done in areas consisting of the Cummings Formation in order to provide knowledge concerning the extent of the interpreted estuary deposits. This thesis only interprets one cored interval, therefore providing only a limited data set. The

determination of paleo-channel margins and tidal flat deposits bordering the estuary would be beneficial for locating possible source rock and reservoir rocks within east central Alberta and western Saskatchewan. It would also be beneficial to correlate sea fluctuations to confirm a depositional model of the entire sedimentary basin. This would increase the understanding of the sequence stratigraphy of the basin and ultimately further the hydrocarbon development within western Canada.

Mineralogical comparisons between the Cummings Formation and the paleotopographical highlands (Kindersley and Wainwright) should be attempted in order to determine the importance of these areas vs. the Cordillera and Rocky Mountain Fold and Thrust Belts in regards to provenance.

The Western Canadian Sedimentary Basin is a highly studied area with numerous drill holes accompanied by downhole geophysics. In order to provide a greater understanding of the depositional environment and sequence stratigraphic relationships, well log data from other areas including the Cummings Formation should be correlated to the observations presented within this thesis.

References

- Allen, J. L. R., 1980. Sand Waves; a model of origin and internal structure: *Sedimentary Geology*, vol. 26, p. 281-328.
- Berner, R. A., De Leeuw, J. W., Spiro, B., Murchison, D. G., Eglinton, G. 1985. Sulphate Reduction, Organic Matter Decomposition and Pyrite Formation. *Philosophical Transactions of the Royal Society of London. Series A, Mathematical and Physical Sciences*, A 315, p. 25-38.
- Bustin, R.M., A.R. Cameron, D.A. Grieve, and W.D. Kalkreuth, 1985, Coal petrology, its principles, methods, and applications: Geological Association of Canada, Short Course Notes, v. 3, Second revised edition, 230 p.
- Buatois, L. A., Mangano, G., Carr, T. R., 1999. Sedimentology and Ichnology of Paleozoic Estuarine Reservoirs, Morrow Sandstone, Lower Pennsylvanian of Southwest Kansas, USA. *Kansas Geological Survey, Current Research in Earth Sciences, Bulletin 243, part 1*
- Cant, D.J. and Abrahamson, B. 1996. Regional distribution and internal stratigraphy of the Lower Mannville. *Bulletin of Canadian Petroleum Geology*, vol. 44, no.3, p. 508-529
- Christopher, V.J. 1984. Sedimentology and Hydrocarbon distribution of the Lower Cretaceous Cadomin Formation, *Canadian Society of Petroleum Geologists*, vol 10, p 175-187.
- Dalrymple, R. W., 1992. Tidal Depositional Systems: *In: Facies Models: Response to Sea Level Change*, R.G. Walker & N. P. James (eds). Department of Geological Sciences, Queen's University, Kingston, Ontario, p. 195-218
- Dalrymple, R. W., Zaitlin, B. A., Boyd, R., 1992. Estuarine facies models; conceptual basis and stratigraphic implications. *Journal of Sedimentary Research*, vol. 62, no. 6, p. 1130-1146
- Hayes, B. J. R., Christopher, J. E., Rosenthal, L., Los, G., McKercher, B., Minken, D., Tremblay, Y. M., Fennell, J. and Smith, D. G., 1994. Cretaceous Mannville Group of the Western Canada Sedimentary Basin. *In: Geological Atlas of the Western Canada Sedimentary Basin*, G. D. Mossop and I. Shetsen (comps.) Canadian Society of Petroleum Geologists and Alberta Research Council, p. 317-334.
- Hopkins, J.C. 1981. Sedimentology of quartzose sandstones of the Lower Mannville and associated units, Medicine River area, central Alberta. *Bulletin of Canadian Petroleum Geology*, vol 29, no. 1, p. 12-41.

Hyde, R. S. and Leckie, D. A. 1994. Provenance of the Lower Cretaceous Paddy Member (Peace River Formation), northwestern Alberta, Bulletin of Canadian Petroleum Geology, vol 42, no. 4, p. 482-498.

Kidston, J., 2003, Depositional environment and provenance of the Dina Formation, Provost oil field, east central Alberta, and a discussion of hydrocarbon distribution within. Honours Thesis submitted to the department of Dalhousie Earth Science.

Jackson, P.C. 1984. Paleogeography of the Lower Cretaceous Mannville Group of Western Canada. *In: Elmworth: Case Study of a Deep Basin Gas Field*. A. J. Masters (ed.). American Association of Petroleum Geologists, p. 49-77.

Leckie, D. A. and Reinson, G.E. 1993. Effects of Middle to Late Albian sea-level fluctuations in the /cretaceous Interior Seaway, western Canada. *In: Evolution of the Western Interior Basin*, W. G. E. Caldwell and E. G. Kauffman (eds.). Geological Association of Canada, Special Paper 39, p. 151-175.

Leckie, D.A., Singh, C., 1991. Estuarine Deposits of the Albian Paddy Member (Peace River Formation) and the Lowermost Shaftesbury Formation, Alberta, Canada. *Journal of Sedimentary Petrology*, vol 61, no. 5, p. 825-849.

Monger, J. W. H., Price, R. A., 1979. Geodynamic Evolution of the Canadian Cordillera; progress and problems. *Canadian Journal of Earth Sciences*, vol 16, no. 3, p. 771-791.

Mossop, G. and Shetsen, I., 1994. Introduction to the Geological Atlas of the Western Canada Sedimentary Basin. *In: Geological Atlas of the Western Canada Sedimentary Basin*, G. D. Mossop and I. Shetsen (comps.). Canadian Society of Petroleum Geologists and Alberta Research Council, p. 1-11.

Nesse, W.D., 1991. *Introduction to Optical Mineralogy*, Second Edition. Oxford University Press, Inc.

Pattison, S. A. J., 1992, Recognition and interpretation of estuarine mudstones (central basin mudstones) in the tripartite valley fill deposits of the Viking Formation, central Alberta; *in*, Applications of Ichnology to Petroleum Exploration--A Core Workshop, S. G. Pemberton, ed.: Society of Economic Paleontologists and Mineralogists, Core Workshop 17, p. 223-249.

Pemberton, S. G., MacEarchern, J. A., and Frey, R. W., 1992 Trace Fossils Facies Models: Environmental and Allostratigraphic Significance: *In: Facies Models: Response to Sea Level Change*, R.G. Walker & N. P. James (eds). Geological Association of Canada, p. 47-73.

Pemberton, S. G., and Wightman, D. M., 1992, Ichnological characteristics of brackish water deposits; *In, Applications of Ichnology to Petroleum Exploration-- A Core Workshop*, S. G. Pemberton, (ed.): Society of Economic Paleontologists and Mineralogists, Core Workshop 17, p. 141-167.

Pemberton, S. G., Van Wagoner, J. C., Wach, G. D., 1992. Ichnofacies of a Wave-Dominated Shoreline. *In: Applications of Ichnology to Petroleum Exploration*. SEPM Core work shop, no. 17, p. 339-379.

Plink-Bjorklund, P., 2005. Stacked fluvial and tide-dominated estuarine deposits in high-frequency (fourth-order) sequences of the Eocene Central Basin, Spitsbergen. *Sedimentology*, vol 52, p.391

Potter, J., L.D. Stasiuk, and A.R. Cameron, 1998, A petrographic atlas of Canadian coal macerals and dispersed organic matter: Canadian Society for Coal Science and Organic Petrology, 105 p.

Poulton, T. P., 1984. The Jurassic of the Canadian Western Interior, from 49 degrees N latitude to the Beaufort Sea. Canadian Society of Petroleum Geologists. Stott, D. F., Glass, D. J. (eds). vol 9, p. 15-41.

Price, R. A., 1994. Cordilleran tectonics and the evolution of the Western Sedimentary Basin. *In: Geological Atlas of the Western Canada Sedimentary Basin*, G. D. Mossop & I. Shetsen (comps.). Canadian Society of Petroleum Geologists and the Alberta Research Council, p. 13-25.

Prothero, D. R. & Shwabb, F., 1996. *Sedimentary Geology: An Introduction to Sedimentary Rocks and Stratigraphy*. W. H. Freeman and Company.

Reineck, H. E. and Singh, I. B., 1980. *Depositional Sedimentary Environments: Second Edition*, Springer-Verlag.

Reinson, G. E., 1992. Transgressive Barrier Island and Estuarine Systems: *In: Facies Models: Response to Sea Level Change*, R.G. Walker and N. P. James (eds). Geological Survey of Canada, p. 179-194.

Reinson, G. E., Clark, J. E., Foscolos, A. E., 1988. Reservoir geology of the Crystal Viking Field, Lower Cretaceous estuarine tidal channel-bay complex, south-central Alberta: American Association of Petroleum Geologists Bulletin, vol. 72, no. 10, p. 1270-1294.

Riediger, C. L., MacDonald, R., Fowler, M. G., Snowdon, L. R., and Sherwin, M. D., 1999. Origin and alteration of the Lower Mannville Group oils from the Provost Oil Field, east central Alberta, Canada. *Bulletin of Canadian Petroleum Geology*, vol 47, no.1, p. 43-62.

Smith, D. G., 1984. Paleogeographic Evolution of the Western Canada Foreland Basin. *In: Geological Atlas of the Western Canada Sedimentary Basin*, G. D. Mossop and I. Shetsen (comps.). Canadian Society of Petroleum Geologists and the Alberta Research Council, p. 277-296.

Stott, D. F. 1984. Cretaceous sequences of the foothills of the Canadian Rocky Mountains. *In: The Mesozoic of Middle North America*, D. F. Stott and D. J. Glass (eds.). Canadian Society of Petroleum Geologists, Memoir 9, p. 85-107.

Taylor, G.H., M. Teichmuller, A. Davis, C.F.K. Diessel, R. Littke, and P. Robert, 1998, *Organic petrology*: Berlin and Stuttgart, Gebruder Borntraeger, 704 p.

Vail, P. R., Mitchum, Jr., R. M. & Thompson, S., 1977. Part Four: Global cycles of relative changes of sea level. *In: Seismic Stratigraphy – applications to hydrocarbon exploration*, C. E. Payton (ed.). American Association of Petroleum Geologists, Memoir 26.

Wightman, D. M., Pemberton, S. G. and Singh, C., 1987. Depositional Modelling of the Upper Mannville (Lower Cretaceous), east central Alberta: Implications of recognition of brackish water deposits. *In: Reservoir Sedimentology*, R. W. Tillman & K. J. Weber (eds). Society of Economic Paleontologists and Mineralogists, Special Publication no. 40, p. 189-220

Williams, G. D., 1963. The Mannville Group (Lower Cretaceous) of Central Alberta. *Bulletin of Canadian Petroleum Geology*, vol 11, no. 4, p. 350-368.

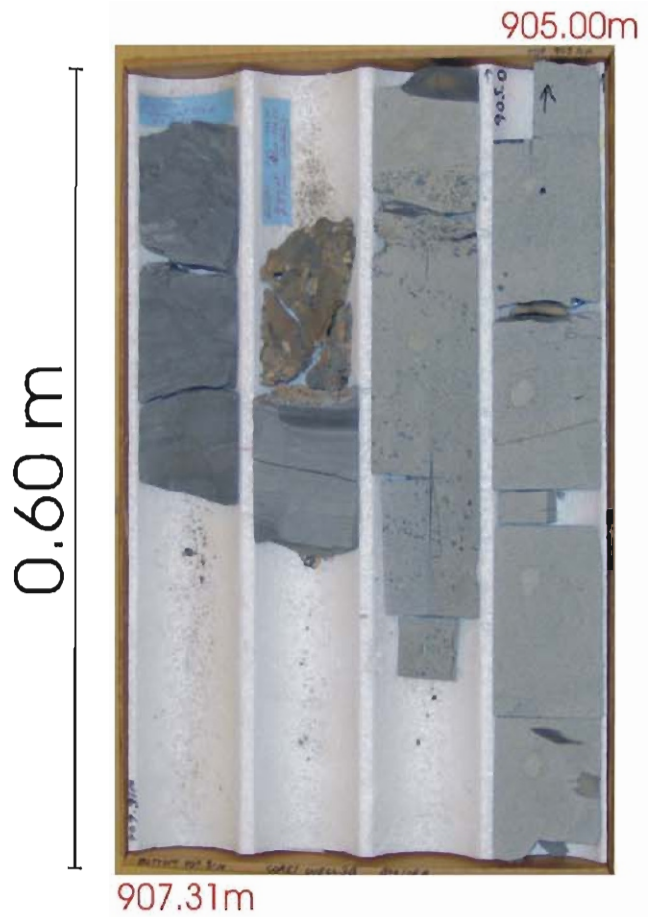
APPENDIX A: PICTURES OF CORE BOXES

Well 3B-36-6W4, Core 1

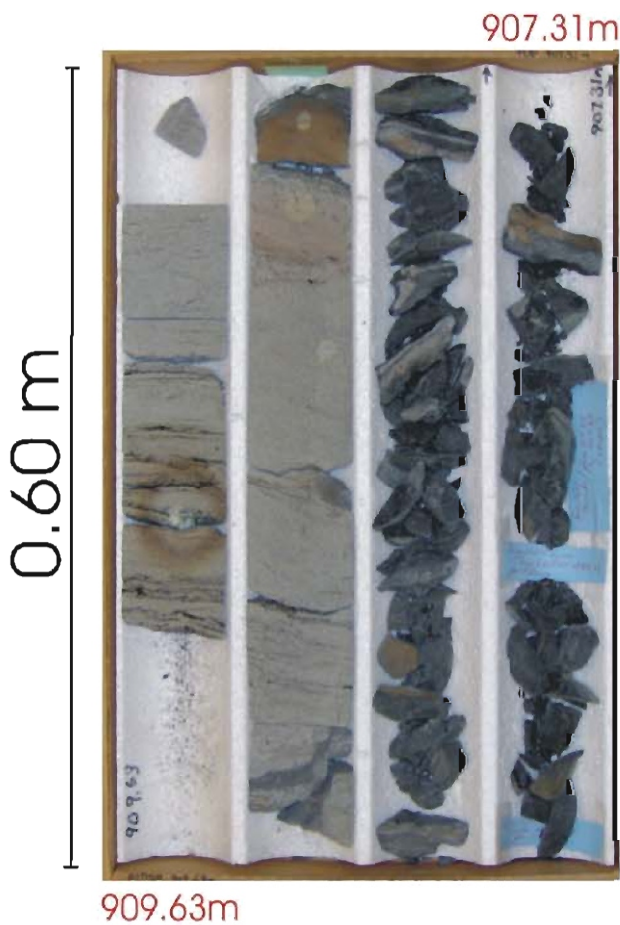
- Box 1... 905.00 - 907.31 m
- Box 2... 907.31 - 909.63 m
- Box 3... 909.63 - 911.95 m
- Box 4... 911.95 - 914.31 m
- Box 5... 914.31 - 916.39 m
- Box 6... 916.39 - 918.15 m

Top of each core box = Upper right corner

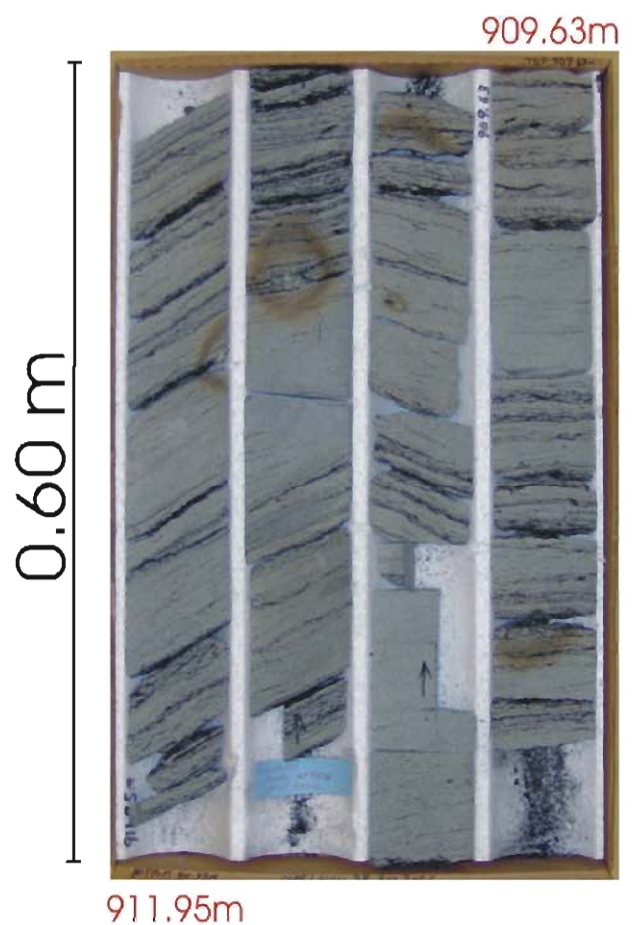
Base of each core box = Lower left corner



BOX 1 OF 6



BOX 2 OF 6



BOX 3 OF 6

0.60m



914.31m

BOX 4 OF 6

916.39m

0.60m



916.39m

BOX 5 OF 6

0.60m



918.15m

BOX 6 OF 6

DEPTH (M)	SAMPLES OR PICS	SEDIMENTARY STRUCTURES	GRAIN SIZE							SURFACE DESC INT	LAMINAE GEOMETRY	BIO- TURBATION INDEX	TRACE FOSSILS	ICHTHO- FACIES	OR STAINED INDEX	Notes	LITHO- FACIES	DEPOSITIONAL ENVIRONMENT	NAME OF ROCK UNIT
			C P G L L A N	V C	C	M	F	V F	S C I L L A T Y										
911.00										S	5		PL			REACTION RIMMING AROUND PYRITE CONCRETIONS			
.10	TS # 3B-2 @ 911.08 & XRD sample									S						POSSIBLE SILICIFIED BED (DIAGENETIC FEATURE)			
.20													PL			MARCASITE CONCRETION			
.30	TS OF ORGANIC MATERIAL @ 911.40												PL			PARTIALLY SILICIFIED (DIAGENETIC FEATURE)			
.40													PL			REACTION RIMMING SROUND PYRITE CONCRETION			
.50																POSSIBLE TIDAL BUNDLES			
.60										CB			PL						
.70																			
.80																			
.90																			
1.0		BOX 4											PL			REACTION RIMMING AROUND PYRITE CONCRETION			
1.1													SK ?						
1.2										GR									
1.3																NEARLY PERFECT TIDAL BUNDLES REPRESENT A COMPLETE LUNAR MONTH (28 CYCLES)			
1.4																			
1.5																			
1.6													PL			MARCASITE CONCRETIONS			
1.7										S						MARCASITE CONCRETIONS			
1.8										GR			PL						
1.9													PL			REACTION RIMMING AROUND PYRITE CONCRETIONS			
													PL						

Transgressive Estuary

CUMMINGS FORMATION

INTER-LAMINATED MEDIUM-GRAINED TO FINE-GRAINED SANDSTONE WITH BIOTURBATED LAMINATIONS OF ORGANIC MATTER

MIXED SKOLITHOS/CRUZIANA

DEPTH (M)	SAMPLES OR PICS	SEDIMENTARY STRUCTURES	GRAIN SIZE										SURFACE DESC INT	LAMINAE GEOMETRY	BIO- TURBATION INDEX 1 2 3 4	TRACE FOSSILLS	ICHTHO- FACIES	OIL STAINED INDEX 1 2 3	Notes	LITHO- FACIES	DEPOSITIONAL ENVIRONMENT	NAME OF ROCK UNIT			
			C P G L L A N	B R L L	V C	C	M	F	V F	S C I L L A T Y															
913.00			[Grain size chart: mostly black bar]											5											
.10			[Grain size chart: black bar]											5											
.20			[Grain size chart: black bar]											5											
.30			[Grain size chart: black bar]										S												
.40			[Grain size chart: black bar]											5											
.50			[Grain size chart: black bar]											5											
.60			[Grain size chart: black bar]											5											
.70			[Grain size chart: black bar]										S												
.80			[Grain size chart: black bar]																						
.90			[Grain size chart: black bar]																						
1.0			[Grain size chart: black bar]																						
1.1			[Grain size chart: black bar]										CB												
1.2			[Grain size chart: black bar]										CB												
1.3			[Grain size chart: black bar]										CB												
1.4		BOX 5 	[Grain size chart: black bar]											15											
1.5			[Grain size chart: black bar]											20											
1.6			[Grain size chart: black bar]											35											
1.7			[Grain size chart: black bar]											5											
1.8			[Grain size chart: black bar]											20											
1.9			[Grain size chart: black bar]											15											
915.00			[Grain size chart: black bar]											15											

MIXED SPACE SKOLITHOS/CRUZIANA

Transgressive Estuary

CUMMINGS FORMATION

MARCASITE

MARCASITE
REACTION RIMMING

MARCASITE CONCRETIONS

MISSING CORE

MARCASITE CONCRETIONS
ELONGATED MUDRIP CLASTS (1/4 THICK, 5cm LONG)

REACTIVATION SURFACE

BIOTURBATION OCCURS IN ORGANIC LAMINAE

MARCASITE CONCRETIONS

INTER-LAMINATED MEDIUM-GRAINED
TO FINE-GRAINED SANDSTONE
WITH BIOTURBATED LAMINATIONS
OF ORGANIC

INTERLAMINATED MEDIUM-GRAINED
TO FINE-GRAINED SANDSTONE
WITH ABUNDANT MARCASITE
CONCRETIONS AND MINOR
BIOTURBATED LAMINAE OF
ORGANIC MATTER

DEPTH (M)	SAMPLES OR PICS	SEDIMENTARY STRUCTURES	GRAIN SIZE							SURFACE DESC INT	LAMINAE GEOMETRY	BIO- TURBATION INDEX 1 2 3 4	TRACE FOSSILS	ICHO- FACIES	OIL STAINED INDEX 1 2 3	Notes	LITHO- FACIES	DEPOSITIONAL ENVIRONMENT	NAME OF ROCK UNIT			
			C P G L L A N	B B R V C	V C	C	M	F	V F											S C I L L A T Y		
917.00	THIN SECTION 3B-1 @ 917.23m & XRD sample																					
0.10																						
0.20																						20
0.30																						
0.40																						40
0.50																						
0.60																						20
0.70																						RARE
0.80																						
0.90																						20
1.00																						
1.10																						VERY LARGE (7 X 7cm) MARCASITE CONCRETION
1.20																						
918.15		END OF CORE																				
1.30																						
1.40																						
1.50																						
1.60																						
1.70																						
1.80																						
1.90																						

Transgressive Estuary

CUMMINGS FORMATION

File: 3B1.D1

9-Feb-2006 18:17

Philips Analytical X-Ray B.V.

PC-APD, Diffraction software

Sample identification: 3B-1

Data measured at: 9-Feb-2006 16:19:00

Diffractometer type: PW3710 BASED

Tube anode: Cu

Generator tension [kV]: 40

Generator current [mA]: 40

Wavelength Alpha1 [Å]: 1.54060

Wavelength Alpha2 [Å]: 1.54439

Intensity ratio (alpha2/alpha1): 0.500

Divergence slit: 1x

Receiving slit: 0.1

Monochromator used: YES

Start angle [x2i]: 5.000

End angle [x2i]: 75.000

Step size [x2i]: 0.010

Maximum intensity: 8537.760

Time per step [s]: 1.000

Type of scan: CONTINUOUS

Minimum peak tip width: 0.00

Maximum peak tip width: 1.00

Peak base width: 2.00

Minimum significance: 0.75

Number of peaks: 60

Angle [x2i]	d-value '1 [Å]	d-value '2 [Å]	Peak width [x2i]	Peak int [counts]	Back. int [counts]	Rel. int [%]	Signif.
8.895	9.9335	9.9579	0.200	31	58	0.4	1.52
12.345	7.1641	7.1817	0.060	790	45	9.2	1.74
12.405	7.1296	7.1471	0.040	734	45	8.6	1.23
13.650	6.4820	6.4979	0.160	26	41	0.3	1.34
17.795	4.9804	4.9926	0.240	16	44	0.2	0.96
19.875	4.4636	4.4746	0.100	121	44	1.4	1.41
20.390	4.3520	4.3627	0.160	123	44	1.4	1.30
20.900	4.2469	4.2574	0.100	1482	44	17.4	18.18
22.550	3.9398	3.9495	0.160	81	45	0.9	1.08
23.590	3.7684	3.7777	0.080	164	45	1.9	0.91
24.925	3.5695	3.5783	0.050	692	45	8.1	1.18
25.725	3.4603	3.4688	0.100	128	46	1.5	1.38
26.465	3.3652	3.3735	0.030	870	46	10.2	0.81
26.650	3.3422	3.3505	0.080	8538	46	100.0	29.53
26.740	3.3312	3.3394	0.040	4396	46	51.5	1.72
27.125	3.2848	3.2929	0.100	193	46	2.3	0.98
27.585	3.2310	3.2390	0.080	222	46	2.6	0.81

27.000	2.7720	3.0001	0.200	117	40	1.1	3.27
30.685	2.9113	2.9185	0.080	557	48	6.5	5.54
31.800	2.8117	2.8186	0.240	42	48	0.5	0.80
32.340	2.7660	2.7728	0.160	45	48	0.5	0.76
33.135	2.7014	2.7081	0.240	35	48	0.4	1.94

File: 381.D1

9-Feb-2006 18:17

Philips Analytical X-Ray B.V.

PC-APD, Diffraction software

Angle [2θ]	d-value '1 [Å]	d-value '2 [Å]	Peak width [2θ]	Peak int [counts]	Back. int [counts]	Rel. int [%]	Signif.
35.045	2.5585	2.5647	0.200	98	49	1.1	1.93
35.590	2.5205	2.5267	0.200	53	49	0.6	1.18
36.015	2.4917	2.4979	0.120	81	49	0.9	1.33
36.560	2.4558	2.4619	0.040	428	49	5.0	1.11
37.190	2.4157	2.4216	0.160	36	49	0.4	0.87
37.740	2.3817	2.3876	0.060	86	49	1.0	1.10
38.490	2.3370	2.3428	0.240	90	50	1.1	4.16
39.495	2.2798	2.2854	0.080	346	50	4.1	3.85
40.330	2.2345	2.2400	0.060	216	50	2.5	2.17
40.895	2.2050	2.2104	0.080	46	50	0.5	0.88
41.750	2.1618	2.1671	0.200	30	50	0.4	1.96
42.460	2.1272	2.1325	0.120	231	50	2.7	6.12
45.800	1.9796	1.9844	0.100	169	55	2.0	2.82
45.940	1.9739	1.9787	0.060	123	55	1.4	1.21
46.920	1.9349	1.9397	0.240	18	53	0.2	1.39
48.175	1.8874	1.8920	0.480	5	53	0.1	0.85
50.180	1.8166	1.8210	0.090	571	53	6.7	8.81
50.305	1.8123	1.8168	0.040	292	53	3.4	4.72
54.895	1.6712	1.6753	0.060	166	49	1.9	1.13
55.050	1.6668	1.6709	0.060	108	49	1.3	1.21
55.345	1.6586	1.6627	0.080	104	49	1.2	1.24
57.045	1.6132	1.6171	0.960	17	49	0.2	2.56
58.735	1.5707	1.5746	0.080	14	49	0.2	0.98
59.990	1.5408	1.5446	0.040	310	48	3.6	0.83
60.160	1.5369	1.5407	0.080	159	48	1.9	2.17
62.295	1.4892	1.4929	0.160	45	48	0.5	0.77
64.050	1.4526	1.4562	0.080	79	48	0.9	1.07
65.220	1.4293	1.4329	0.320	17	48	0.2	0.91
67.755	1.3819	1.3853	0.100	246	46	2.9	4.10
67.950	1.3784	1.3818	0.060	144	46	1.7	1.81
68.160	1.3747	1.3781	0.040	250	46	2.9	0.80
68.340	1.3715	1.3749	0.060	361	46	4.2	2.84
68.535	1.3681	1.3714	0.060	128	46	1.5	1.31
70.275	1.3384	1.3417	0.400	12	46	0.1	1.03
71.315	1.3214	1.3247	0.080	10	46	0.1	0.84
72.435	1.3037	1.3069	0.640	15	46	0.2	1.30
73.525	1.2871	1.2902	0.080	83	46	1.0	1.19
73.730	1.2840	1.2871	0.060	49	46	0.6	1.00

C:\APDJ\DATA\3B1.IDN

9-Feb-2006 18:19

Analyzed DI file : C:\APDJ\DATA\3B1.DI
Sample identification : 3B-1
Last update of results file : 9-Feb-2006 18:19

Database used : C:\IDENTDB

MEASUREMENT PARAMETERS

Diffractometer : PW3710
Start angle [x2θ] : 4.995
Final angle [x2θ] : 75.005
Step size [x2θ] : 0.010
Time per step [s] : 1.0
Anode material : Cu

Date and time of measurement : 9-Feb-2006 16:19

PEAK SEARCH PARAMETERS

Minimum peak width : 0.00
Maximum peak width : 1.00
Peak base width : 2.00
Minimum significance : 0.75

Number of peaks detected : 60

SEARCH-MATCH PARAMETERS

Number of strong lines of the
reference patterns used in SEARCH : 5
Intensity threshold : 3.02
Confidence threshold : 20
Minimum specimen displacement : -40
Maximum specimen displacement : 35
Step size in specimen displacement: 75

Restrictions file : GENERAL

Results:

Card.	Match	Rel m	I [%]	Displ	QM	Formula
ident.	score	score		[fm]		
1	31-0966	35.24	0.37	1	-14	S KAlSi3O8
2	33-1161	15.78	0.79	61	12	S SiO2
3	35-0610	29.53	0.34	2	-129	S MgSiO3
4	37-0447	25.57	0.35	4	83	S Cu3(AsO4)(OH)3
5	25-0618	26.77	0.33	1	-14	S K(Si3Al)O8
6	19-0932	25.20	0.32	1	17	I KAlSi3O8
7	29-1488	12.70	0.60	3	-112	O Al2Si2O5(OH)4
8	19-1227	22.32	0.34	2	-125	S (K,Na)(Si3Al)O8

C:\APDJ\DATA\381.IDN

9-Feb-2006 18:19

Name

Orthoclase
Quartz, syn
Clinoenstatite, syn
Clinoclase
Sanidine, disordered
Microcline, intermediate
Xaolinite-1M
Sanidine

C:\APDJ\DATA\381.IDN

9-Feb-2006 18:19

Card.	Match	Rel m	I [%]	Disp	QM	Formula
ident.	score	score		[fm]		
9	19-1263	21.78	0.30	1	62	S Na2Zn(SO4)2!4H2O
10	31-0782	14.38	0.42	1	-122	I (Mg,Al)3(Si,Al)2O5(OH)4
11	13-0004	14.93	0.40	1	-64	O (Mg,Al)3(Si,Al)2O5(OH)4
12	41-0607	17.75	0.33	1	-122	I Ca2Mg(AsO4)2!2H2O
13	44-1426	19.78	0.29	1	-64	S Fe2(SO4)3!7H2O
14	29-0380	21.37	0.27	1	58	I Ca5(SiO4)2(OH)2
15	12-0724	14.41	0.37	1	-3	O Hg3(SO4)O2
16	36-0439	16.54	0.31	1	-57	O Na11(Na,Ca)4MnTi4(Si207)2
17	44-1410	15.07	0.33	1	-43	I LiNaSi2O5!2H2O
18	25-1187	16.90	0.28	1	-99	C Ag3SbS3
19	35-1013	15.16	0.31	1	-3	C Pd9Te4
20	25-0624	13.97	0.33	1	-46	I KB5O8!4H2O
21	14-0195	11.51	0.40	1	-99	O (Mn,Ca)4(Mn,Fe)9SbSi2O24
22	21-0435	14.03	0.32	1	-99	I Fe2(TeO3)2SO4!3H2O
23	06-0214	17.12	0.26	1	-79	I CuAl6(PO4)4(OH)8!4H2O
24	23-1461	14.22	0.31	1	-117	O UC2.86!1.5H2O
25	43-0633	13.50	0.32	2	30	S BaSnSi3O9

C:\APDJ\DATA\3E1.IDN

9-Feb-2006 16:19

```
-----  
+-----+  
|Name  
+-----+  
|Zincbl\PIodite, syn [NR]  
|Lizardite-6(3)T, aluminian  
|Lizardite-6(2)T, aluminian  
|Wendwilsonite  
|Kornelite  
|Reinhardbraunsite, syn  
|Schuetteite, syn  
|Sobolevite  
|Silinaite  
|Pyrostilpnite  
|Telluropalladinite, syn  
|Santite, syn  
|Langbanite  
|Poughite  
|Turquoise  
|Paraschoepite, syn  
|Pabstite, syn  
+-----+
```

File: SAMPLE2.DI

9-Feb-2006 20:23

Philips Analytical X-Ray B.V.

PC-APD, Diffraction software

Sample identification: Sample2

Data measured at: 9-Feb-2006 18:26:00

Diffractometer type: PW3710 BASED

Tube anode: Cu

Generator tension [kV]: 40

Generator current [mA]: 40

Wavelength Alpha1 [Å]: 1.54060

Wavelength Alpha2 [Å]: 1.54439

Intensity ratio (alpha2/alpha1): 0.500

Divergence slit: 1x

Receiving slit: 0.1

Monochromator used: YES

Start angle [x2i]: 5.000

End angle [x2i]: 75.000

Step size [x2i]: 0.010

Maximum intensity: 4369.210

Time per step [s]: 1.000

Type of scan: CONTINUOUS

Minimum peak tip width: 0.00

Maximum peak tip width: 1.00

Peak base width: 2.00

Minimum significance: 0.75

Number of peaks: 48

Angle [x2i]	d-value '1 [Å]	d-value '2 [Å]	Peak width [x2i]	Peak int [counts]	Back. int [counts]	Rel. int [%]	Signif.
8.865	9.9671	9.9916	0.160	100	100	2.3	1.38
12.420	7.1210	7.1385	0.040	506	74	11.6	1.24
13.800	6.4119	6.4276	0.240	11	61	0.2	0.96
14.970	5.9133	5.9278	0.320	4	58	0.1	0.82
17.775	4.9859	4.9982	0.160	32	62	0.7	0.87
19.890	4.4603	4.4712	0.280	256	66	5.9	7.80
20.385	4.3531	4.3638	0.080	222	66	5.1	0.88
20.880	4.2510	4.2614	0.080	1082	66	24.8	9.02
21.265	4.1749	4.1851	0.100	161	67	3.7	0.88
22.095	4.0199	4.0298	0.080	123	69	2.8	0.87
23.065	3.8530	3.8624	0.200	110	71	2.5	1.30
23.600	3.7668	3.7761	0.120	161	71	3.7	1.38
24.260	3.6658	3.6748	0.160	128	72	2.9	0.79
24.915	3.5709	3.5797	0.160	520	72	11.9	12.07
25.735	3.4590	3.4675	0.120	142	74	3.2	1.95
26.665	3.3404	3.3486	0.080	4369	76	100.0	19.58
26.745	3.3306	3.3388	0.050	1962	76	44.9	1.08

27.100	3.2072	3.2702	0.030	100	70	4.0	0.71
27.525	3.2379	3.2459	0.160	174	76	4.0	1.24
27.960	3.1885	3.1964	0.120	169	77	3.9	2.33
29.910	2.9850	2.9923	0.160	81	79	1.9	0.91
30.835	2.8975	2.9046	0.160	52	81	1.2	0.93

File: SAMPLE2.D1

9-Feb-2006 20:23

Philips Analytical X-Ray B.V.

PC-APD, Diffraction software

Angle [2θ]	d-value '1 [Å]	d-value '2 [Å]	Peak width [2θ]	Peak int [counts]	Back. int [counts]	Rel. int [%]	Signif.
31.865	2.8061	2.8130	0.320	42	83	1.0	2.39
35.095	2.5549	2.5612	0.240	132	83	3.0	3.41
36.005	2.4924	2.4985	0.240	72	81	1.7	3.38
36.535	2.4575	2.4635	0.070	266	79	6.1	3.46
37.750	2.3811	2.3870	0.120	76	77	1.7	2.60
38.480	2.3376	2.3434	0.280	85	77	1.9	3.87
39.500	2.2796	2.2852	0.070	266	76	6.1	3.06
39.610	2.2735	2.2791	0.030	121	74	2.8	0.78
40.305	2.2359	2.2414	0.050	128	74	2.9	0.81
42.480	2.1263	2.1315	0.070	193	71	4.4	2.15
45.810	1.9792	1.9840	0.060	128	67	2.9	3.15
47.960	1.8953	1.9000	0.480	14	62	0.3	1.02
49.265	1.8481	1.8527	0.040	25	61	0.6	1.23
50.165	1.8171	1.8215	0.080	331	61	7.6	6.01
50.285	1.8130	1.8175	0.050	177	61	4.0	1.08
51.195	1.7829	1.7873	0.240	14	59	0.3	0.77
52.355	1.7461	1.7504	0.400	2	59	0.1	0.83
54.865	1.6720	1.6761	0.100	114	67	2.6	2.39
55.330	1.6591	1.6631	0.160	59	71	1.4	1.05
59.960	1.5415	1.5453	0.100	199	64	4.6	3.52
62.470	1.4855	1.4891	0.320	41	62	0.9	2.73
64.035	1.4529	1.4565	0.120	37	62	0.9	1.73
67.760	1.3818	1.3852	0.120	98	61	2.2	3.11
68.135	1.3751	1.3785	0.100	154	62	3.5	2.82
68.315	1.3719	1.3753	0.060	151	62	3.5	1.53
73.455	1.2881	1.2913	0.080	37	58	0.9	0.80

C:\APDJ\DATA\SAMPLE2.IDN

9-Feb-2006 20:25

Analyzed DI file : C:\APDJ\DATA\SAMPLE2.DI
Sample identification : Sample2
Last update of results file : 9-Feb-2006 20:25

Database used : C:\IDENTDB

MEASUREMENT PARAMETERS

Diffractometer : PW3710
Start angle [x2i] : 4.995
Final angle [x2i] : 75.005
Step size [x2i] : 0.010
Time per step [s] : 1.0
Anode material : Cu

Date and time of measurement : 9-Feb-2006 18:26

PEAK SEARCH PARAMETERS

Minimum peak width : 0.00
Maximum peak width : 1.00
Peak base width : 2.00
Minimum significance : 0.75

Number of peaks detected : 48

SEARCH-MATCH PARAMETERS

Number of strong lines of the
reference patterns used in SEARCH : 5
Intensity threshold : 3.02
Confidence threshold : 20
Minimum specimen displacement : -40
Maximum specimen displacement : 35
Step size in specimen displacement: 75

Restrictions file : GENERAL

Results:

Card.	Match	Rel m	I [%]	Displ	QM	Formula
ident.	score	score		[fm]		
1	19-1184	42.04	0.33	2	8	I NaAlSi3O8
2	33-1161	16.35	0.82	35	-4	S SiO2
3	20-0528	31.69	0.36	2	93	C (Ca,Na)(Al,Si)2Si2O8
4	31-0966	32.23	0.34	2	93	S KAlSi3O8
5	35-0610	29.42	0.34	3	-125	S MgSiO3
6	14-0164	25.40	0.38	1	93	I Al2Si2O5(OH)4
7	20-0452	23.32	0.40	10	73	I CaAl2Si2O8·4H2O
8	37-0447	25.31	0.35	10	126	S Cu3(AsO4)(OH)3

C:\APOJ\DATA\SAMPLE2.IDN

9-Feb-2006 20:25

```
-----+
|Name|
|-----+
|Albite, ordered|
|Quartz, syn|
|Anorthite, sodian, ordered|
|Orthoclase|
|Clinoenstatite, syn|
|Kaolinite-1A|
|Gismondine|
|Clinoclase|
|-----+

```

C:\APDJ\DATA\SAMPLE2.IDN

9-Feb-2006 20:25

Card.	Match	Rel m	I [%]	Displ	QM	Formula
ident.	score	score		[fm]		
9	25-0618	26.76	0.33	1	-68	S K(Si3Al)O8
10	09-0466	19.64	0.44	5	65	S NaAlSi3O8
11	37-0440	26.66	0.30	1	-132	I (K,Na)Ca2Si3O8(F,OH)
12	41-1480	22.88	0.35	3	78	I (Na,Ca)Al(Si,Al)3O8
13	29-0989	22.80	0.35	1	-59	I K5Ca2(Al9Si23O64)·24H2O
14	31-0062	24.38	0.33	1	-125	S ((NH4)2Ni(SO4)2·6H2O
15	41-1486	24.04	0.32	3	119	S CaAl2Si2O8
16	19-1227	22.57	0.34	2	-122	S (K,Na)(Si3Al)O8
17	27-0380	23.93	0.30	1	58	S K2Cr2O7
18	16-0606	21.45	0.32	1	111	I Al2Si2O5(OH)4
19	19-1418	20.86	0.33	1	-29	I Ca5Ba4Al9Si11O41(OH)2(SO4
20	41-1358	21.54	0.32	1	-122	O K2FeCl4·2H2O
21	11-0046	20.87	0.32	1	-24	I Al2SiO5
22	19-1263	22.00	0.30	2	62	S Na2Zn(SO4)2·4H2O
23	24-1035	21.36	0.30	1	-122	S BaSO4
24	31-0788	19.21	0.32	1	103	I Mg3B11O15(OH)9
25	41-1372	19.31	0.31	2	28	S CaFeSi2O6

C:\APD\DATA\SAMPLE2.IDN

9-Feb-2006 20:25

```
+-----+
|Name|
+-----+
|Sanidine, disordered|
|Albite, ordered|
|Densovite|
|Albite, calcian, ordered|
|Merlinoite|
|Nickelbousingaultite, syn|
|Anorthite, ordered|
|Sanidine|
|Lopezite, syn|
|Nacrite-2M2|
|Wenkite|
|Douglasite|
|Kyanite|
|Zincbl\PIodite, syn [NR]|
|Barite, syn|
|Preobrazhenskite|
|Hedenbergite|
+-----+
```

File: 3B2.D1

10-Feb-2006 13:52

Philips Analytical X-Ray B.V.

PC-APD, Diffraction software

Sample identification: 3B-2

Data measured at: 10-Feb-2006 11:55:00

Diffractometer type: PW3710 BASED

Tube anode: Cu

Generator tension [kV]: 40

Generator current [mA]: 40

Wavelength Alpha1 [Å]: 1.54060

Wavelength Alpha2 [Å]: 1.54439

Intensity ratio (alpha2/alpha1): 0.500

Divergence slit: 1x

Receiving slit: 0.1

Monochromator used: YES

Start angle [x2θ]: 5.000

End angle [x2θ]: 75.000

Step size [x2θ]: 0.010

Maximum intensity: 4583.290

Time per step [s]: 1.000

Type of scan: CONTINUOUS

Minimum peak tip width: 0.00

Maximum peak tip width: 1.00

Peak base width: 2.00

Minimum significance: 0.75

Number of peaks: 66

Angle [x2θ]	d-value '1 [Å]	d-value '2 [Å]	Peak width [x2θ]	Peak int [counts]	Back. int [counts]	Rel. int [%]	Signif.
7.780	11.3545	11.3824	0.120	7	67	0.1	0.89
8.820	10.0178	10.0425	0.240	24	59	0.5	0.86
12.415	7.1239	7.1414	0.030	317	48	6.9	1.10
13.860	6.3842	6.3999	0.120	29	44	0.6	1.74
15.065	5.8762	5.8906	0.480	7	42	0.1	0.95
16.230	5.4569	5.4703	0.400	4	42	0.1	0.75
17.745	4.9943	5.0066	0.480	14	42	0.3	1.18
19.885	4.4614	4.4724	0.200	67	44	1.5	1.46
20.890	4.2490	4.2594	0.060	858	44	18.7	4.33
22.090	4.0208	4.0307	0.060	108	45	2.4	1.58
22.550	3.9398	3.9495	0.240	76	45	1.7	1.60
23.580	3.7700	3.7792	0.080	154	45	3.4	1.04
23.935	3.7149	3.7240	0.060	164	45	3.6	2.53
24.275	3.6636	3.6726	0.120	96	45	2.1	0.86
24.910	3.5716	3.5804	0.140	313	46	6.8	6.36
25.675	3.4669	3.4754	0.160	102	46	2.2	1.09
26.660	3.3410	3.3492	0.060	4583	46	100.0	12.94

26.740	3.3312	3.3374	0.040	2007	46	43.6	1.73
27.150	3.2818	3.2899	0.060	132	46	2.9	0.85
27.570	3.2328	3.2407	0.180	196	48	4.3	5.49
27.970	3.1874	3.1953	0.100	199	48	4.3	2.67
29.860	2.9898	2.9972	0.160	98	48	2.1	1.07

File: 3E2.D1

10-Feb-2006 13:52

Philips Analytical X-Ray B.V.

PC-APD, Diffraction software

Angle [x2 θ]	d-value '1 [Å]	d-value '2 [Å]	Peak width [x2 θ]	Peak int [counts]	Back. int [counts]	Rel. int [%]	Signif.
30.705	2.9095	2.9166	0.090	1592	49	34.7	10.44
30.790	2.9016	2.9088	0.050	1163	49	25.4	1.13
33.075	2.7062	2.7129	0.160	96	49	2.1	1.04
33.260	2.6916	2.6982	0.060	114	49	2.5	0.75
35.050	2.5581	2.5644	0.240	67	50	1.5	1.88
36.065	2.4884	2.4945	0.160	44	50	1.0	0.88
36.545	2.4568	2.4629	0.040	299	50	6.5	0.89
36.655	2.4497	2.4557	0.060	159	52	3.5	0.83
37.200	2.4150	2.4210	0.120	108	52	2.4	1.80
37.780	2.3793	2.3851	0.240	37	52	0.8	1.68
38.395	2.3426	2.3483	0.200	30	52	0.7	0.99
39.485	2.2804	2.2860	0.040	188	52	4.1	0.89
39.595	2.2743	2.2799	0.030	86	52	1.9	0.82
40.295	2.2364	2.2419	0.100	94	53	2.1	2.30
40.875	2.2060	2.2114	0.080	151	53	3.3	1.14
41.735	2.1625	2.1678	0.160	30	53	0.7	0.94
42.475	2.1265	2.1318	0.060	156	53	3.4	1.88
44.670	2.0270	2.0320	0.120	90	55	2.0	1.92
45.805	1.9794	1.9842	0.080	88	55	1.9	1.36
48.130	1.8890	1.8937	0.280	7	56	0.1	0.97
49.040	1.8561	1.8607	0.240	31	56	0.7	0.96
50.165	1.8171	1.8215	0.050	328	58	7.1	1.85
50.310	1.8122	1.8166	0.060	177	58	3.9	1.85
50.645	1.8010	1.8054	0.100	161	58	3.5	1.64
54.895	1.6712	1.6753	0.040	110	53	2.4	0.78
55.035	1.6672	1.6713	0.060	71	53	1.5	1.49
55.325	1.6592	1.6633	0.120	34	53	0.7	0.90
56.345	1.6316	1.6356	0.200	14	55	0.3	0.75
57.440	1.6030	1.6070	0.060	6	55	0.1	0.86
57.805	1.5938	1.5977	0.240	8	55	0.2	1.01
58.670	1.5723	1.5762	0.240	13	56	0.3	1.32
59.980	1.5411	1.5449	0.050	180	56	3.9	1.39
60.135	1.5375	1.5412	0.060	100	56	2.2	1.13
61.335	1.5102	1.5139	0.090	7	58	0.2	1.37
63.035	1.4735	1.4772	0.120	24	58	0.5	1.01
64.050	1.4526	1.4562	0.400	28	59	0.6	2.30
67.085	1.3941	1.3975	0.240	18	55	0.4	1.64
67.760	1.3818	1.3852	0.080	85	53	1.8	1.09
68.160	1.3747	1.3781	0.080	88	53	1.9	0.77
68.345	1.3714	1.3748	0.070	161	53	3.5	2.59
68.505	1.3686	1.3720	0.080	45	52	1.0	0.80
70.220	1.3393	1.3426	0.960	10	49	0.2	2.50
72.415	1.3040	1.3072	0.480	10	46	0.2	1.01
73.460	1.2880	1.2912	0.100	22	45	0.5	0.80

```

=====
Analyzed DI file       : C:\APOJ\DATA\3B2.DI
Sample identification  : 3B-2
Last update of results file : 10-Feb-2006 13:54

```

```

Database used        : C:\IDENTDB

```

MEASUREMENT PARAMETERS

```

Diffractometer       : PW3710
Start angle           [x2θ] : 4.995
Final angle           [x2θ] : 75.005
Step size             [x2θ] : 0.010
Time per step         [s]   : 1.0
Anode material        : Cu

```

```

Date and time of measurement : 10-Feb-2006 11:55

```

PEAK SEARCH PARAMETERS

```

Minimum peak width    : 0.00
Maximum peak width    : 1.00
Peak base width       : 2.00
Minimum significance  : 0.75

```

```

Number of peaks detected : 66

```

SEARCH-MATCH PARAMETERS

```

Number of strong lines of the
reference patterns used in SEARCH : 5
Intensity threshold             : 3.02
Confidence threshold           : 20
Minimum specimen displacement  : -40
Maximum specimen displacement  : 35
Step size in specimen displacement: 75

```

```

Restrictions file : GENERAL

```

Results:

	Card.	Match	Rel m	I [%]	Displ	QM	Formula
	ident.	score	score		[fm]		
1	19-1184	45.12	0.36	2	25	I	NaAlSi3O8
2	31-0966	39.10	0.41	3	-14	S	KAlSi3O8
3	19-1220	38.29	0.38	2	-42	S	Na2Ni(SO4)2·4H2O
4	33-1161	16.90	0.84	43	12	S	SiO2
5	41-0586	19.06	0.64	29	-46	S	Ca(Fe,Mg)(CO3)2
6	35-0610	32.42	0.37	3	-129	S	MgSiO3
7	41-1369	33.85	0.34	1	-145	S	Pb(Zn,Cu)VO4(OH)
8	20-0528	29.97	0.34	2	111	C	(Ca,Na)(Al,Si)2Si2O8

C:\APDJ\DATA\3B2.IDN

10-Feb-2006 13:54

Name
Albite, ordered
Orthoclase
Nickelbl\Iodite, syn
Quartz, syn
Ankerite
Clinoenstatite, syn
Descloizite, cuprian
Anorthite, sodian, ordered

C:\APDJ\DATA\3B2.IDN

10-Feb-2006 13:54

Card.	Match	Rel m	I [%]	Displ	QM	Formula
ident.	score	score		[fm]		
9	37-0447	27.00	0.37	8	111	S Cu ₃ (AsO ₄)(OH) ₃
10	43-1476	29.59	0.33	1	136	S CuPb ₁₃ Sb ₇ S ₂₄
11	41-1480	25.09	0.39	3	-47	I (Na,Ca)Al(Si,Al) ₃ O ₈
12	43-1470	24.49	0.40	2	41	S FeAsS
13	19-0932	27.03	0.34	3	73	I KAlSi ₃ O ₈
14	20-0452	22.95	0.40	3	45	I CaAl ₂ Si ₂ O ₈ !4H ₂ O
15	25-0618	26.94	0.33	1	-31	S K(Si ₃ Al) ₀₈
16	19-1263	24.83	0.34	2	17	S Na ₂ Zn(SO ₄) ₂ !4H ₂ O
17	41-1486	24.61	0.33	2	123	S CaAl ₂ Si ₂ O ₈
18	09-0466	19.17	0.43	3	65	S NaAlSi ₃ O ₈
19	19-1227	22.96	0.35	2	-145	S (K,Na)(Si ₃ Al) ₀₈
20	29-0989	22.68	0.35	1	-64	I K ₅ Ca ₂ (Al ₉ Si ₂₃ O ₆₄)!24H ₂ O
21	29-0288	21.34	0.37	1	-109	I Ca ₂ Al ₂ Mn(Si ₄)(Si ₂₀₇)(O, ₀
22	43-0695	14.23	0.55	7	144	S Ca(Mn,Mg)(CO ₃) ₂
23	44-1426	22.97	0.34	1	-47	S Fe ₂ (SO ₄) ₃ !7H ₂ O
24	39-1376	23.61	0.33	1	-24	I K(Ca,Ba)(Si ₅ Al ₃) ₀₁₆ !6H ₂ O
25	22-0633	23.88	0.31	4	50	S FeSO ₄ !7H ₂ O

C:\APOJ\DATA\3B2.IDN

10-Feb-2006 13:54

Name-----
Clinoclase
Meneghinite
Albite, calcian, ordered
Arsenopyrite
Microcline, intermediate
Gismondine
Sanidine, disordered
Zincblende, syn [NR]
Anorthite, ordered
Albite, ordered
Sanidine
Merlinoite
Piemontite
Kutnohorite, magnesian
Kornelite
Wellsite [NR]
Melanterite, syn

C:\APDJ\DATA\3B1.IDN

10-Feb-2006 13:58

Analyzed DI file : C:\APDJ\DATA\3B1.DI
 Sample identification : 3B-1
 Last update of results file : 10-Feb-2006 13:58

Database used : C:\IDENTDB

MEASUREMENT PARAMETERS

Diffractometer : PW3710
 Start angle [x2 θ] : 4.995
 Final angle [x2 θ] : 75.005
 Step size [x2 θ] : 0.010
 Time per step [s] : 1.0
 Anode material : Cu

Date and time of measurement : 9-Feb-2006 16:19

PEAK SEARCH PARAMETERS

Minimum peak width : 0.00
 Maximum peak width : 1.00
 Peak base width : 2.00
 Minimum significance : 0.75

Number of peaks detected : 60

SEARCH-MATCH PARAMETERS

Number of strong lines of the
 reference patterns used in SEARCH : 5
 Intensity threshold : 3.02
 Confidence threshold : 20
 Minimum specimen displacement : -40
 Maximum specimen displacement : 35
 Step size in specimen displacement: 75

Restrictions file : GENERAL

Results:

	Card.	Match	Rel m	I [%]	Displ	QM	Formula
	ident.	score	score		[fm]		
1	31-0966	35.24	0.37	1	-14	S	KAlSi3O8
2	33-1161	15.78	0.79	61	12	S	SiO2
3	35-0610	29.53	0.34	2	-129	S	MgSiO3
4	37-0447	25.57	0.35	4	83	S	Cu3(AsO4)(OH)3
5	25-0616	26.77	0.33	1	-14	S	K(Si3Al)O8
6	19-0932	25.20	0.32	1	17	I	KAlSi3O8
7	29-1488	12.70	0.60	3	-112	O	Al2Si2O5(OH)4
8	19-1227	22.32	0.34	2	-125	S	(K,Na)(Si3Al)O8

C:\APDJ\DATA\3B1.IDN

10-Feb-2006 13:58

Name

Orthoclase
Quartz, syn
Clinoenstatite, syn
Clinoclase
Sanidine, disordered
Microcline, intermediate
Kaolinite-1Md
Sanidine

C:\APDJ\DATA\3B1.IDN

10-Feb-2006 13:58

	Card ident.	Match score	Rel m score	I [%]	Disp1 [fm]	QM	Formula
9	19-1263	21.78	0.30	1	62	S	Na2Zn(SO4)2·4H2O
10	31-0782	14.38	0.42	1	-122	I	(Mg,Al)3(Si,Al)2O5(OH)4
11	13-0004	14.93	0.40	1	-64	O	(Mg,Al)3(Si,Al)2O5(OH)4
12	41-0607	17.75	0.33	1	-122	I	Ca2Mg(AsO4)2·2H2O
13	44-1426	19.78	0.29	1	-64	S	Fe2(SO4)3·7H2O
14	29-0380	21.37	0.27	1	58	I	Ca5(SiO4)2(OH)2
15	12-0724	14.41	0.37	1	-3	O	Hg3(SO4)O2
16	36-0439	16.54	0.31	1	-57	O	Na11(Na,Ca)4MnTi4(Si207)2
17	44-1410	15.07	0.33	1	-43	I	LiNaSi2O5·2H2O
18	25-1187	16.90	0.28	1	-99	C	Ag3SbS3
19	35-1013	15.16	0.31	1	-3	C	Pd9Te4
20	25-0624	13.97	0.33	1	-46	I	KB5O8·4H2O
21	14-0195	11.51	0.40	1	-99	O	(Mn,Ca)4(Mn,Fe)9SbSi2O24
22	21-0435	14.03	0.32	1	-99	I	Fe2(TeO3)2SO4·3H2O
23	06-0214	17.12	0.26	1	-79	I	CuAl6(PO4)4(OH)8·4H2O
24	23-1461	14.22	0.31	1	-117	O	UO2.86·1.5H2O
25	43-0633	13.50	0.32	2	30	S	BaSnSi3O9

7

Appendix D – Rock Evaluation Data of the upper cored interval of well 3B

Sample	Qty	S1	S2	PI	S3	Tmax	Tpeak	S3CO	PC(%)	TOC	RC%	HI	OICO	OI
9107	70.9	0.67	11.19	0.06	0.47	443	483	0.04	1.02	5.11	4.09	219	1	9
9107	70.3	0.71	11.69	0.06	0.59	443	483	0.12	1.06	5.11	4.05	229	2	12
		Well 3B Provost Field												
907.58	70.5	0.69	12.18	0.05	3.99	428	468	2.28	1.34	8.46	7.12	144	27	47
910.23	25.1	2.08	27.70	0.07	19.97	415	455	15.00	3.99	38.17	34.18	73	39	52

MINC%	S4CO	S4CO2	RCCO(%)	S4CO2	S5aCO2	S5bCO2	KFID	RCCO2(%)
4.3	20.5	117.6	0.880	0.0	0.0	0.0	1112	3.21
4.4	21.0	115.4	0.900	0.0	0.0	0.0	1112	3.15
0.4	46.2	188.4	1.980	0.0	0.0	0.0	1112	5.14
3.1	212.4	919.5	9.100	0.0	0.0	0.0	1112	25.08